INFORMATION TO USERS

This manuscript has been reproduced from the microfilm master. UMI films the text directly from the original or copy submitted. Thus, some thesis and dissertation copies are in typewriter face, while others may be from any type of computer printer.

The quality of this reproduction is dependent upon the quality of the copy submitted. Broken or indistinct print, colored or poor quality illustrations and photographs, print bleedthrough, substandard margins, and improper alignment can adversely affect reproduction.

In the unlikely event that the author did not send UMI a complete manuscript and there are missing pages, these will be noted. Also, if unauthorized copyright material had to be removed, a note will indicate the deletion.

Oversize materials (e.g., maps, drawings, charts) are reproduced by sectioning the original, beginning at the upper left-hand corner and continuing from left to right in equal sections with small overlaps.

Photographs included in the original manuscript have been reproduced xerographically in this copy. Higher quality 6" x 9" black and white photographic prints are available for any photographs or illustrations appearing in this copy for an additional charge. Contact UMI directly to order.

ProQuest Information and Learning
300 North Zeeb Road, Ann Arbor, MI 48106-1346 USA
800-521-0600

The NMR Properties, Photochromism and Efficient Syntheses of Several [e]-Annelated Dimethyldihydropyrenes

by

Timothy Robbins Ward

B.Sc. University of Victoria, Canada, 1987.

A Dissertation Submitted in Partial Fulfillment
of the Requirements for the Degree of

DOCTOR OF PHILOSOPHY

in the Department of Chemistry

We accept this dissertation as conforming
to the required standard

Dr. R. H. Mitchell (Department of Chemistry)

Dr. T. M. Fyles (Department of Chemistry)

Dr. R. G. Hicks (Department of Chemistry)

Dr. R. W. Olafson (Department of Biochemistry)

Dr. R. V. Williams (Department of Chemistry, University of Idaho)

Supervisor: Dr. R. H. Mitchell

ABSTRACT

A systematic and efficient route to [e]-annelated derivatives of 2,7-di-*t*-butyl-*trans*-10b,10c-dimethyl-10b,10c-dihydropyrene **34** has been achieved which provides access to the benzo, naphtho, and anthro derivatives of **34**, by means of a Diels - Alder reaction of an aryne with a furan. Reaction of the annulyne derived from bromide **50** with furan gave adduct **52** which could be both deoxygenated to benzo derivative **53** and reacted with tetrazine **54** to yield the annuleno furan **55** which subsequently with benzyne and 2,3-naphthalyne yielded adducts which were deoxygenated to naphtho and anthro derivatives **57** and **59**. Reaction of the furan **55** with the benzoannulyne derived from **65** gave the cyclophane fused pyrene **68**, while reaction of the annulyne derived from **50** with the bisfuran **62** gave the chrysene bis pyrene **60**. These fused dihydropyrene derivatives are all photochromic, and the photoisomerizations were studied in each case. Dihydropyrenes **53**, **57**, **59**, and **65** are simple photo-switches, while **60** and **68** are more complex multiple state switches. In each case the kinetics of the MCD to DMDHP reaction was followed to obtain the activation energy, enthalpy, and entropy. It was found that the activation enthalpies and energies decreased through the series, from the benzo to the naphtho to the anthro system. This suggested that the transition states for the MCD to DMDHP reactions were stabilized by resonance with the respective annelated fragments.

Detailed analysis of the NMR data of all compounds yielded an experimental aromaticity scale in which δ(Me) or $\delta(H^4)$ could yield information to obtain the relative resonance energy of the annelating fragment. Correlations between methyl and H^4 protons were obtained and compared to related systems.

Examiners:

Dr. R. H. Mitchell (Department of Chemistry)

Dr. T. M. Fyles (Department of Chemistry)

Dr. R. G. Hicks (Department of Chemistry)

Dr. R. W. Olafson (Department of Biochemistry)

Dr. R. V. Williams (Department of Chemistry, University of Idaho)

Table of Contents

Chapter one Introduction

Chapter two Synthesis

Chapter three Results and Discussion

Chapter four Conclusions

Chapter five Experimental

List of Tables

List of Figures

List of Abbreviations

Ar	arene
^{13}C NMR	carbon-13 nuclear magnetic resonance spectrum
BuLi	butyllithium
CI	chemical ionization
δ	chemical shift in ppm
DCM	dichloromethane CH_2Cl_2
dec.	decomposition
DMDHP	dimethyldihydropyrene
DMF	dimethylformamide
EtOH	ethanol
EI	electron impact
h	hour
^{1}H NMR	proton nuclear magnetic resonance spectrum
HRMS	high resolution mass spectrum
IR	infrared spectrum
KO^{t}Bu	potassium *t*-butoxide
LDA	lithium diisopropylamide
LFP	laser flash photolysis
LSIMS	liquid secondary ion mass spectrometry
MCD	metacyclophanediene
Me	methyl

MeOH	methanol
min	minute
mp	melting point
MS	mass spectrum
NBS	N-bromosuccimide
NMP	N-methylpyrrolidone
NMR	nuclear magnetic resonance
NOE	nuclear Overhauser enhancement
s	second, singlet
d	doublet
t	triplet
dd	doublet of doublets
m	multiplet
ppm	parts per million
RE	resonance energy
TBAF	tetra-n-butylammonium fluoride
THF	tetrahydrofuran
TMS	trimethylsilyl group
UV-visible	ultraviolet and visible spectrum

Acknowledgments

The author wishes to express his deep appreciation to Dr. R. H. Mitchell for his constant guidance and encouragement during the course of this work.

Financial support from the University of Victoria and from NSERC Canada is gratefully acknowledged.

My thanks also go to Mrs. Christine Greenwood for recording many NMR spectra, and to Dr. David McGillivray for mass spectrometric analysis.

To Byrl and David.

Chapter one Introduction

1.1.1 What is Aromaticity?

The discovery of benzene by Faraday in 1825[1] opened a field of enquiry now known as aromaticity. Practical and theoretical results stemming from benzene and aromatics have entered into discussions and developments of broad chemical interest. Valency and bonding theory in the 19th and 20th centuries and pericyclic reaction transition state theory in the 20th century have both looked to benzene as an important model, electronically and structurally[2-7]. As a colloquial usage, aromaticity is typically taken to mean benzene-like, because most chemists have a feel for the reactivity of benzene.

The concept of aromaticity is also vital to heterocyclic chemistry. Heterocycles support life itself, and many medical and industrial uses of heterocycles are known.

Aromaticity is usually used qualitatively, though a general quantitative method to measure aromaticity would be desirable, which encompasses both carbocycles and heterocycles. Fundamental preconditions for aromaticity usually include a planar monocyclic π system with $4n + 2$ mobile π electrons, $n = 0,1,2,...$ This is central in Huckel's molecular orbital (HMO) theory[4]. In contrast, some of the 4n electron homologues[8,9] display destabilization, great reactivity, π bond localization, and have thus become known as antiaromatics. Post Huckel (HMO) modification by Streitweiser has helped explain properties of conjugated heterocycles[10]. Another important adjunct to HMO is Randic's circuit theory[11], for polycyclic conjugated systems. In this theory, regardless of the total π electron

count, systems with only 4n + 2 electron conjugated circuits are aromatic, while those with only 4n electron circuits are antiaromatic. Composite systems (biphenylene for example) with both 4n and 4n + 2 circuits usually have one prevalent character, not both. The most widely held criteria of aromaticity are geometry, energy (the pair are termed classical), and magnetic effects. Quantitative measures of aromaticity have been proposed in each of these catagories[12].

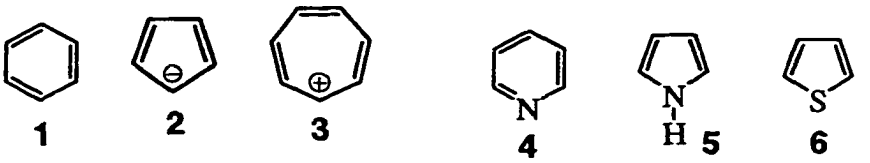

1 2 3 4 5 6

Huckel aromatics. Heteroaromatics.

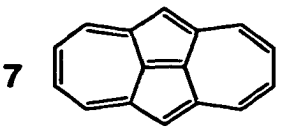

7

Non-Huckel (Randic) aromatic

Larger monocyclic conjugated systems often have difficulty in maintaining the planarity necessary for aromaticity. Two successful approaches to solving this problem have been developed. The first approach, used by Sondheimer [13] and Nakagawa[14] independently, is to introduce acetylenic bonds and large substituents. The second approach, independently used by Boekelheide [15] and Vogel[16a], is to use internal bridging groups to give structural rigidity. This second approach serendipitously introduces aromaticity probe groups for instrumental detection, by nuclear magnetic resonance (NMR) spectroscopy.

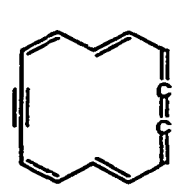

8

Sondheimer

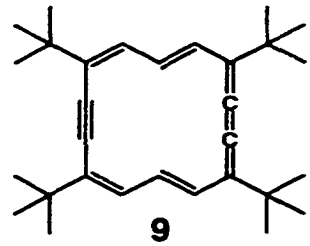

9

Nakagawa

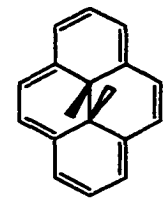

10

Boekelheide

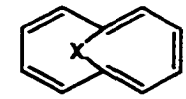

11, X = CH_2

(X = CH_2, O, NR)

Vogel

Geometric affirmation of aromaticity requires bond length equalization, arising from cyclic electron delocalization[12,17]. Benzene has perfect bond equalization, but higher condensed aromatics display significant alternation, and so great care is required in application of the geometric criterion. Boekelheide's bridged [14] annulene **10** shows close to bond equivalence.

Energetic stabilization (resonance energy, RE) in (4n + 2) aromatics arises from the cyclic π molecular orbital system having additional bonding stabilization compared to non-cyclic or non contiguous cyclic systems. Unfortunately, the value of the stabilization depends on the reference system chosen. For example, just three comparisons for benzene give considerable variance[18,19];

3 x cyclohexene = benzene + 2 x cyclohexane ΔH = -35.2 Kcal/mol

3 x ethene + cyclohexane = benzene + 3 x ethane ΔH = -48.9 Kcal/mol

3 x butadiene = benzene + 3 x ethene ΔH = -21.7 Kcal/mol

When strained systems are considered, even more difficulty is encountered (eg C_{60} , Vogel's bridged [10]-annulene **11**[16a])[20].

A third consequence of the general electronic preconditions of aromaticity (above) is magnetic effects. Diamagnetic susceptibility exaltation (Λ) was noted almost a century ago by Pascal[21], and has been proposed as the best criterion for aromaticity, by Schleyer[22]. "Compounds which exhibit significantly exalted diamagnetic susceptibility are aromatic." Here again, a calculation is necessary, and a reference set must be chosen.

1.1.2 Aromaticity and NMR

Another magnetic effect is found in NMR chemical shifts, and proton chemical shifts are perhaps the most popular accessible characterization of aromaticity and antiaromaticity. The theory used to account for aromaticity effects on NMR signals actually had its origin in the diamagnetic susceptibility exaltation noted in the early decades on the 1900's. Pauling advanced a quantitative theory assuming Larmor precession of the π electrons in benzene to account for the diamagnetic exaltation[5a]. Ultimately, this model points to the macroscopic observations of current flow induced in cyclic conductors moving in magnetic fields. In macroscopic systems, current flow is induced in a cyclic conductor to produce an opposing magnetic field. This classical model has been co-opted for the molecular model[23]. At the molecular level, the applied magnetic field is said to induce a ring current in the aromatic molecule, such that a magnetic field produced by the molecule opposes the applied field, within the molecule. Outside the ring, the induced magnetic field augments the applied field. The external protons of the aromatic are thus more strongly deshielded

Outside the ring, the induced magnetic field augments the applied field. The external protons of the aromatic are thus more strongly deshielded than for an analogous alkene, and the aromatic protons therefore resonate at lower field in an NMR spectrometer. This is depicted for benzene in **Figure 1**.

Figure 1. Induced π electron ring current, and induced magnetic field.

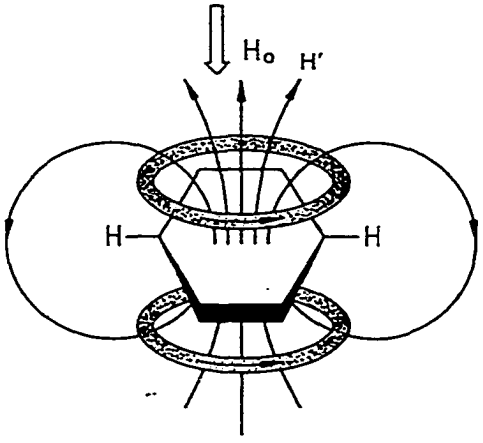

There is no current proof that ring currents exist, at the molecular level. The ring current theory is used widely, however, to explain the chemical shifts of annulenes. The putative ring current in $4n + 2$ π electron diamagnetic annulenes is termed diatropic. In the $4n$ π electron systems, a paramagnetic ring current is said to be induced, and these systems are called paratropic. The classical model cannot be used for 4n systems, since in classical systems, induced magnetism always opposes the applied field, at the center of the cyclic conductor.

An interesting example illustrating the above model is the bridged [14]annulene dimethyldihydropyrene **10**. This system has an NMR spectrum with aromatic deshielded protons between δ 8.67 to 7.95, and shielded internal

paramagnetically deshielded internal methyl protons at δ 21 and shielded external proton resonances upfield at δ -3.2 to -4.0 [25]. Caution is required for assignment of aromaticity based on NMR resonances, as some metal hydrides and some organometallics show great upfield proton resonances, while simple acidic, and carbonyl proton signals are quite downfield. Structure must always be kept in mind. Examples of diatropic and paratropic systems appear below and in Table 1.

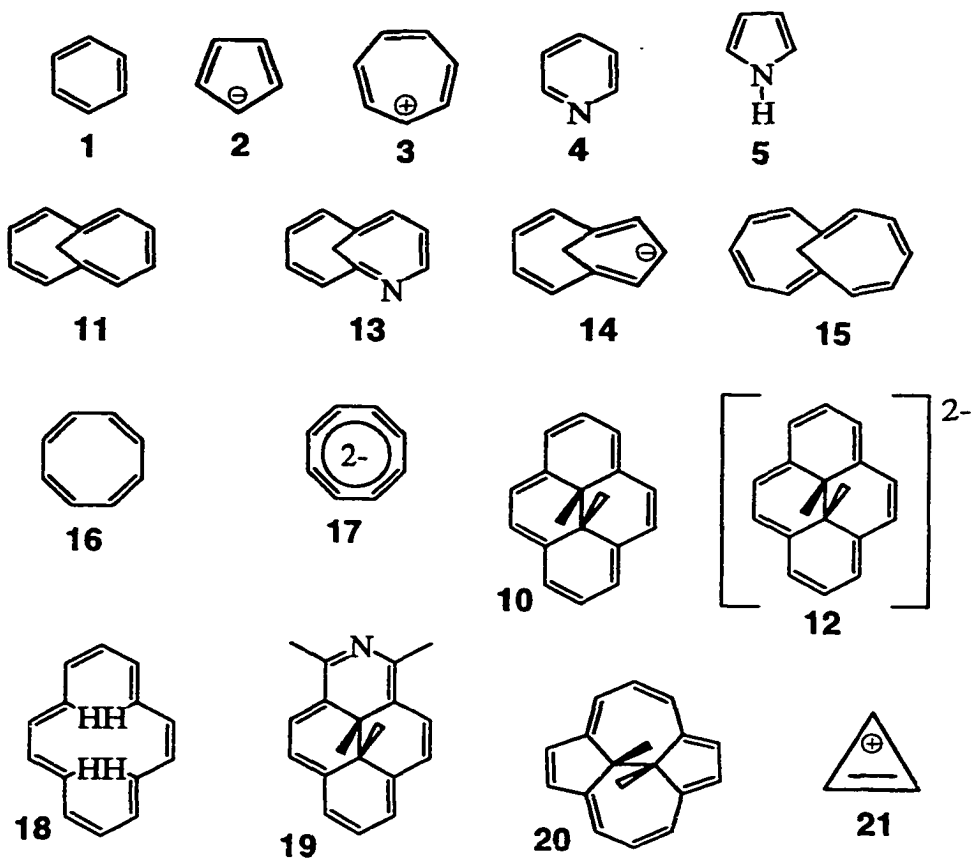

Table 1 Proton NMR (δ) shifts of illustrative π systems.

Compound	π electrons	δ outer protons	δ inner protons	reference
1	6	7.27		26
2	6	5.60		27a
3	6	9.20		27a
4	6	8.50 - 7.46		27b
5	6	7.70 - 6.05		27b
11	10	7.27 - 6.95	-0.52	16a, 28
13	10	8.23 - 6.50	0.65 to -0.40	29
14	10	6.80 - 5.40	-0.70 & -1.20	30
15	12	5.50 - 5.20	6.06	31
16	8	5.70		32
17	10	5.70		32
10	14	8.67 - 7.98	-4.25	24
12	16	-3.19 to -3.96	21.00	25
18	14	7.88	-0.61	33
19	14	9.50 - 8.70	-3.75 & -3.80	34
20	14	8.77 - 8.04	-4.53	35
21	2	11.10		36

Various electronic factors influence the experimentally observed proton chemical shifts of real molecules. The examples illustrate shielding and deshielding effects in conjugated systems.

Archetypal benzene **1** has its proton NMR resonance at δ 7.27, 1.5 ppm downfield of typical olefins. This serves as a benchmark, implying that an additional deshielding effect is operative in benzene, the ring current. Aromatic cyclopropenium, **21**, has an additional deshielding factor. The cation effect on deshielding in **21** is much stronger than the aromatic effect, and the proton resonance is strongly shifted, to δ 11.1. Contrasting effects of charge are displayed by cyclopentadienide **2**, and tropylium **3**, in comparison to **1**. Increased charge density shields **2**, almost perfectly offsetting the aromatic deshielding, to result in δ ~ 5.5. In **3**, the reduced charge density acts in concert with the aromatic deshielding, resulting in a strong downfield shift, to δ ~ 9.2.

Structural rigidity in the isoelectronic annulenes **10** and **20** contributes to a large shielding effect. The internal methyl proton resonances of **10** and **20** at δ -4.25 and δ -4.53 respectively, appear to be similarly affected ($\Delta\delta$ ~ 5 ppm) as are the internal protons of **18** at δ -0.61, but the internal methyls of **10** and **20** and the internal alkene protons of **18** are not similarly located. The annulene **18** is much less rigid than **10** and **20**, resulting in reduced π overlap, and ultimately less induced magnetic field. Annulenes **10** and **20** have near planar peripheries, with near optimal π overlap, and thus high magnetically induced shielding. Deviation from planarity reduces ring current. In bridged annulene **11**, the

methano bridge protons resonate at δ -0.52, implying reduced shielding and reduced ring current, resulting from a bent periphery. The bending of the periphery of **11**, τ_{max}, is ~35° [16b].

Examples **16** and **17** show how effects can oppose one another. Cyclooctatetraene **16** shows a typical olefin proton resonance at δ 5.70. The molecule **16** is not planar, but tub shaped. Adding two electrons to the π system results in the planar aromatic **17**. The expected aromatic deshielding effect is perfectly balanced by the shielding effect of negative charge, to give **17** the same proton resonance as **16**.

Paratropic ring current effects are illustrated in **15** and **12**. Nearly planar **15** shows a bridge methano proton resonance at δ 6.06, strongly deshielded from typical allylic methylene signals ~ δ 2. The more rigid planar paratropic system **12** shows a very strongly deshielded internal methyl proton resonance at δ 21.

Heterocycles exhibit additional effects. Pyridine **4** displays proton signals ~δ 8.5 - 7.46, downfield of those of pyrrole **5**, at ~δ 7.7 - 6.05. Pyridine is more aromatic/delocalized than pyrrole. Pyridine behaves more like an electron poor deactivated aromatic (downfield shift) while pyrrole behaves more as an activated, electron rich (upfield shift) aromatic. Differences are also seen in polarization. Pyridine is polarized toward nitrogen, while pyrrole is polarized away from nitrogen. The chemical shift differences have been attributed to the dipole differences. Since the respective aromatic characters and dipoles result

from the molecular orbital structures of each, a more appropriate explanation would derive from the molecular orbital descriptions of the systems.

Additional influences of hetero substitution may be seen in **13** and **19**, compared to **11**, and **10** respectively.

Examples above show that the shielding or deshielding of protons resulting from ring current is not the only influence on chemical shift differences. To address this, Vogler has put forward a linear equation (1), relating observed shielding (σ) to the sum of ring current, and other factors[37].

(1) $$\sigma = \sigma^{RC} + \sigma^{LA} + \sigma_{\mu}^{\circ} + \sigma_{v}^{q}.$$

σ^{RC} = shielding from ring current

σ^{LA} = shielding from local anisotropy

σ_{μ}° = zero of chemical shift scale.

σ_{v}^{q} = shielding from excess π electron density.

Thus extreme caution is required in the interpretation of chemical shifts in annulenes. In charged systems and heterocycles, shielding from local anisotropy and from perturbation in π electron density are of equal import[38]. With these caveats in mind, the diatropicity of annulenes are of considerable interest in the estimation of aromaticity.

Magnetic susceptibility anisotropy is another possible arbiter of aromaticity, though again, calculation is required, and reference sets must be chosen.

All the criteria of aromaticity are held to stem from the fundamental preconditions (above), and a fundamental theoretic relationship between the properties would be desirable. In 1978, Haddon proposed that resonance energy (RE) is proportional to ring current (RC)[40];

(2) $RE = \pi^2(RC)/3S$ or $RC = 3S(RE)/\pi^2$ where S is ring area.

This relationship would appear to allow the various aromaticity scales to be united, as magnetic properties should depend on ring current. However, for wider classes of aromatics, including heterocycles, some discussion has arisen in the literature as to whether aromaticity is really unified. Schleyer has demonstrated quantitative relation between magnetic, energetic and geometric criteria for a specific set of five membered heterocycles[17,41], while Katritzky has demonstrated that for a representative set in which the number of heteroatoms varies, no linear relationship holds between the various criteria[42].

1.1.3 Estimation of Relative Aromaticity: the Mitchell Method.

In developing a hypothetical aromaticity scale, whether unified or multidimensional, one must first show that the scale is well behaved for the most traditional aromatics, the benzenoid and annulene hydrocarbons. The most desirable scale would provide a direct instrumental value as a function of aromaticity, with a minimum of calculation. Fusion of annulenes actually helps us solve the problem. The relative contributions of the ring currents of the annelated fragments to the overall ring current pattern of the fused system depends on the resonance energies of the fragments[40,43]. Thus we can use the effects of one

ring current to tell us about an annelated ring current, and in turn it's resonance energy.

These concepts have been used to develop an experimental aromaticity scale[44], based on the bridged [14]annulene dimethyldihydropyrene **10**[14]. This planar system with aliphatic internal methyl groups held rigidly close to the center of a strongly shielding diatropic ring current has proven very sensitive and responsive to annelated aromatic fragments, and of limited response to singly bound substituents. That is, in the Vogler equation, (1), the contribution for local anisotropy is small compared to the term for ring current, and to a close approximation, may be neglected. Internal methyl proton resonances for the parent compound are at δ -4.25, while the [a]-benzannelated derivative **22** has these at δ -1.62, an impressive shift of 2.63 ppm. The 2-phenyl derivative **23** has corresponding signals at δ -4.03 and -4.00, a rather small shift from **10**. The [e]-fused derivative **24** had an internal methyl proton chemical shift of δ -1.85, close to that of **22**. Detailed study of the proton NMR chemical shifts of internal methyl resonances, distant external ring protons, and $^3J_{H,H}$ coupling constants, shows strong correlations for a series of [a]-annelated derivatives of **10**. These correlations allow the estimation of the aromaticity of fused systems relative to benzene, and that is the essence of the Mitchell method of estimating aromaticity. Gratifying agreement of the estimated aromaticities with Dewar resonance energies[45] has prompted analogous investigation of less well established aromaticities, such as those of cyclopentadienide[46] and biphenylene[47]. Positive results in these cases were obtained. Metal complexed

annelated systems formed the basis of a more recent study, which indicated that metal complexation greatly increased the bond localizing ability of annelated fragments[48].

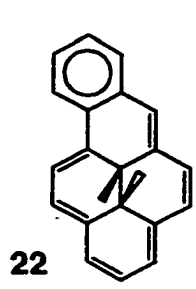

22

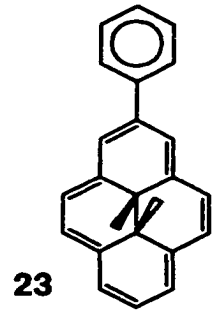

23

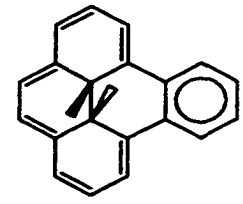

24

Theoretically, the generality of results obtained in the [a]-fused DMDHP systems above, should extend to the [e]-fused DMDHP systems. Impetus to explore such [e]-fused systems actually derives from a second intriguing behaviour displayed by DMDHPs; they are photochromic. This thesis in part presents results in both the investigation of aromaticity in [e]-annelated DMDHP systems, and the photochromism of such systems.

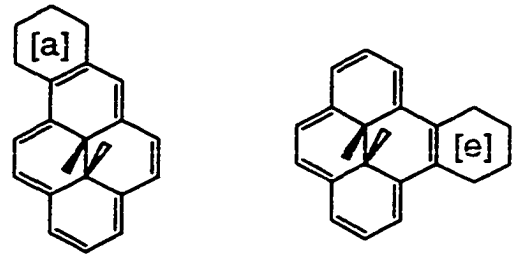

Positions and labels for [a] and [e] fused DMDHP.

1.2 Photochromism[49]

Photochromism is a property of a system signifying that the electronic spectrum of the system alters, on absorption of light. To our eye, this may appear as a color change or as a greying or lightening. A subset of photochromic molecules are termed bistable optical switches. For these, two different ground state forms or structures exist, which may be interconverted by light of different wavelengths, with no thermal interconversion of the isomers. Some types show a thermal back reaction also. These are called t - type. Those with photoisomerism, but no thermal return are termed p - type. Useful lifetime depends on function. Optical data storage would require indefinite longevity for both isomers. On the other hand, some signal transductions and some switching operations do not require long lifetimes .

1.2.1 Types of Photochromic Molecules

Molecular photoswitches may be conveniently classed according to the photoisomerization reaction involved;

1) E/Z (trans - cis) isomerization.
2) electrocyclization.
3) heterolysis.
4) tautomerism.
5) homolysis.

The most commonly encountered photoswitches in modern studies are 1) the azobenzenes[50] **25**, 2) the diarylethenes (heteroaryl) [51] **26**, 3) the spiropyrans[52] **27**, and 4) bacteriorhodopsin[53]. Other types are also used , such as fulgides[54], spirooxazines[52], and dianthracenes[55], but the three above have the lion's share of studies. Of the synthetic switches, currently some members of the dithienylethenes/diaryethenes[51] and fulgides[54] are closest to ideal as far as thermal irreversibility (p - type) at ordinary temperature. The photochromic ability of coronene is not due to any of the above mechanisms, but derives from the triplet form having more light absorption in the visible wavelengths[56].

Azobenzenes

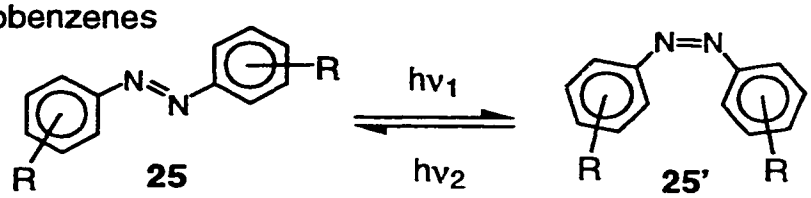

Dithienylethenes

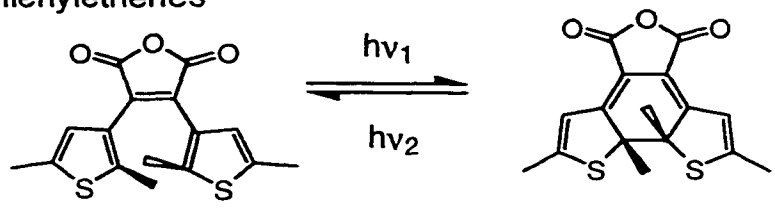

26
colorless

26'
colored

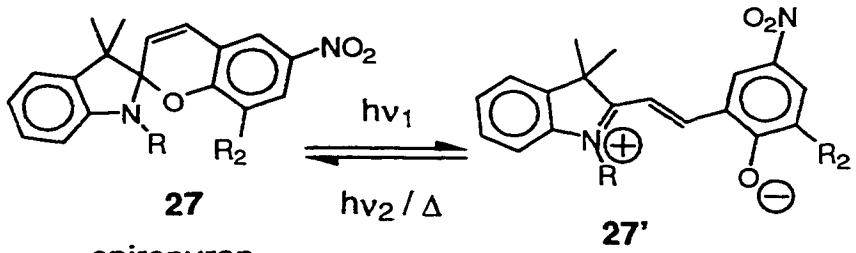

27
spiropyran
colorless

27'
merocyanine
colored

Photochromic molecules which show reversibility with stimuli other than light include electronic (redox), ionic, and proton gated systems.

A major concern in all photoswitches is fatigue resistance, in cycling between the photoisomers. The dithienylethenes have members with over 10^4 cycles capability. Tautomerism (proton shift) switches also have good stability, in excess of 10^4 - 10^5 cycles. Bacteriorhodopsin may be cycled > ~ 10^6 times.

1.2.2 The Photochromism of DMDHPs

An intriguing aspect of dimethyldihydropyrene **10** (DMDHP) is its photochromic behaviour[57]. DMDHP belongs to the second class of bistable optical switches, it is an electrocyclization photoswitch. The photoisomerization of DMDHP to metacyclophanediene (MCD) **10'** is related to the dihydrophenanthrene - *cis*-stilbene photosystem[58], but has some advantages. Dehydrogenation and E/Z isomerization mitigate against the *cis*-stilbene photosystem. Methyl substitution solves the dehydrogenation problem for dihydrophenanthrene, and cyclic fusion of the ethene linker prohibits E/Z isomerization. The very rapid thermal return is solved by turning to hetero diarylethenes. Irie's dithienylethenes are thermally irreversible at ordinary temperatures[51].

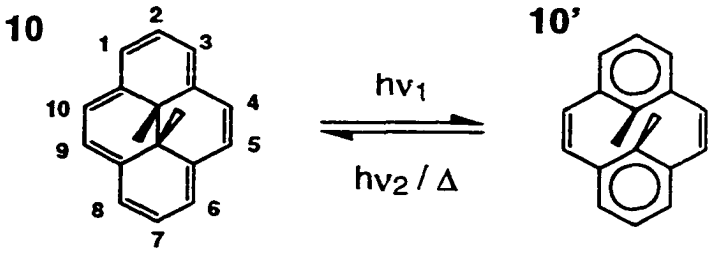

emerald green colorless

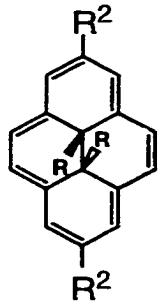

28 $R = R^2 = H$

29 $R = CH_3$, $R^2 = C(CH_3)_3$

Although the parent 10b,10c-dihydropyrene, **28**, readily oxidizes to pyrene, DMDHP suffers from neither dehydrogenation, nor E/Z isomerization. The photodecoloration/opening reaction for DMDHP **10** has a quantum yield $\phi = 0.015$ to 0.02, at 466 nm[59,60], and the thermal coloration/closing reaction rate of **10'** is $k = 0.0010\ min^{-1}$ at 30 °C[59].

The doubly alkyl substituted 2,7-di-*t*-butyl derivative of DMDHP, **29**, has a quantum yield of decoloration/opening of $\phi = 0.002$, about an order of magnitude smaller than for DMDHP[60]. The thermal coloration rate of **29'** to **29** is k = ~0.0008 min^{-1} at 30 °C[59], slightly slower than that of DMDHP **10**. The decreased quantum yield for photobleaching is comprehensible, as the photophysical parameters of aromatics are often detrimentally impacted by alkyl groups, like *t*-butyl. These alkyl groups often lead to increased rates of non-radiative decay from the first excited singlet state, and this parasitizes all competing photophysical processes. The photoisomers of the alkylated derivatives **30** and **31** has the same coloration rates as **10'**.

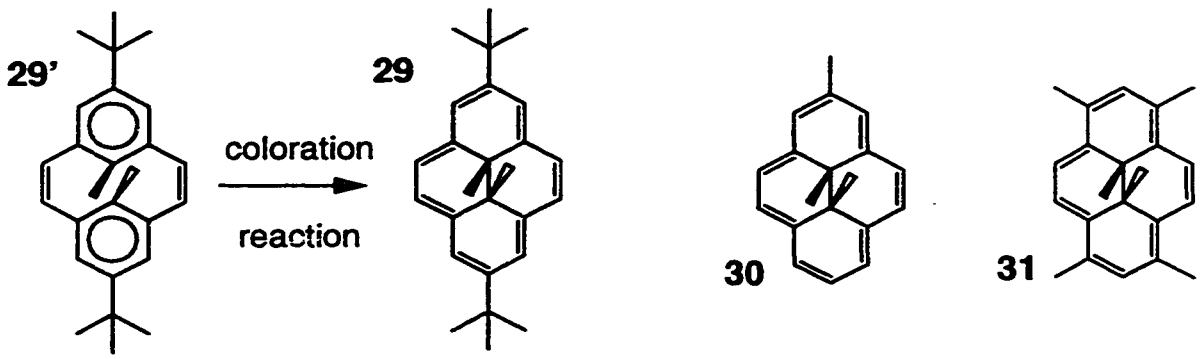

Substituent effects on the thermal return reaction rate have shown weak trends[59,60], though no Hammett substituent correlation has been found. Substitution of **29** at the 4 position with electron withdrawing groups decreased the thermal coloration rate. For example, the photoisomers of **32**, **33**, **34** and **35**, respectively, have coloration rates of 0.0018, 0.0028, 0.0016, and 0.0012 min^{-1} at 40 °C, while **10'** has a coloration rate of 0.0031 min^{-1} at 40 °C.

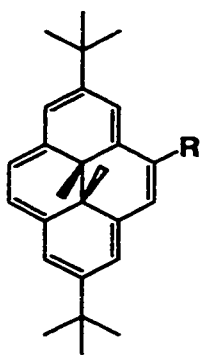

32 R = NO_2
33 R = COC_6H_5
34 R = $COCH_3$
35 R = COC_2H_5

Increasing the size of the alkyl substituents within the cavity of the π-electron cloud has little effect on the quantum yield of opening, but actually increases the rates of coloration[59,60]. For example, coloration rates for the

photoisomers of **36**, **37**, and **38** are 0.0044, 0.0047, and 0.012 min^{-1} at 40 °C. This increase possibly stems from increased repulsion between the larger alkyl groups and the stepped MCD benzene rings. Closure/coloration relieves this slightly, as the internal groups project away from the plane of the molecule. The thermal stability of systems with larger alkyl groups within the π electron cavity decreases. The larger alkyl groups migrate more readily, destroying the electronic structure of the dihydropyrene.

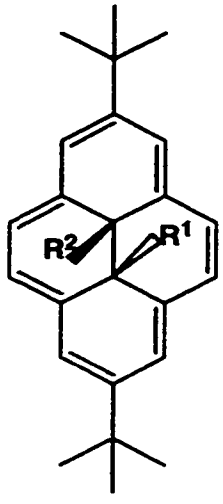

36 $R^1 = CH_3$, $R^2 = C_2H_5$

37 $R^1 = CH_3$, $R^2 = CH_2Br$

38 $R^1 = R^2 = C_2H_5$

Multiple substitution has also been studied[59,60], with results comparable to single substitution. Perhaps the most striking behavior is seen in the donor acceptor system of the 2-acetamido-7-formyl derivative of DMDHP, **39**. The photodecoloration/opening quantum yield (0.17) approaches those for DMDHPs substituted in the 2 position with an electron acceptor, as might be expected. The formyl and benzoyl derivatives, **40** and **41**, have quantum yields

respectively of 0.26 and 0.25. The coloration reaction of the photoisomer of **39**, however, is very fast at k = 1.59 min^{-1} at 30 °C, for a half life of only 26 seconds. The half life for the coloration of MCD to DMDHP is ~11.6 hours, while the photoisomer of **40** has a coloration half life of ~13 minutes.

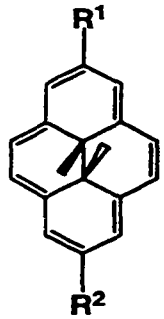

39 $R^1 = NHCOCH_3$, $R^2 = CHO$

40 $R^1 = CHO$, $R^2 = H$

41 $R^1 = COC_5H_6$, $R^2 = H$

An interesting hetero analogue is the azapyrene **19**[34]. Both **19** and **39** readily photobleach, to the respective metacyclophanedienes **19'** and **39'**. The thermal dark reaction is quite slow at room temperature, ~0.00020 min^{-1} for **19'** to **19**. This dark reaction is proton gated, as protonation alters the rate by four orders of magnitude to ~4.8 min^{-1} at 17 °C, for **39'** to **39**, one of the fastest colorizing non-annelated MCDs known.

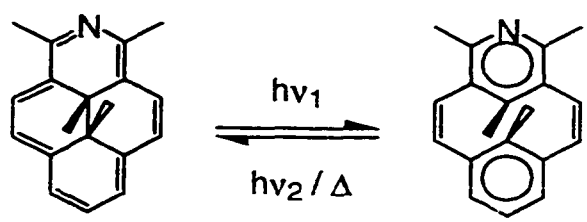

19 **19'**

42 = **19** :HCl **42'** = **19'**:HCl

Annelation of the DMDHP/MCD nucleus has large consequences in quantum yields and thermal return rates. The [a]-benzannelated dihydropyrene **22** shows no substantial photobleaching (< ~4%),[61] while the [e]-benzo analogue **24** is readily photodecolorized[61] and has a slow coloration rate of ~0.00078 min^{-1} at 22 °C. Bis annelation shows differential effects. Dibenzo derivative **43** does not photobleach significantly[61], while the [e,l]-dibenzo system **44** actually has the MCD form as the thermally stable form[62]. The green [e,l]-dibenzodihydropyrene **44'** is obtained on irradiation of **44** at reduced temperatures. Thermal decoloration is quite rapid, 0.256 min^{-1} at -10 °C. Presumably, **44** is more stable than **44'**, because of the greater degree of resonance stabilization in four benzene rings compared to that in the dihydropyrene system **44'**.

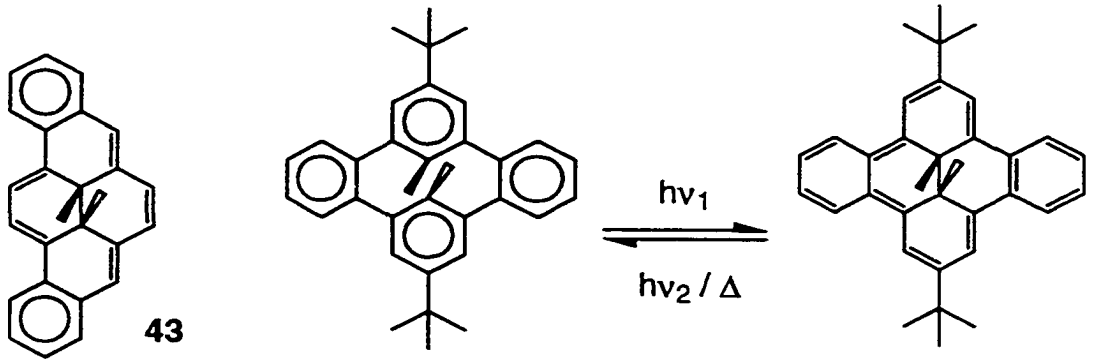

43 **44** **44'**

Introduction of strain tips the balance in favor of the MCD forms for the dimethylarene annelated MCDs **45, 46, 47** [63]. The dihydropyrene forms **45', 46', 47'**, are formed on irradiation with UV followed by evaporation of solvent.

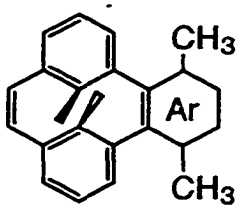

45 Ar = benzo

46 Ar = 2,3-naphtho

47 Ar = 2,3-anthro

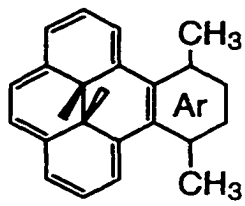

45' Ar = benzo

46' Ar = 2,3-naphtho

47' Ar = 2,3-anthro

Systems with two DMDHPs (**48** and **49**) have also been obtained[64]. The photochemistry of these has not been reported.

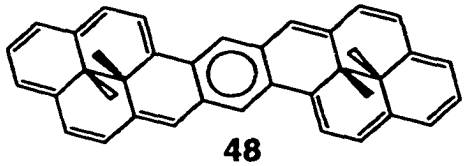

48

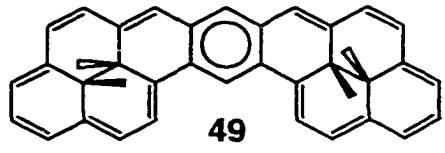

49

1.3 Thesis Research Objectives

In light of the results of the efforts of previous investigators, briefly introduced above, and with the relative ease of obtaining the 2,7-di- *t*-butyldimethyldihydropyrene **29**[65], it has become clear that a structure function study of unstrained [e]-arene annelated derivatives of **29** should be undertaken. The very slow thermal coloration rate for the photoisomer of **24** prompts this. In designing, testing, and optimizing systems based on the DMDHP to MCD photoisomerization, [e]-annelated derivatives of **29** would be a most economical choice since **29** is much more readily obtained than the parent DMDHP **10**. Previous [e]-annelated derivatives of DMDHP **10** (without *t*-butyls) have been made through a tedious low yielding route requiring the synthesis and cyclization of teraryls.

The goals of this thesis research are thus;

- to investigate and try to develop efficient routes to [e]-annelated derivatives of DMDHP **29**;
- to observe aromaticity effects of [e]-annelated derivatives of **29** as displayed by the NMR probe behaviour of the DMDHP core;
- to test the photoisomerizations and thermal coloration rates of the [e]-annelated DMDHPs obtained.

Chapter two Synthesis

2.1 Introduction

A practical outcome of the study of theoretically interesting molecules has been the development of efficient routes to obtaining those molecules. One such route which has benefited the study of novel conjugated aromatics, and DMDHPs in particular, is the thiacyclophane / dithiacyclophane method[66].

This method requires formation of a cyclic thioether (thiacyclophane) typically by dilution methods. In subsequent steps, the sulfur is extruded to form a carbon-carbon bond. This is achieved by first contracting the C-S-C bond and then eliminating the sulfur bearing residue. This is illustrated below in Scheme 1 for the synthesis of **10**.

All DMDHPs are prepared by synthesis of cyclophanedienes. The DMDHP is obtained by valence isomerization, of the cyclophanediene synthesized.

SCHEME 1

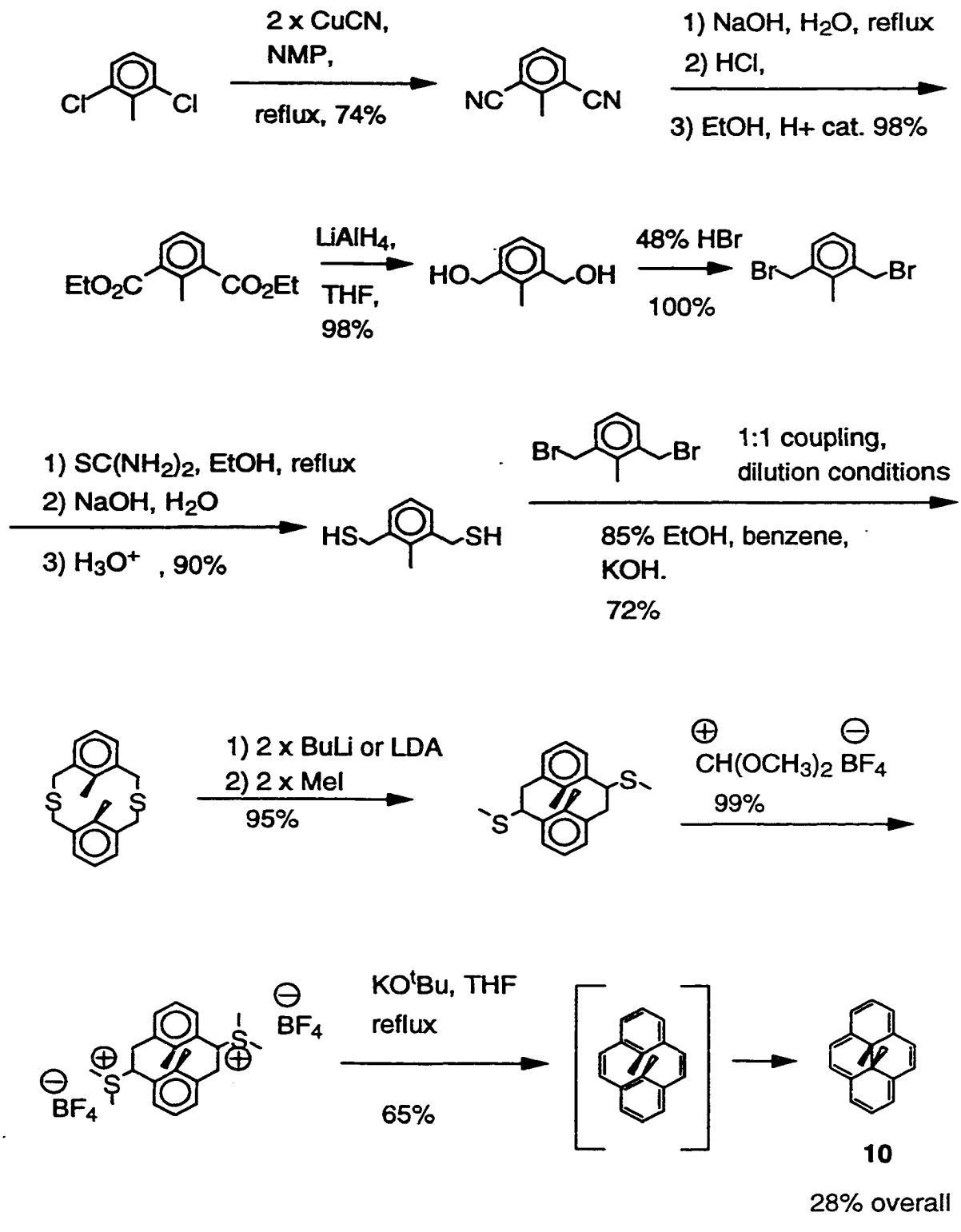
2 x CuCN,
NMP,
reflux, 74%
1) NaOH, H2O, reflux
2) HCl,
3) EtOH, H+ cat. 98%
LiAlH4,
THF,
98%
48% HBr
100%
1) SC(NH2)2, EtOH, reflux
2) NaOH, H2O
3) H3O+ , 90%
1:1 coupling,
dilution conditions
85% EtOH, benzene,
KOH.
72%
1) 2 x BuLi or LDA
2) 2 x MeI
95%
CH(OCH3)2 BF4
99%
KOtBu, THF
reflux
65%
10
28% overall

For [e]-annelated DMDHPs, a variation of this method begins with formation of a teraryl, which is then transformed to a thiacyclophane in several steps[44a, 62, 67]. The final product is obtained analogous to **10**, by extrusion, and ultimately elimination of sulfur.

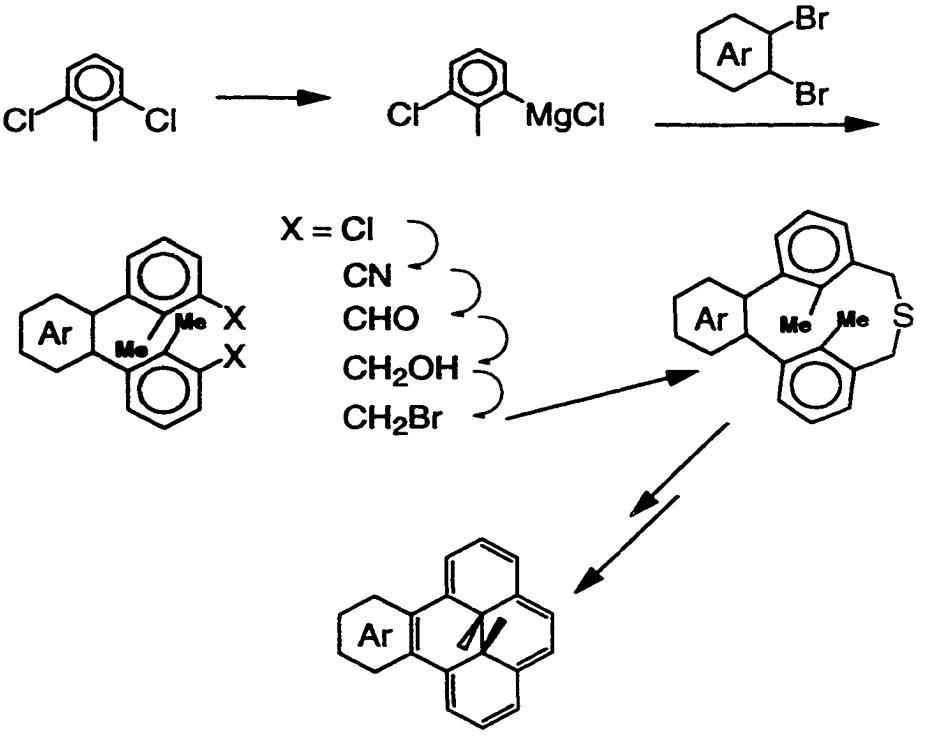

[e]-annelated DMDHP

Many [a]-annelated DMDHPs, and polysubstituted DMDHPs have been synthesized using the same core reaction sequences, as in Scheme 1, previous page. One difficulty has been the production of the appropriate 2,6-bis(bromomethyl)toluene derivative. Once this has been obtained, the thiacyclophane route has been usually fairly straightforward.

Alternatively, substituted or annelated DMDHPs have been obtained after producing the DMDHP core **10** or an analogue.

Diels-Alder cycloaddition has proven an excellent method to obtain annelated aromatics. Previous work has shown that the convergent modular approach to forming annelated DMDHPs from a preformed DMDHP nucleus to be of particular value, using aryne-furan cycloadditions[44a,47]. Retrosynthesis shows the DMDHP fragment may be supplied as either an aryne equivalent or an isoarenefuran. This is illustrated for [e]-annelated derivatives of **29** in Scheme 2, next page. Both strategies have been successfully employed in obtaining [a], [a,h], [a,i], and [e,l] DMDHP adducts. In the past, [e]-fused DMDHP Diels-Alder adducts of the type we desired have been obtained as side products from [e,l] syntheses. Aryne generation by elimination of the elements of HBr using $NaNH_2$, and by the metallation/metal halide elimination reaction have both been successful on DMDHPs.

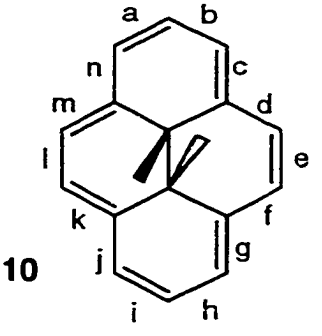

10

Position labels for annelated derivatives of **10**.

2.2 Synthesis of [e] systems

Scheme 2

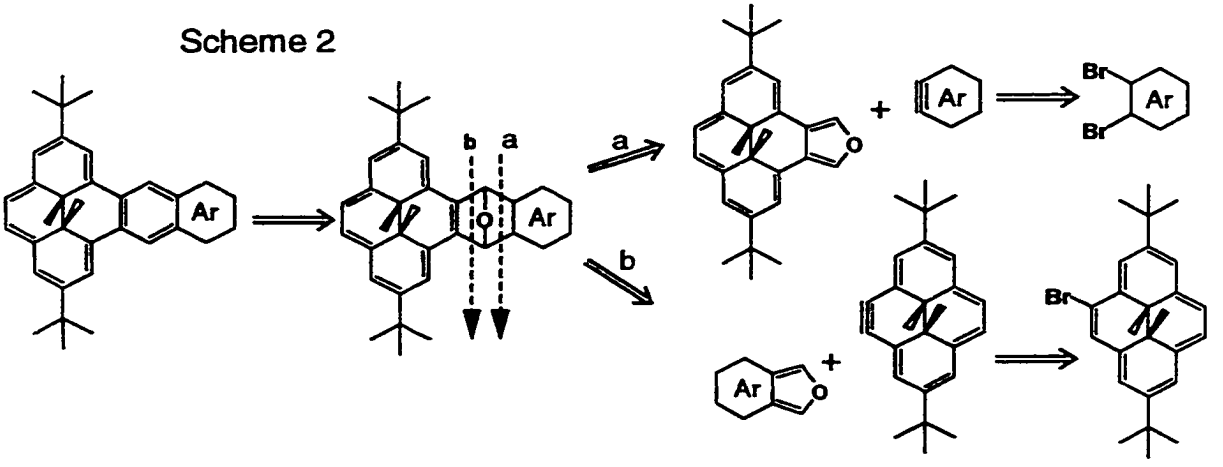

A most convenient and expedient route into the [e]-annelated DMDHPs would be from DMDHP **29**, as reactivity is confined to lateral 4 and 5 (and 9 and 10) positions, because the 2,7 positions are blocked by *t*-butyl groups. The most convenient substrate to apply a Diels - Alder approach for this would be the 4-bromo-2,7-di-*t*-butyldihydropyrene **50**.

2.2.1 Bromination

The DMDHP **29** brominates smoothly with N-bromosuccimide in dimethylformamide with dichloromethane[62,68], (NBS/DMF - CH_2Cl_2), to form the 4-bromo derivative **50** in excellent yield, ~92%. This was confirmed by the proton NMR spectrum by two singlets at δ -3.93 and -3.95, indicating that the product was a DMDHP, and that the symmetry had been eliminated. Integration showed

seven aromatic hydrogens, to six internal methyl hydrogens, and eighteen hydrogens for the two *t*-butyl groups, all as expected. Carbon NMR spectroscopy showed all expected carbons for $C_{26}H_{31}Br$. Mass spectrometry (methane CI) supported the product identity, with an isotopic pattern for a monobromo hydrocarbon, with *m/z* 422 (MH^+,^{79}Br) and 424 (MH^+,^{81}Br). The impurity in the final product was ~3% each of **29** and dibromide **51**, as shown by NMR spectroscopy. The amounts of these other DMDHPs in the product decreased with lower reaction temperatures. Best results were obtained at -78 °C, although for most purposes 0 °C was sufficient. Product purity also decreased with increasing concentration of the DMDHP precursor under the reaction conditions. Dilution improved the purity of the product.

Full characterization for all compounds is given in the experimental section. Only significant data is reported here as used for product identification.

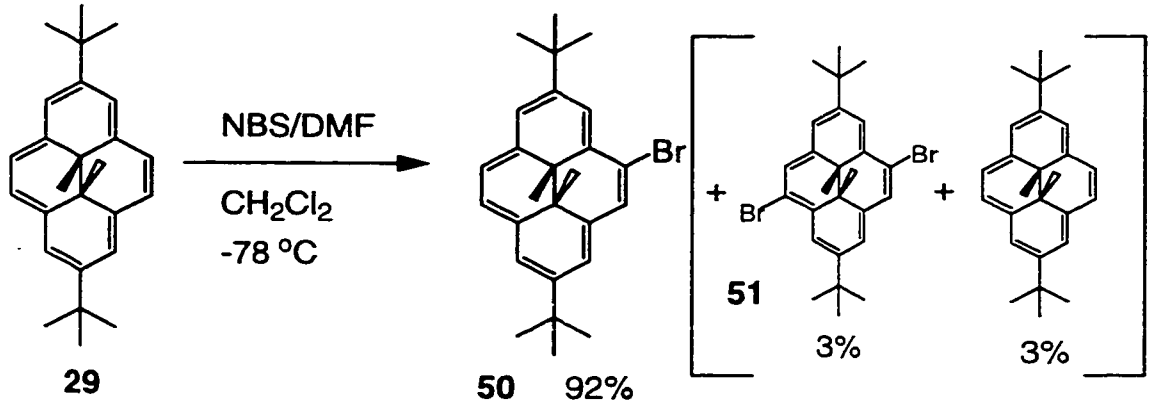

2.2.2 Aryne reaction of **50** and benzannelation

Reaction of bromide **50** with furan under sodium amide conditions in THF, gave the 4,5-didehydropyrene aryne adduct with furan, **52**, in 86% yield. The adduct **52** was a dark green microcrystalline powder which lost oxygen on melting, and also slowly in solution in chloroform, or dichloromethane. Solutions of **52** in THF or benzene were relatively stable. Adduct **52** had limited solubility in hexane. Product identity was confirmed in the proton NMR spectrum by two singlets at δ -3.18 and -3.42 indicating the presence of a non-symmetrical DMDHP. The ethene bridge of the fused fragment was indicated by signals at δ 7.13 - 6.98, and the bridgehead ether hydrogens were at δ 6.49 - 6.45. Carbon NMR spectroscopy showed all expected carbons for $C_{30}H_{34}O$, with two ether carbons at δ 81.6 and 81.3. Mass spectrometry (methane CI) supported the product identity, showing MH+ *m/z* 411. NOE experiments showed that the ethene bridge was closer in space to the internal methyl with a proton resonance at δ -3.42, that is, they were on the same face of the molecule.

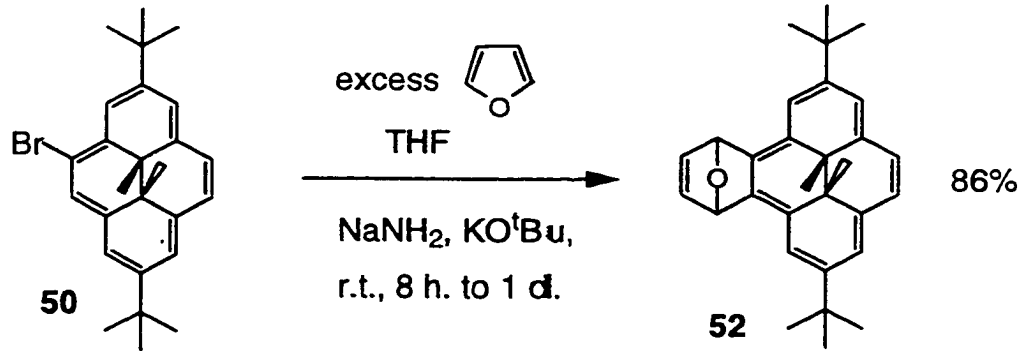

A variety of reagents have been used to aromatize Diels - Alder adduct analogues of **52** by deoxygenation[69]. The use of $Fe_2(CO)_9$ was introduced by Wege[70] for this purpose. The desired benzo[e]dimethyldihydropyrene **53** was obtained by reaction of **52** with $Fe_2(CO)_9$ in refluxing benzene for one to two hours in the dark. After chromatography, **53** was obtained as an intense red crystalline solid, mp 172 °C. Dihydropyrene **53** was readily soluble in chloroform, benzene, THF, dichloromethane, or hexane, forming strawberry red solutions which oxidized very slowly under air. These solutions bleached on exposure to light, to form the photoisomeric metacyclophanediene **53'** which was virtually colorless. For this reason, chromatography of **53**, reactions with **53**, and general handling of **53** (such as for NMR spectroscopy), were best accomplished in the dark or under subdued light. Dihydropyrene **53** was reobtained by exposure of **53'** to 350 nm UV light, or by heating in solution.

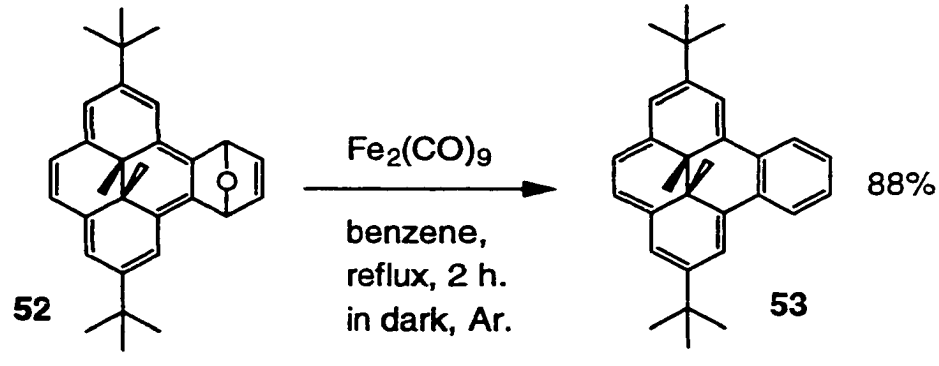

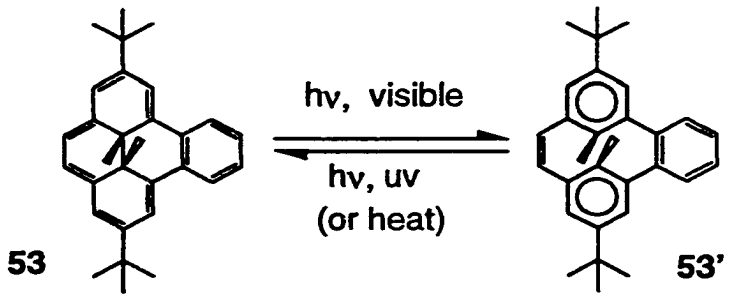

Characterization of the product confirmed the identity as the benzo[e]dimethyldihydropyrene **53**. Proton NMR spectroscopy showed a single resonance at δ -1.58, very near the corresponding signals for the internal methyl proton resonances for benzo[a]dimethyldihydropyrene **22**[61] and benzo[e]-dimethyldihydropyrene **24**[62], compounds previously obtained. An AA'XX' pattern was evident, as expected for the benzo fragment. The proton NMR spectrum also appeared to confirm the expected C_2 symmetry of the molecule, with one signal for the protons of the *t*-butyl groups and one signal for the protons of the internal methyls. Also, the six aromatic protons showed three resonances, of two protons each, in keeping with the symmetry. Two of the resonances were coupled to one another, as shown in a COSY NMR experiment, with coupling constant 1.0 Hz, appropriate for meta coupling. The pair of protons vicinal to the *t*-butyl groups would show just such a meta coupling pattern. The remaining two protons were a singlet .

The carbon NMR spectrum showed 13 resonances as expected, for a molecule with C_2 symmetry. Mass spectrometry (methane CI) supported the identity of **53**, with *m/z* 394 (M+.) and 395 (MH+). Correct elemental analysis was obtained.

2.2.3 Isoarenefuran formation

Successful obtainment of **52** admitted the possibility of forming an isoarenefuran using Warrener's[71] mild, facile method to such compounds, using the dipyridyltetrazine[72] **54** to remove the ethene bridge. In the event, reaction of **52** with **54** in THF in the dark gave the grape purple isoarenefuran **55** in 90 % yield. The crystalline solid **55** was stable under inert atmosphere, in pleasant contrast to the [a]-fused analogue, which was less stable[64].

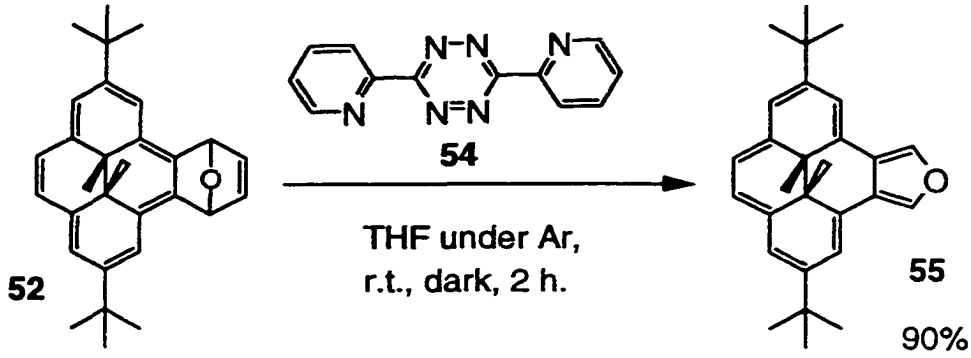

The facile method of obtaining isoarenefuran **55** was slightly unusual, in that room temperature reaction of **52** with tetrazine **54** directly resulted in **55**. Often such reactions result in an intermediate Diels - Alder adduct, which is thermolyzed above room temperature, to yield the isoarenefuran.

Isoarenefurans are usually highly reactive[73]. Special care must be exercised to obtain the simplest member of the series, isobenzofuran, to avoid

polymerization, oxidation, or acid catalyzed additions. Isoarenefuran **55** decomposed on alumina or silica gel chromatography agents, if long columns or long elution times were used. Short filtration columns, with basic chromatography agents, helped to optimize yields. Isoarenefuran **55** also oxidized, and so inert atmospheres were best used in handling, though short exposure to air did not materially reduce yields. Isoarenefuran **55** was best prepared, purified, used in reactions, and handled generally (for NMR spectroscopy and the like) in the dark or under subdued light.

The identity of the isoarenefuran product **55** was supported both spectroscopically, and chemically. Proton NMR spectroscopy supported C_2 symmetry, as *t*-butyl protons and internal methyl protons each showed only one resonance. The remaining aryl protons signals occured in only four peaks, of equal integrations, two protons each. Carbon NMR spectroscopy also showed the symmetry of the molecule, with all resonances at appropriate chemical shifts for the structure.

Mass spectrometry (methane CI) confirmed the identity of **55**, with *m/z* 384 (M+.) and 385(MH+). Elemental analysis also supported the theoretical mass composition.

The chemical reactivity of **55** also confirmed the structure. Isoarenefuran **55** reacted virtually quantitatively in minutes with electron poor dienophiles like dimethyl acetylenedicarboxylate (DMAD) and fumaronitrile, to give dark green adducts with regenerated DMDHP chromophore. Isoarenefurans react rapidly

with just such electrophilic dienophiles[73]. These reactions are discussed further below.

With the isoarenefuran **55** successfully in hand, short syntheses of other annelated DMDHPs were possible.

2.2.4 Benzyne adduct of isoarenefuran **55**

The naphtho[e]dimethyldihydropyrene **57** was produced in two steps from **55**, using *o*-dibromobenzene as an aryne precursor. Isoarenefuran **55** reacted with *o*-dibromobenzene under *n*-butyllithium conditions in toluene at -40° . The course of the reaction was color indicated, as the initial intense purple solution passed through red brown to green brown and finally became green to signal the end of the reaction, in 16 minutes. This color change occured as the purple isoarenefuran chromophore was replaced by the DMDHP chromophore which is green. The epoxynaphthacene product, **56**, obtained in 85% yield, was isolated as a green crystalline solid which lost oxygen on heating, or in solution in chloroform.

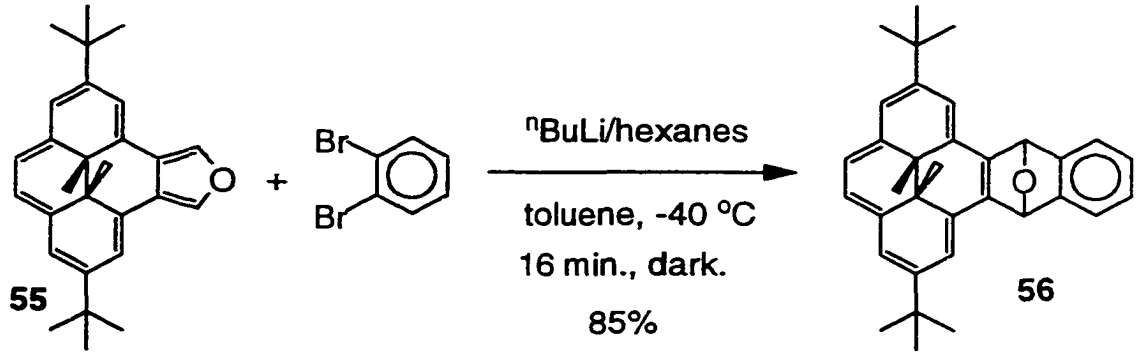

55 **56**

The structure of the adduct **56** was indicated by its proton NMR spectrum which showed the bridgehead hydrogens adjacent to the oxygen at δ 6.99 and 6.98, internal methyl protons at δ -3.49 (syn to oxygen) and -4.14, an AB pattern for the 4,5 hydrogens and four meta coupled doublets for the hydrogens adjacent to the *t*-butyl groups. These could be assigned by COSY/NOESY experiments. Likewise, the carbon NMR spectrum showed bridgehead ether carbons at δ 82.5 and 82.1. The mass spectrum (methane CI) supported the product identity with *m/z* 461 (MH+).

2.2.5 Naphthannelated DMDHP **57**

Preparative deoxygenation of **56** with $Fe_2(CO)_9$ in refluxing benzene gave the intense purple naphtho[e]dihydropyrene **57**. Naphthopyrene **57** was readily soluble in the usual organic solvents, and these solutions bleached on exposure to light, to give yellow solutions of the metacyclophanediene form, **57'**. The naphthannelated cyclophanediene **57'** was reconverted to **57** by illumination with 350 nm UV light, or by warming. It was best to handle **57** under subdued light or in the dark for preparations and purification.

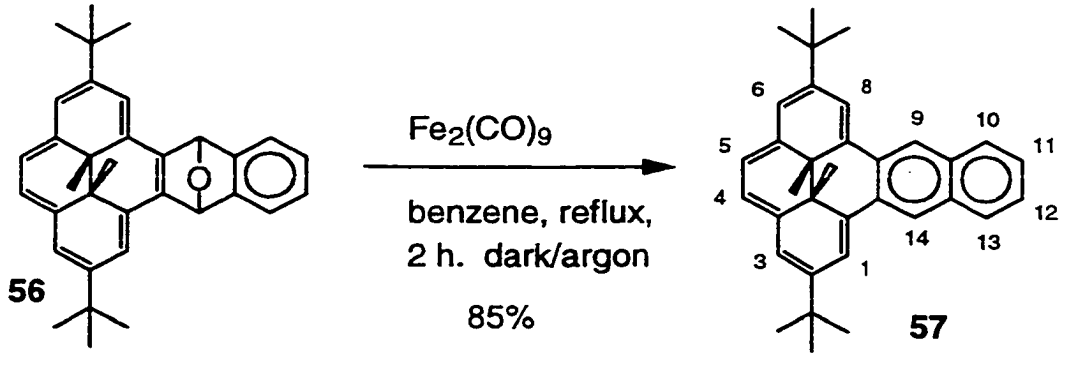

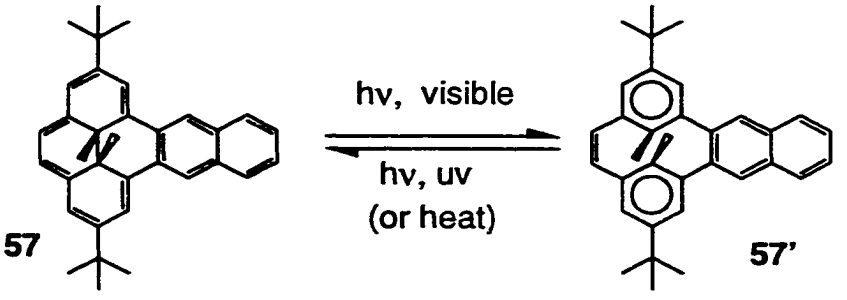

Compound **57** showed a single internal methyl peak at δ -0.54, a singlet for H-9 at δ 9.01 which showed NOESY interaction with H-10 and H-8. The latter at δ 8.00 showed COSY with H-6 at δ 6.90, which showed NOESY interaction to the singlet for H-4,5 at δ 6.66. Hydrogens 10 and 11 showed an AA'XX' pattern, with COSY interactions. The internal methyl proton signal reflected increased bond localization, as it was shifted 3.52 ppm down field, quite far from the corresponding signal of **29**.

Carbon NMR spectroscopy also supported C_2 symmetry, and had all resonances in positions expected for the structure. Mass spectrometry (methane CI) supported the molecular composition with *m/z* 445 (MH+), and elemental analysis was satisfactory.

2.2.6 Anthannelated DMDHP **59**

We were also able to obtain the epoxyanthro[e]dihydropyrene **58** by reaction of **55** with 2,3-dibromonaphthalene[74] and *n*-butyllithium, in toluene.

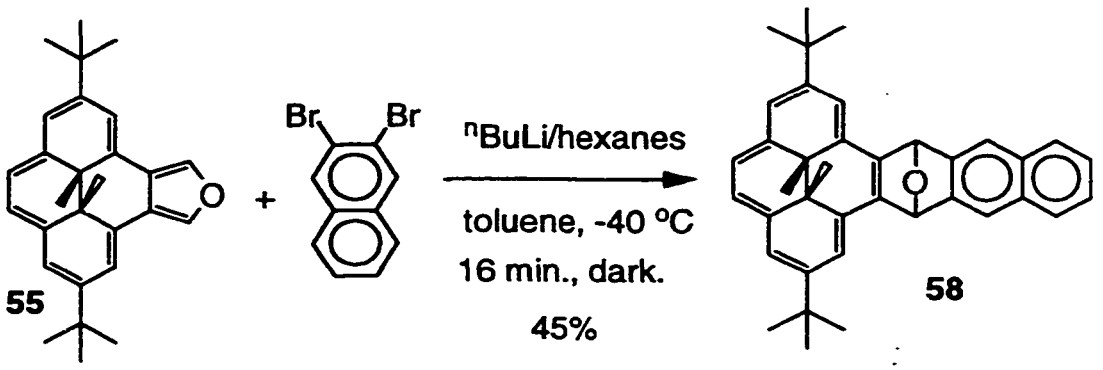

The proton NMR spectrum of the adduct **58** indicated two internal methyl proton resonances, at δ -3.62 and -4.30, positions similar to other Diels - Alder adducts obtained above. The proton spectrum showed the expected positions for all resonances, and integration of the proton signals indicated the correct ratio of hydrogens. Carbon NMR spectroscopy also supported the structure of **58** with the correct number and position of carbon resonances. Ether carbon peaks appeared at δ 82.35 and 81.90. Mass spectrometry of **58** was not possible by ordinary methane CI, as the sample would not volatilize. LSIMS showed *m/z* 510 (M+.) and 511(MH+). The fragmentation pattern from *m/z* 511(MH+) showed characteristic loss of methyl and *t*-butyl groups. Exact mass spectrometry (HRMS) indicated the correct atomic composition, with an exact mass of 510.2924; $C_{38}H_{38}O$ requires 510.2922.

The green adduct **58** was deoxygenated with $Fe_2(CO)_9$ in refluxing benzene, to give the blue green anthro[e]dihydropyrene **59**. This compound, like tetracene, was much more oxygen sensitive than previous analogues [5b]. Solutions of **59** did not bleach rapidly, under light. This was the first anthannelated DMDHP obtained without additional substituents on the fused anthracene.

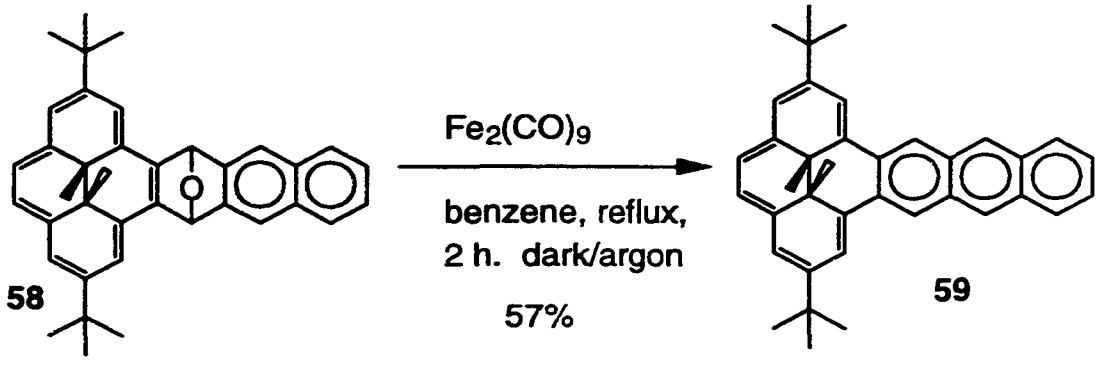

Proton NMR spectroscopy of the product **59** supported the product identity, showing an AA'XX' pattern, and single resonances each for internal methyl proton and *t*-butyl groups, appearing respectively at δ 0.004 and 1.41. Symmetry also was evident in the proton spectrum. Carbon NMR spectroscopy also showed the correct number and positions of carbon resonances expected for the structure. LSIMS showed peaks at *m/z* 494 (M+), 479(M+ - 15). An exact mass determination supported the formula of **59** as $C_{38}H_{38}$ with HRMS peak at 494.2971. The calculated exact mass was 494.2973.

2.2.7 Bis(dimethyldihydropyreno)chrysene **60**

The general method of aryne-furan cycloaddition opens many additional possibilities for obtaining arene annelated DMDHPs. The group of Dr Dibble at the University of Lethbridge has synthesized several different isoarenefurans,[75] one of which made possible the synthesis of the bis pyrene system **60**, with both DMDHPs [e]-fused to a chrysene linker. With the precursor **61**[75] supplied by Dr. Dibble, we embarked on the synthesis of this large aromatic system, **60.**

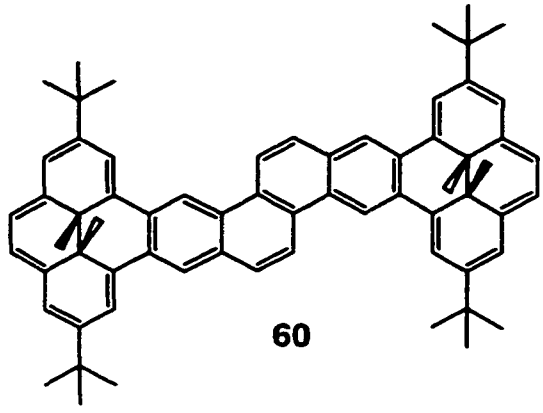

60

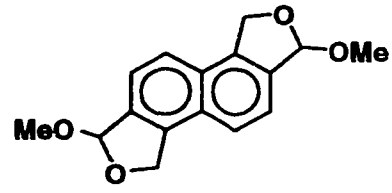

61

The acetal **61** eliminated two equivalents methanol by the action of strong bases, to generate the isoarenefuran **62**[75]. This intermediate was isolated and purified by filtration through basic alumina. Proton NMR spectroscopy confirmed the product **62**, by correspondence with the published chemical shifts.

Reaction of **62** with 2.7 equivalents of bromodihydropyrene **50** in THF using sodium amide conditions at room temperature over 24 hours gave a

surprisingly good yield (81 %) of the double aryne - isoarenefuran adduct **63**, as a mixture of isomers.

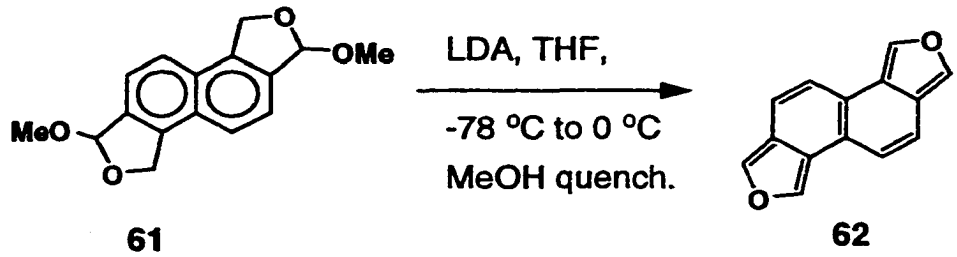

61 **62**

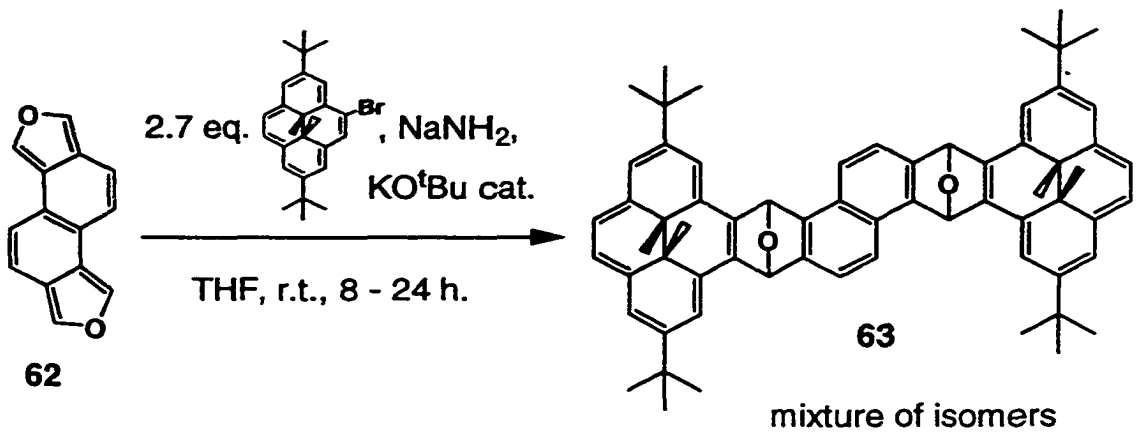

62 **63**

mixture of isomers

Characterization of **63** supported the expected structure. Proton NMR spectroscopy showed signals in the region δ -3 to -4, indicating asymmetric DMDHPs were present. Arene and *t*-butyl proton signals appeared as expected. Since the desired product was a double aryne - isoarenefuran adduct, the possibility existed of obtaining a mono Diels - Alder adduct, with the second isoarenefuran either remaining intact or reacting in some other manner. Such

compounds would still show DMDHP signals, but the structure would be incorrect. The combination of proton NMR spectroscopy and mass spectroscopy firmly supported the structure **63**. LSIMS revealed a strong peak at *m/z* 893 (MH+), and a fragmentation pattern showing loss of methyls and *t*-butyls from protonated **63**. HRMS confirmed with exact mass peak *m/z* 893.5268 (MH+). The calculated exact mass is 893.5219 (MH+).

The intermediate **63** deoxygenated smoothly with $Fe_2(CO)_9$ in refluxing benzene to give the bis(dimethyldihydropyreno)chrysene **60** in good yield, 82%.

The structure **60** was well supported by proton NMR spectroscopy, which showed an unresolved system at δ -0.29 (C_6D_6) for the internal methyl protons, arising from two isomers, **60a** and **60b**. All twenty arene protons were readily discerned in the NMR spectrum, with expected bay type protons at δ 10.35, 9.39, and 9.21 - 9.15. LSIMS indicated a molecular ion at *m/z* 860.5 (M+), and the fragmentation pattern, showed loss of methyl and *t*-butyl groups. HRMS for **63**, $C_{66}H_{68}$, indicated *m/z* 860.5323, and the calculated exact mass is 860.5321, for (M+.).

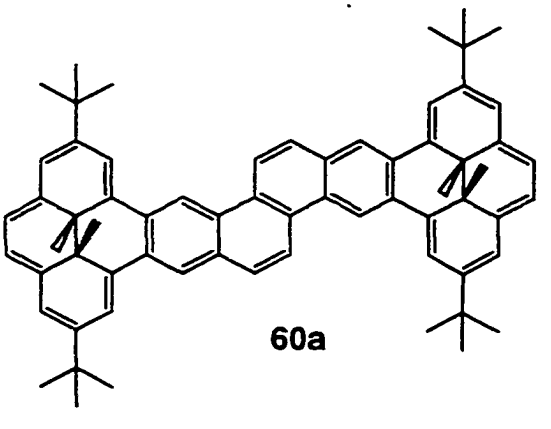

60a

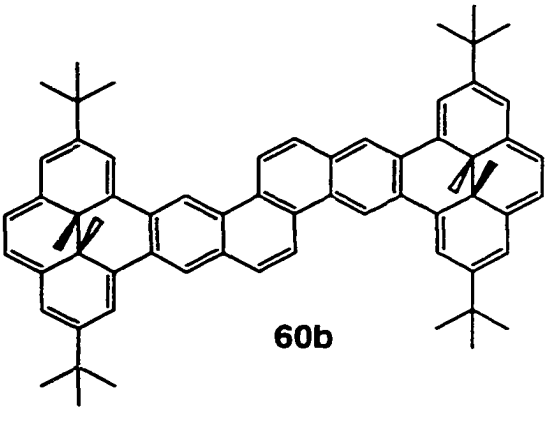

60b

2.3 Annulenometacyclophanes

Successful syntheses of [e]-annelated DMDHPs as above, prompted the question whether bis-annelated MCDs may be constructed by analogous methods. Retrosynthesis indicated several possibilities, Scheme 3, next page.

2.3.1 Bromobenzodihydropyrenes

Since benzo[e]dimethyldihydropyrene **53** had been obtained above, and since the most expedient test of aryne - furan adduct formation utilizes furan itself, it appeared that it would be best to try to obtain **64** and **65** from **53**, following retrosynthetic path a of Scheme 3, next page.

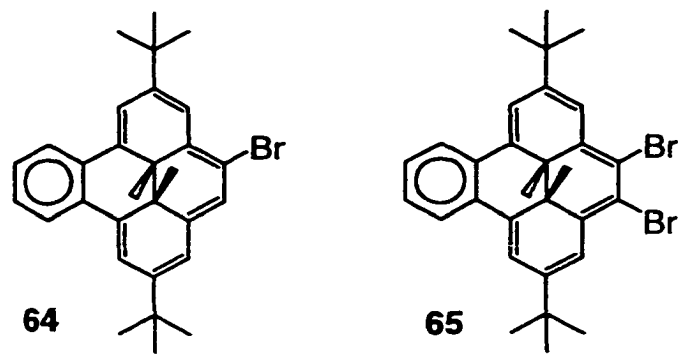

64 **65**

Bromination of **53** using 1 equivalent NBS in DMF/DCM in an ice bath in the dark yielded 92% of the red bromide **64**, mp 178 - 179 °C.

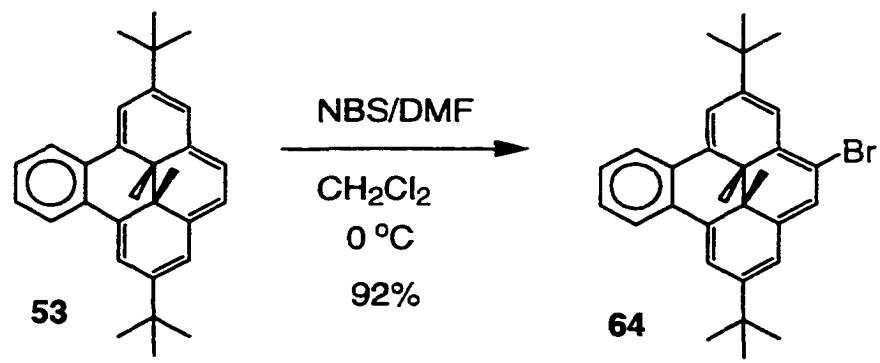

53 **64**

Scheme 3

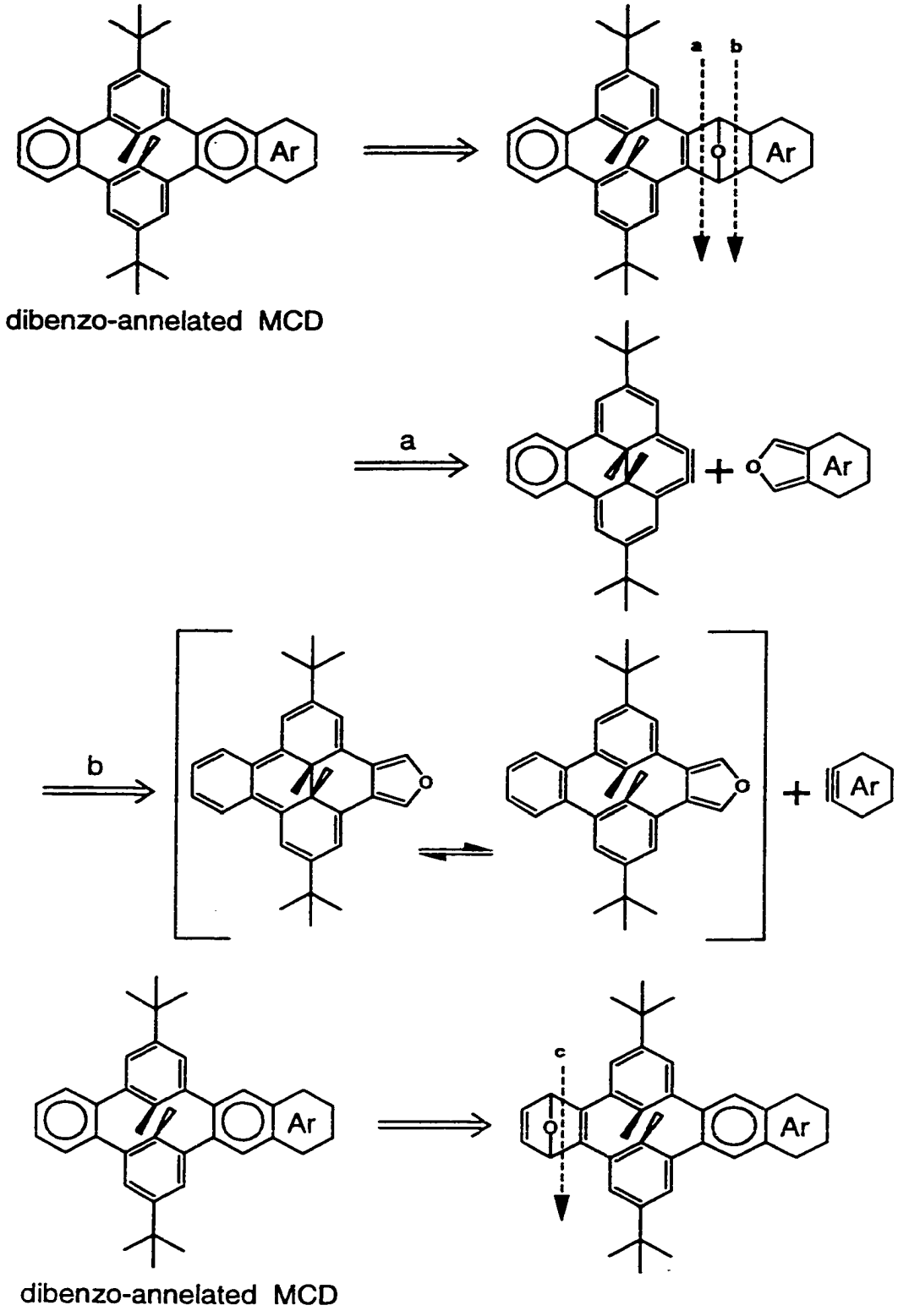
Ar
a
b
Ar
dibenzo-annelated MCD
a
Ar
b
Ar
c
Ar
dibenzo-annelated MCD

Characterization by proton NMR spectroscopy showed that the product **64** was likely a substituted benzodimethyldihydropyrene, with two singlets δ -1.43 and -1.44 indicating asymmetry. The benzo fragment was represented by a system similar to an ABXY system, with integration 2 protons : 2 protons. Integration of the other down field signals indicated five arene protons, implying mono-substitution of **53.** The presence of coupling and NOESY interactions showed that four protons vicinal to the *t*-butyl groups were still present. Thus mono-substitution appeared to be exclusively at the 4 position. Carbon NMR spectroscopy signals were also consistent with the structure **64.**

Mass spectroscopy gave peaks at *m/z* 472 and 474 for ^{79}Br and ^{81}Br isotope peaks for (M+.), and *m/z* 473 and 475 for ^{79}Br and ^{81}Br isotope peaks for (MH+), consistent for $C_{30}H_{33}Br$. Elemental analysis confirmed structure **64** with a satisfactory analysis.

The dibromobenzo[e]dimethyldihydropyrene **65** was produced by reaction in the dark of an ice chilled solution of one equivalent **53** in dry CH_2Cl_2, with two equivalents NBS in dry DMF. Intense purplish red **65** was obtained in modest yield of about 50 % as crystals after repeated chromatography. Closely eluting fluorescent compounds necessitated four fold chromatography. Scrupulous attention to anhydrous conditions was necessary to obtain **65.**

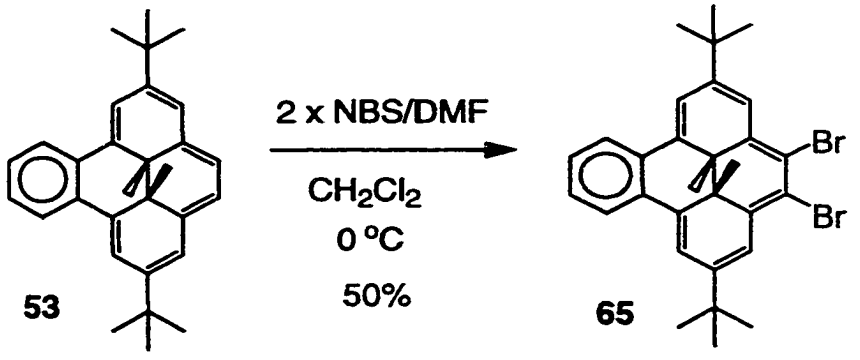

53 **65**

Proof of structure for **65** was partially provided in the NMR spectra which revealed symmetry. Single peaks in the proton NMR spectrum for internal methyl and *t*-butyl protons at δ -1.30 and 1.49 respectively indicated a symmetric substituted benzodihydropyrene. An AA'XX' like system was also apparent. The only other signals were a pair of coupled down field resonances, 2 protons each, shown by COSY and NOESY NMR spectra to be the meta coupled protons vicinal to the *t*-butyls, of the DMDHP fragment. The only positions unaccounted for were the 4 and 5 positions which must therefore be substituted. Mass spectroscopy confirmed the presence of two bromines, by isotope pattern, and supported the formula of **65** as $C_{30}H_{32}Br_2$, with *m/z* 553 (MH+, ^{79}Br and ^{81}Br). Elemental analysis supported the composition $C_{30}H_{32}Br_2$.

2.3.2 Aryne reactions derivatizing benzo[e]dimethyldihydropyrenes

With aryne synthons **64** and **65**, we performed aryne - furan reactions with a view to constructing bisannelated metacyclophane compounds.

Reaction of **64** with furan in THF, with sodium amide/potassium t-butoxide conditions resulted in a modest yield of **66**, 41 %. Larger amounts of parent hydrocarbon **53** were recovered, ~ 55 %.

Reaction of **65** with furan in THF at -78 °C using *n*-butyllithium produced a small amount of **66**, ~20 %, and large amounts of **53**, ~ 50 %.

More useful amounts of **66** were finally obtained by reaction of **65** with furan in toluene at - 40 °C, with *n*-butyllithium. After chromatography, 66 % yield of **66** was obtained. This aryne reaction was optimized at 15 to 16 minutes. Shorter reaction times returned some unreacted **65**, and longer reaction times resulted in increasing decomposition.

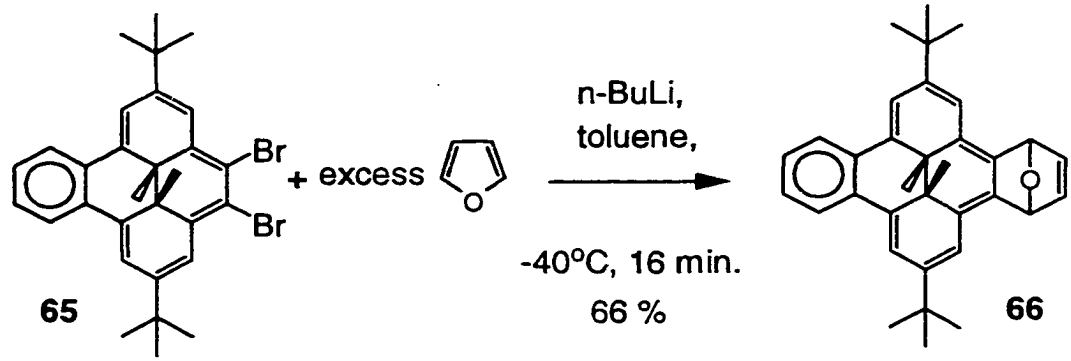

Compound **66** was obtained as an orange - brown microcrystalline solid, mp 212 - 213 °C. Proton NMR spectroscopy indicates asymmetry with two internal methyl proton resonances at δ - 0.98 and - 1.20. An ABXY like pattern

was evident in the proton spectrum, as were meta coupled protons vicinal to the *t*-butyl groups. Alkene and ether bridge proton signals also appeared. Ether carbon resonances occurred in the carbon NMR spectrum, at δ 80.22 and 80.15, in addition to other expected signals for **66**. Mass spectrometry (methane CI) supported **66** as $C_{34}H_{36}O$, with *m/z* 461 (MH+).

The aryne - furan reactions of monobromopyrene **50** and the two benzopyrene bromides **64** and **65** displayed significant reactivity differences.

Aryne reaction of **50** with furan in THF gave 86% yield of adduct **52**, 86 %, and small amounts of **29**. The analogous aryne reactions of **64** or **65** with furan in THF retumed large amounts of hydrodehalogenated **53**, and modest amounts of adduct **66**.

It may be that the aryne from **50** can be significantly stabilized by bond localization, reducing the reactivity and improving the selectivity for the Diels - Alder adduct. The aryne from **64** or **65** may suffer destabilization, by the contrary bond localizing influence of the benzo group. Significant cumulene character could diminish selectivity, and increase the arynes ability to attack solvent. In the event, aryne reactions of **65** produced better yields in toluene than THF.

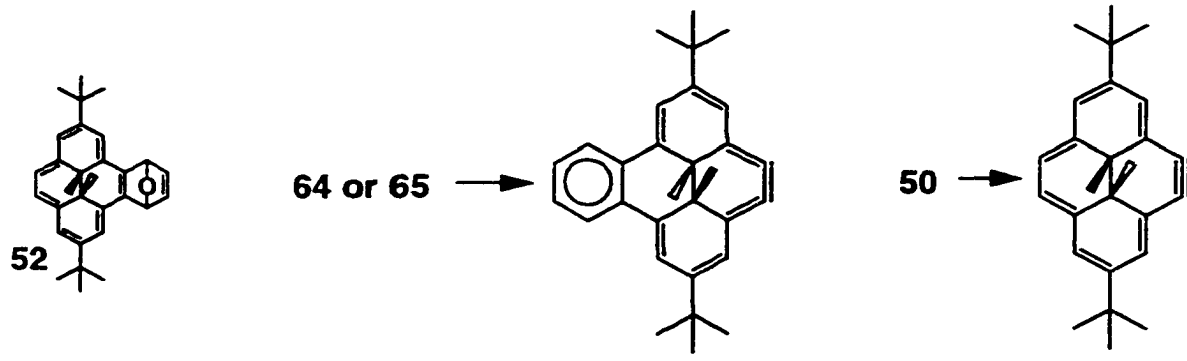

2.3.3 Benzo[e]dimethyldihydropyreno annelated metacyclophane

Successful production of adducts from benzo[e]dihydropyrene aryne synthons with furan above prompted the attempt to couple the isoarenefuran **55** with a benzo[e]dimethyldihydropyrene.

Reaction of dibromo-benzopyrene **65** with isopyrenefuran **55** in toluene at - 40°C with *n*-butyllithium did result in a small amount (12 %) of the adduct **67**.

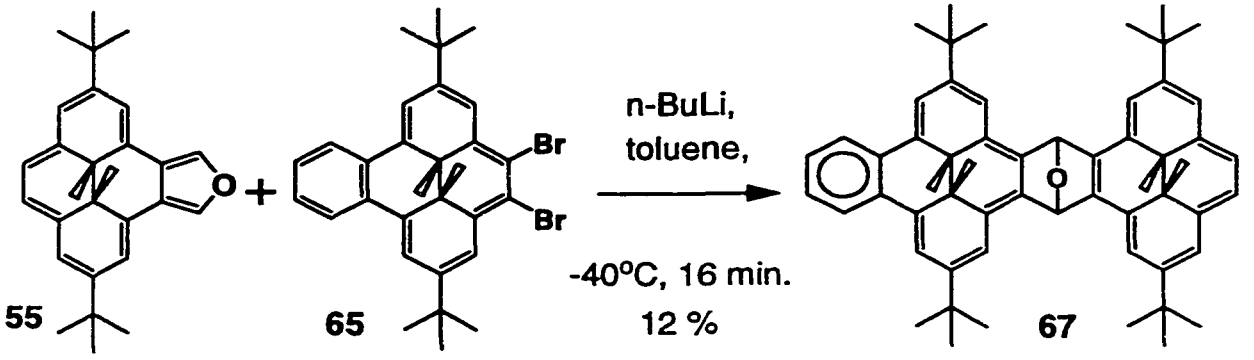

Golden malt colored aryne adduct **67** was obtained as a mixture of isomers, mp < 154 °C. With chromatography, one isomer was obtained, mp 222 - 225 °C. Proton NMR spectroscopy of the single isomer showed four distinct internal methyl proton resonances, at δ -4.18, -3.60, -1.99 and -1.04, appropriate for a system with both a DMDHP and a benzo[e]dimethyldihydro-pyrene. Four distinct *t*-butyl proton resonances were also found, and signals appropriate for the protons vicinal to the *t*-butyl groups appeared, as did two discrete resonances for the two ether protons.

Mass spectroscopy confirmed **67**, with LSIMS showing the peak *m/z* 776.5 (M+.), and a fragmentation pattern showing loss of methyl and *t*-butyl

groups. Exact mass found for M+. *m/z* 776.4977, while calculation for $C_{58}H_{64}O$ (M+.) gave 776.4957.

Deoxygenation of **67** with $Fe_2(CO)_9$ in refluxing benzene yielded 60% of the DMDHP - MCD system **68**.

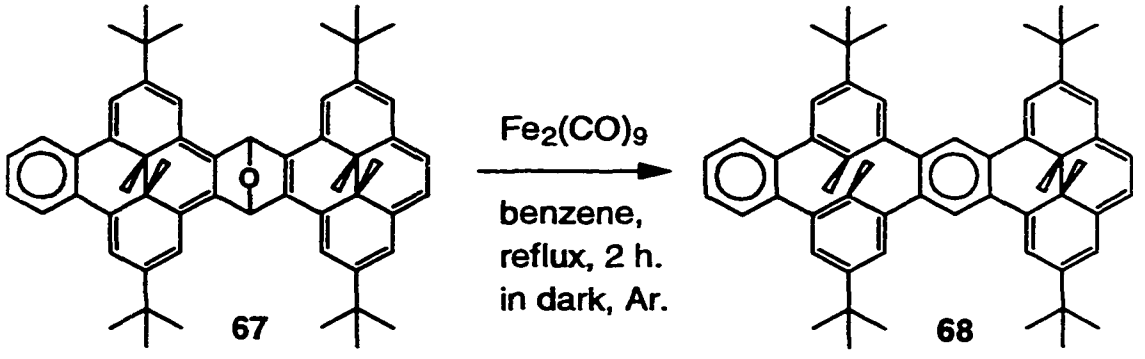

67 **68**

System **68** was somewhat oxygen sensitive and was best handled carefully under inert gas in the dark. Proton NMR spectroscopy confirmed the presence of DMDHP and MCD systems, with single resonances at δ -1.37 and 1.18, respectively.

The proton NMR spectrum appeared to show a single isomer. An AA'XX' pattern appeared, and two distinct *t*-butyl proton resonances.

Mass spectrometry confirmed **68** as $C_{58}H_{64}$ by EI MS with *m/z* 760.5 (M+.), and HRMS exact mass 760.5004 (M+.). The exact mass of $C_{58}H_{64}$ was calculated as 760.5008.

Of the two possible isomers of **68a** or **68b**, it was not determined which was obtained as the single isomer.

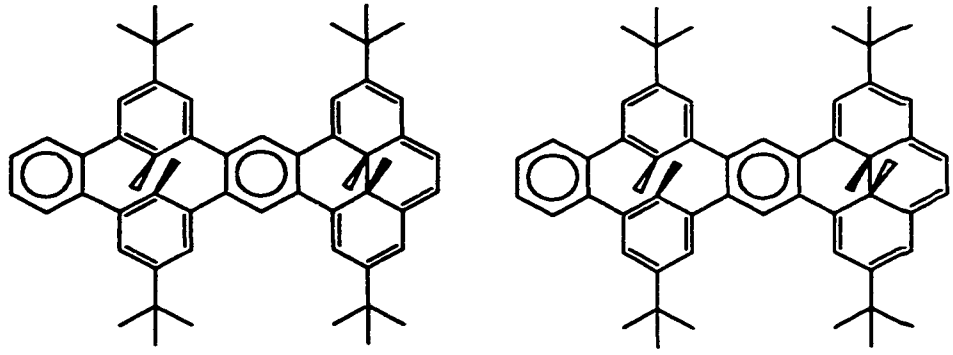

68a and **68b**, two isomers

Compound **68** was photoisomerizable and bleached readily to a double MCD system, which could be returned to **68** by 350 nm UV, or by warming in solution.

2.3.4 Alternate attempts to obtain **67**: furano-metacycophanes

Since adduct **67** was somewhat difficult to obtain by reaction of **55** and **65**, we also attempted to obtain **67** by one of the other retrosynthetic paths in Scheme 3 above. Experience with aryne reactions from bromopyrene **50** showed that good yields of adducts may be obtained, even with limited amounts of furans. Therefore we elected to try to obtain **69**, from reaction of **66** with tetrazine **54**, and then react **69** with **50** under aryne generating conditions.

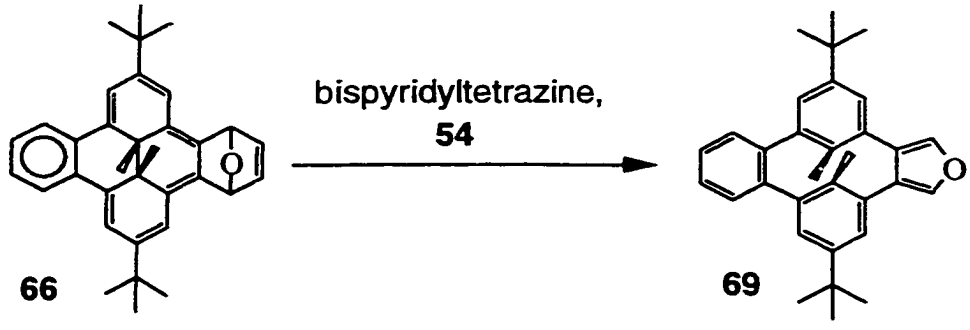

Product **69** was expected to be a metacyclophane, as all previous bis-annelated MCD analogues have been more stable as MCDs rather than DMDHPs.

Stirring **66** with **54** in dry THF in the dark produced a purple solution. From this a purple compound was isolated and purified by chromatography on deactivated alumina, in the dark, to yield a crystalline purple solid. Proton NMR spectroscopy showed that pyridyl residues were present. It is believed that the compound obtained was **70**, analogous to adducts obtained by Warrener[71] and others. To eliminate the pyridazine fragment in a retro Diels - Alder reaction, we first tried mild photolysis, with pyrex filtered visible light, from an incandescent tungsten source. An ice chilled solution of the purple intermediate was exposed for 0.5 hour to such light and bleached to pale yellow. After concentration and chromatography, we isolated a colorless crystalline compound, that proved to be the desired furanocyclophane system **69**, 67 % yield. Subsequently, it was found unnecessary to isolate the adduct **70**. Photolysis of the adduct solution of **70**, with excess tetrazine **54** present, gave **69** in 67% yield.

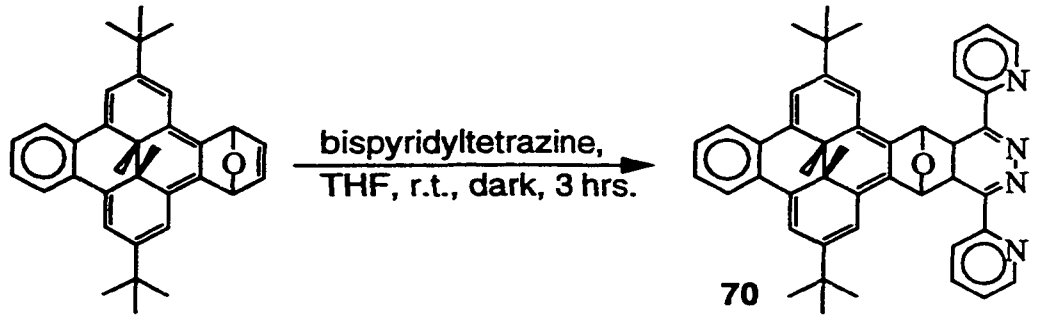

66 **70**

Isolable and chromatographable

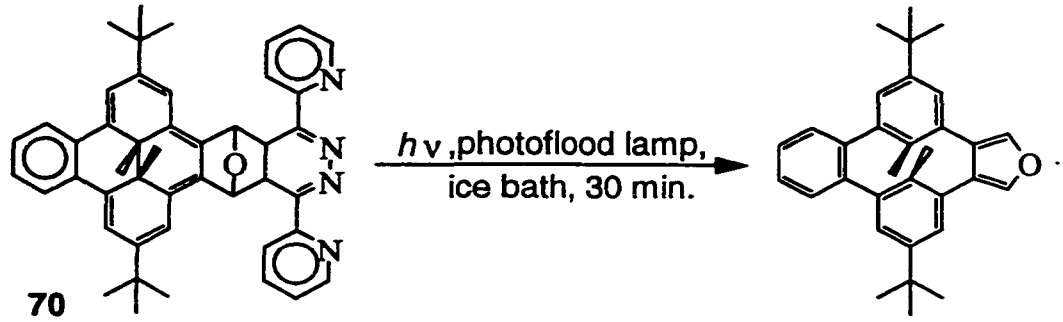

70 **69**

Characterization supported the product as the required cyclophane **69**. Proton NMR spectroscopy showed single peaks each for *t*-butyl and methyl protons, at δ 1.28 and 0.93 respectively. The methyl proton signals appear in the characteristic up field region for MCDs ~ δ 1. Mass spectrometry (methane CI) indicated a peak at *m/z* 435 (MH+), appropriate for **69**. Elemental analysis was satisfactory.

Successful production of **69** prompted us to attempt to form the bisfuranocyclophane **72** from the known **71** [68b,c].

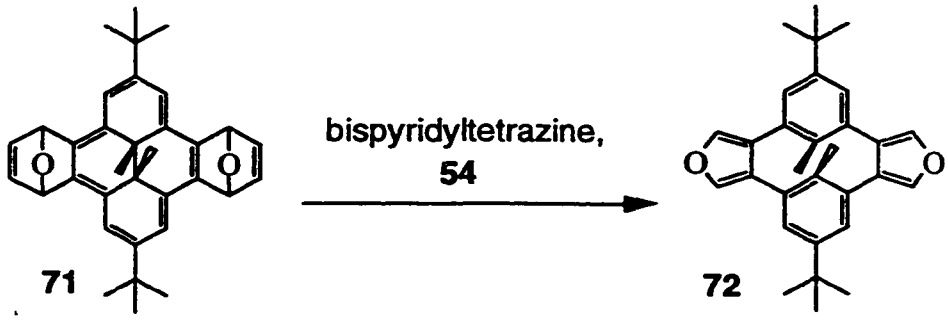

Reaction of adduct **71** with tetrazine **54** in dry THF produced an intense purple solution. Photolysis of this, conducted as for **70** above, resulted in bleaching. After concentration and chromatography, a colorless crystalline solid was obtained. Characterization confirmed that the product was the bis-furanocyclophane **72.**

Proton NMR spectroscopy indicated a high degree of symmetry, with only four peaks evident. Two aromatic peaks at δ 7.73 and 6.99 and two aliphatic peaks at δ 1.28 and 0.81 appeared, with the MCD methyl peak in the appropriate region. Only eight types of carbon resonances appeared in the carbon NMR spectrum, supporting the symmetry and the structure. Mass spectroscopy indicated the appropriate ion for MH+ with *m/z* 425. Elemental analysis was satisfactory.

With **69** in hand, we tried the aryne reaction with bromopyrene **50** in the same manner as for other furans, but with no success. Three trials resulted in no satisfactory indication of product **67**.

2.4 Aryne generation methods

The aryne reactions of monobromoarenes with sodium amide/potassium t-butoxide are somewhat different than the reactions of *ortho*-dibromoarenes with *n*-butyllithium. Alkali amides are kinetically more efficient bases than the alkyllithiums. It is known that furans are susceptible to kinetic deprotonation with alkali amides[73b] ,while alkyllithiums tend not to deprotonate furans. Aryne reactions under sodium amide conditions often return polymeric side products. The more rapid exchange of alkyllithiums with arylbromides may lead to a cleaner production of arynes, with fewer side products arising from deprotonation of furans present. The alkyllithium exchange method also operates at considerably reduced temperatures. A 4,5-dibromodimethyldihydro-pyrene would thus be desirable to allow aryne generation by alternate methods. Reaction of cyclopentadiene with tetrabromopyrene **73** and butyllithium yields **74**, but reaction of cyclopentadiene with dibromopyrene **51** under sodium amide conditions does not.

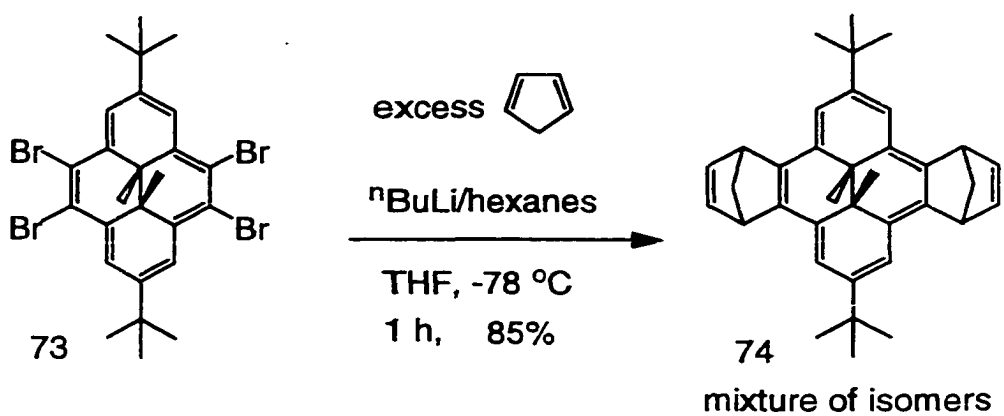

73 74

mixture of isomers

The topic of aryne generation overlaps another topic of interest in DMDHPs, that of vicinal functionalization. Vicinal arene dibromides are useful in obtaining bisacetylene substituted arenes. DMDHPs with vicinal bisacetylenes are of some interest because of the possibilities of forming other types of annelation deriving from the acetylenes. Thus a target of multiple potential uses would be the 4,5-dibromodimethyldihydropyrene **75**.

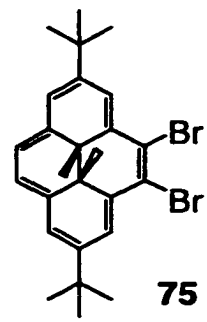

75

2.4.1 Vicinal functionalization: use of a protecting group

In order to impose vicinal bromination, some restricting protecting group for the 9, 10 positions would be required. We elected to try protection using a trimethylsilyl group, as subsequent removal is usually facile.

In the event, lithium exchange on bromide **50** with excess *n*-butyllithium at -78 °C, followed by quenching with TMSCl produced a deep green compound. The product was stable to water and dilute acids. Oxidation by air occurred slowly. The product was more mobile in chromatography than DMDHP **29**. Purification by chromatography yielded the trimethylsilylpyrene **76**, as shown by characterization.

Proton NMR spectroscopy revealed a singlet at δ 0.67, in the range for TMS groups. The integration of this peak (δ 0.67) was close to half the integration for the *t*-butyl groups, at δ 1.68 and 1.67. Two peaks appeared for the internal methyl protons at δ -4.02 and -4.05. Integration of the aryl proton region showed seven hydrogen were present, supporting mono substitution of **29**. Carbon NMR spectroscopy showed a strong peak at δ 1.04, supporting the presence of the TMS group. Other carbon signals appeared as expected for the structure.

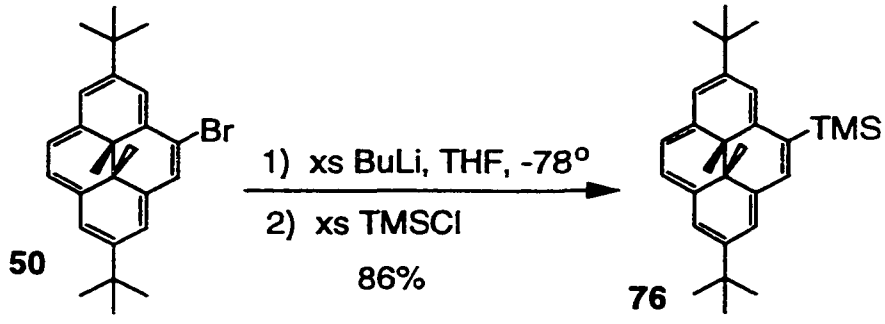

50 **76**

Mass spectroscopy (CI) showed peaks appropriate for TMS-DMDHP **76** $C_{29}H_{40}Si$, with *m/z* 417 (MH+), and 416 (M+.). Elemental analysis was satisfactory.

Bromination of **76** was attempted with two equivalents NBS in DMF/DCM, analogous to other DMDHPs, to try to obtain **77**. Analysis of the reaction product by proton NMR spectroscopy showed a mixture of products, with retention of the TMS group. It appeared that the bromination was occurring, though incompletely. Excess NBS (3 eq.) was tried, for 24 hours reaction time, and this

proved successful. A dark green crystalline solid was obtained after work up, in good yield, 95 %.

Proof of identity of **77** was provided by the usual characterizations. Proton NMR spectroscopy indicated an asymmetric DMDHP with penta substitution, by two internal methyl proton resonances and five aryl proton resonances. The TMS group was revealed in both proton and carbon NMR specta. A NOESY 2-D spectrum showed that two aryl protons interacted with the TMS group. This implied that the position vicinal to the TMS group was unsubstituted, and therefore bromination had occurred at the 4,5 positions.

Mass spectroscopy (methane CI) showed an appropriate isotope pattern for the molecular ion, centered at *m/z* 575 for MH+ (^{79}Br, ^{81}Br). Elemental analysis found a slight excess of carbon, 61.73 % C. Calculation gave for **77**, $C_{29}H_{38}Br_2Si$, 60.63 % C. Proton NMR spectroscopy indicated 5% of the monobromide derivative of **76** was present, which would raise the carbon analysis to 61.2%.

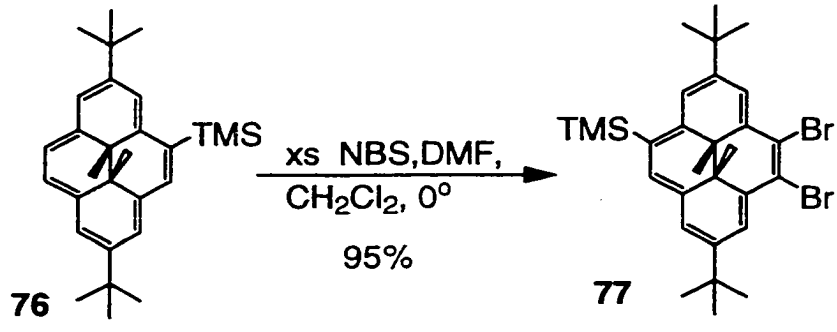

With the successful synthesis of **77**, final removal of the TMS group was attempted. The action of 10 % H_2SO_4 /THF was ineffective at deprotection. Use of fluoride (TBAF) was tried next. Room temperature reaction of **77** with TBAF in THF showed a small amount of TMS removal after 24 hours. Reflux of **77** with TBAF in THF for 24 hours was found to completely remove the TMS group to give **75**.

Identification of 4,5-dibromopyrene **75** by the usual characterization methods supported the target structure. Proton NMR spectroscopy indicated symmetry, with a single peak each for internal methyl proton and *t*-butyl proton resonances. Aromatic protons were distributed in three resonances, two showing coupling, as expected for the meta proton vicinal to the *t*-butyl groups, with coupling constant 1.3 Hz. The carbon NMR spectrum also indicated a two fold symmetry, with eleven resonances.

Mass spectroscopy (methane CI) indicated a dibromohydrocarbon with an appropriate isotope pattern centered at *m/z* 503 for MH+, for $C_{26}H_{30}Br_2$. A fragment peak for loss of HBr from MH+ appeared, with isotope pattern, centered at *m/z* 423. Elemental analysis indicated a slight excess of carbon, with 62.84 % C found. Calculation for **75** gives 62.17 % C. Since a small amount of **50** was present, ~3%, indicated by proton NMR spectroscopy, the elemental analysis would be expected to be in slight excess for carbon.

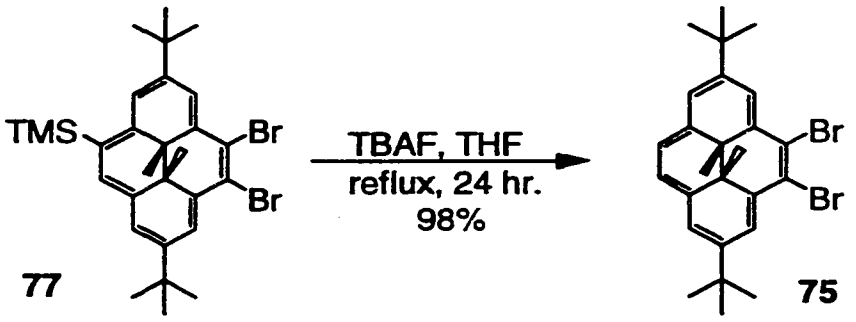

With characterization supporting the product **75** as a dibromo derivative of **29**, it must be proven which of three possible isomers was obtained. Isomer **51** has been obtained previously, as has the third isomer, **78** [68]. The melting point of **51** was reported as 220 - 222 °C [68], while the product **75** melted at 198 - 200 °C. Both **51** and **78** have different aryl proton patterns in their proton NMR spectra [68], than the product **75** obtained. Isomer **78** showed two internal methyl proton peaks in the proton NMR spectrum. The 4,5-dibromo orientation of the precursor **77** was also indicated by NOESY interactions of the TMS group with two aryl protons.

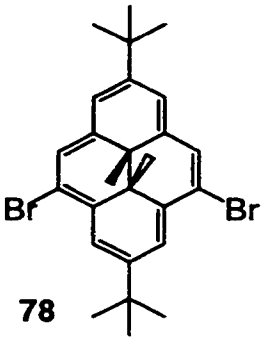

More positive evidence of the structure of **75** was obtained from its reaction chemistry. Collaborative work with Dr. M. Haley[76a] has shown that coupling reactions on **75** introduce vicinal acetylenes in positions 4 and 5 of DMDHP. The metal exchange - salt elimination aryne generation method has also been successfully employed with **75** and **77**, as demonstrated by professor T. Sawada[76b], to obtain Diels - Alder adducts with cyclopentadiene. From the characterization and chemical reactivity, it appeared well supported that **77** and **75** had the desired 4,5-dibromo substitution pattern.

2.5 Diels - Alder reactions of the isoarenefuran **55**

Successful syntheses of various annuleno[e]dihydropyrenes above demonstrated the usefulness of aryne - furan adduct formation. The reactivity of isoarenefurans[71,73] suggested that other dienophiles might react well with isopyrenefuran **55**, possibly providing routes to annelated DMDHPs not accessible using arynes. To test this possibility, reactive dienophiles were also reacted with **55**.

Dimethylacetylenedicarboxylate (DMAD) is highly reactive with electron rich dienes, furans, and isoarenefurans[73], and so reaction of **55** with DMAD was tested.

A solution of purple **55** was stirred with excess DMAD in THF at room temperature in subdued light. The solution became an intense green color in about 20 minutes. Dark green crystalline **79** could be obtained on work up.

Performing the reaction in an NMR tube and monitoring by NMR spectroscopy indicated the reaction was virtually quantitative.

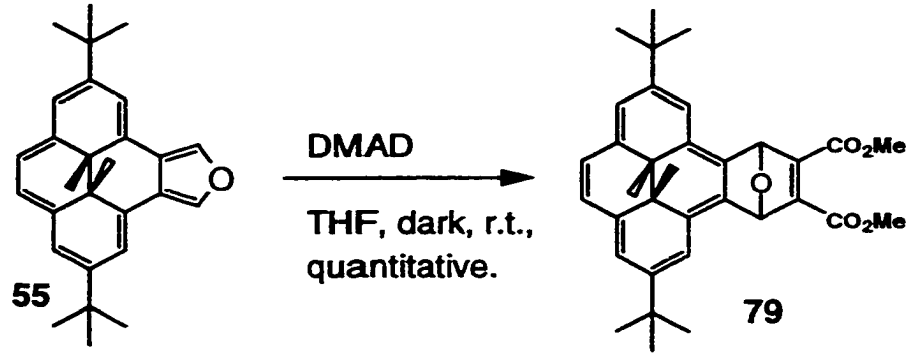

Characterization showed the product as an asymmetric DMDHP, with two internal methyl proton signals in the proton NMR spectrum, at δ -3.17 and 3.52. Two different methoxyl fragments were indicated by signals at δ 3.72 and 3.67, for the ester residues. Carbon NMR spectroscopy also showed two methoxyl residues at δ 52.06 and 52.03. Strong IR absorbtions at 1747 and 1722 cm^{-1} indicated the presence of the carboxyl fragments. Mass spectroscopy supported the structure with an ion at *m/z* 527 (MH+). An acceptable elemental analysis was obtained.

A second Diels - Alder reaction of **55** was attempted, using fumaronitrile, to form **80**. A preliminary test of the reaction was tried in an NMR tube. Monitoring the reaction by proton NMR spectroscopy appeared to show the reaction to be virtually quantitative. On a preparative scale, **55** reacted with fumaronitrile in ~20 minutes to give an intense green solution in THF. After work

up, a green microcrystalline solid was obtained. Purification by chromatography gave a 95 % yield of **80** as a mixture of isomers.

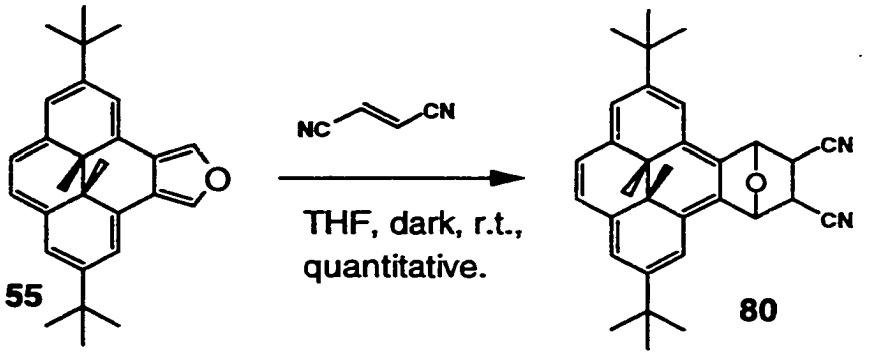

Characterization supported the identity of **80**. Proton NMR spectroscopy indicated an asymmetric DMDHP was obtained, with signals in the δ -3.90 to -4.10 region. IR showed the presence of a nitrile with absorbtion at 2240 cm^{-1}. Mass spectroscopy gave a molecular ion at *m/z* 463 for MH+, from **80**, $C_{32}H_{34}N_2O$.

Chapter three Results and Discussion

1.1 NMR properties

1.1.1 Internal and external protons

A consequence of the theoretical considerations on aromatic ring currents as discussed in the introduction would be that the different sets of chemically equivalent protons of DMDHP should experience different magnetic fields. This arises in part as each set of equivalent protons is a different distance from the centre of the ring current induced magnetic field. A ramification of this would be that changes in ring current would result in different changes in chemical shifts for the sets of chemically equivalent protons. The sensitivity of each set of protons tc changes in ring current was calculated by Haddon [77]. These sensitivity factors, expressed inversely as the magnitude of the ratio of the change in internal methyl chemical shift to the change in external proton chemical shift $|\Delta\delta(Me)/\Delta\delta(H^n)|$ were calculated as 2.38, 2.08 and 1.96 respectively for H^2, H^3, and H^4 of DMDHP **10**.

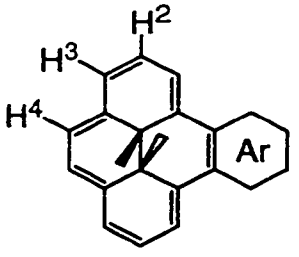

[e] annelated derivatives of **10**.

Several [e]-annelated derivatives of **29** were obtained for this thesis. A series of these products, called the **[e]-2,7-Di-*t*-butyl** series is shown below. The chemical shifts of the internal methyl protons and the H^4 protons of the **[e]-Di-*t*-butyl** series are collected in Table 2. These data were plotted to find the NMR sensitivity factor of the internal methyl protons to the H^4 protons. For the acene series **29**, **53**, **57**, and **59**, plotted in Figure 2, below, the equation relating the chemical shifts of the internal methyl and external Ar-H^4 protons was found to be;

(3) $$\delta(H\ Me_{internal}) = 13.035 - 2.036[\delta(H^4)] \qquad R = 0.99945\ .$$

The magnitude of the slope, 2.036, was within 4% of Haddon's theoretical value of 1.96[77].

The magnitude of the slope of the plot in Figure 3 for all compounds in Table 2 was 1.968, very close to theoretical value of 1.96. The relationship between the internal methyl and external Ar-H^4 proton chemical shifts for the **[e]-2,7-Di-*t*-butyl** series was thus;

(4) $$\delta(\ Me_{internal}) = 12.593 - 1.968[\delta(H^4)]. \qquad R = 0.9954$$

Table 2 [e]-2,7-Di-*t*-butyl series internal and H^4 proton chemical shifts

compound	δ ($Me_{internal}$)	δ (H^4)
29	-4.06	8.41
53	-1.58	7.14
57	-0.54	6.66
59	0.004	6.43
60	-0.74	6.84
68a	-1.37	7.16
68b	-1.67	7.31
55	0.18	6.21

(all δ values in Table obtained in $CDCl_3$)

[e]-2,7-Di-*t*-butyl series compounds

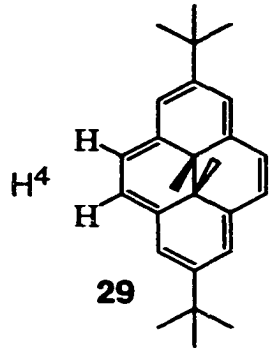

29

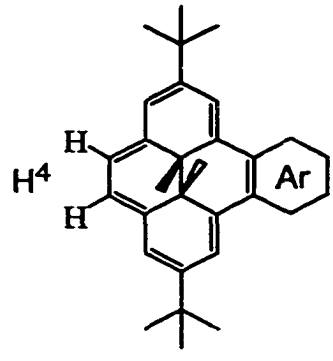

annuleno[e]DMDHPs

53 Ar = benzo
57 Ar = 2,3-naphtho
59 Ar = 2,3-anthro
55 Ar = 3,4-furano

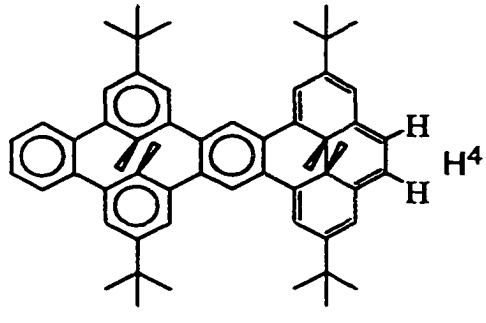

two isomers, **68a, 68b**

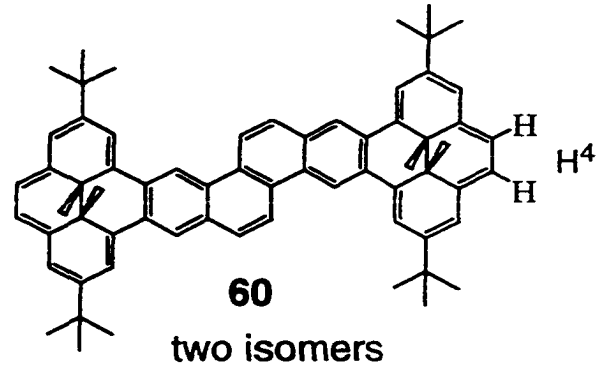

60

two isomers
(not separated)

Figure 2

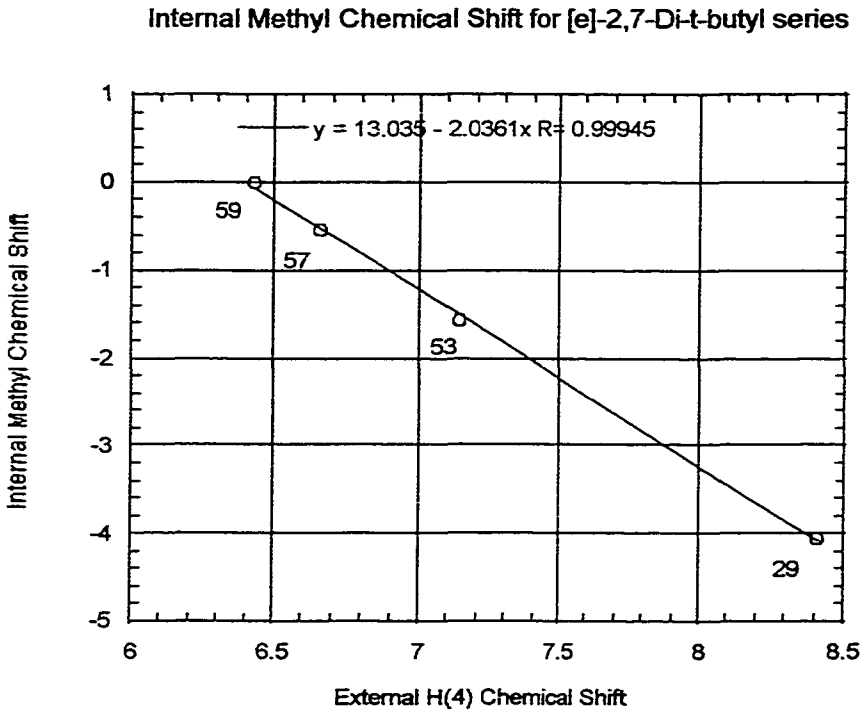

Figure 3

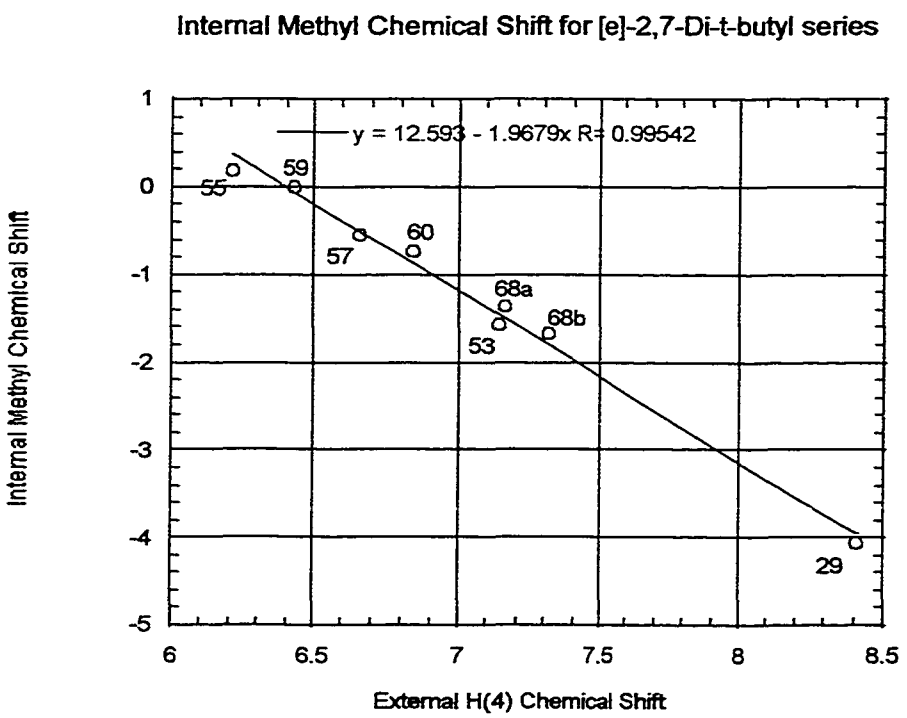

A previous study[44a] has shown that for the **[e]-2,7-H** series below, the relative sensitivity of internal methyl proton chemical shift to external Ar-H^4 chemical shift was 1.909.

[e]-2,7-H series

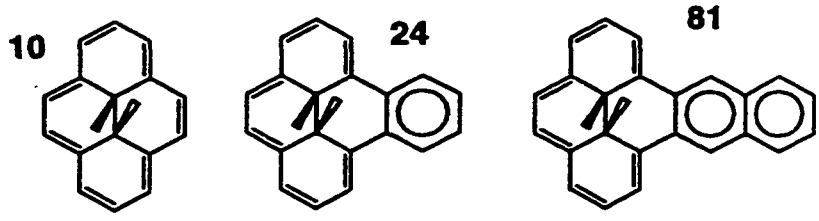

The relationship of the internal methyl chemical shift to the external Ar-H chemical shift is important, for it provides a ready test for additional effects. For example, if charge were present, distribution of charge over the π framework would be expected to affect the Ar-H^4 more than the internal methyls. The through bond distance of the internal methyls from the annulene perimeter would reduce the effect of charge at the perimeter on the internal methyls. Perimeter Ar-H^4 would be much more affected through bond, by perimeter charge. (The principle effect of the annulene perimeter on the internal methyls is a through space magnetic effect, not through bond.)

Additionally, the linear relationship of δ(Me) and δ(H^4) allows us to use the H^4 NMR signals to probe for aromaticity effects, instead of using δ(Me), as is discussed below.

3.1.2 The Mitchell method of estimating aromaticity

Aromaticity as a concept has proven controversial[78]. No general method of quantifying aromaticity has been agreed upon[42,79]. Empirically, NMR spectroscopy is the method most often used to judge whether a system is aromatic. Other methods such as diamagnetic susceptibility exaltation were briefly discussed in the introduction. The Mitchell method of estimating aromaticity as outlined in the introduction has been developed as an experimental method of determining the aromaticity of systems relative to benzene. No molecular model calculations and no hypothetical structures are involved in the Mitchell method, in contrast to the energetic and magnetic criteria of aromaticity discussed in the introduction.

As discussed on page 11, resonance energy (RE) is proportional to ring current (RC)[40] and the relative contributions of two fused arene fragments to overall ring current depends on the REs of the fragments[40,43]. Thus the magnetic effects arising from the ring current of one fragment will tell us about the resonance energy of the other fragment. In this context, RE is taken as a measure of aromaticity. We can use as the magnetic effect, the change of the chemical shift of the internal methyl protons δ(Me) of **10** arising on annelation, to gauge RE. The low sensitivity of δ(Me) to single substituents[80], and the small through space deshielding of the internal methyls by arene fusion[81] makes **10** a good probe for aromaticity.

In its most simple form, the method of obtaining the aromaticity of a

system relative to benzene would estimate the relative aromaticity as the ratio of the change in chemical shift of the internal methyl protons of **10** caused by annelation with the system, to the chemical shift change of **10** caused by benzannelation.

This is shown using the **[a]-2,7-H** series below, for the naphtho derivative **82.**

[a]-2,7-H series

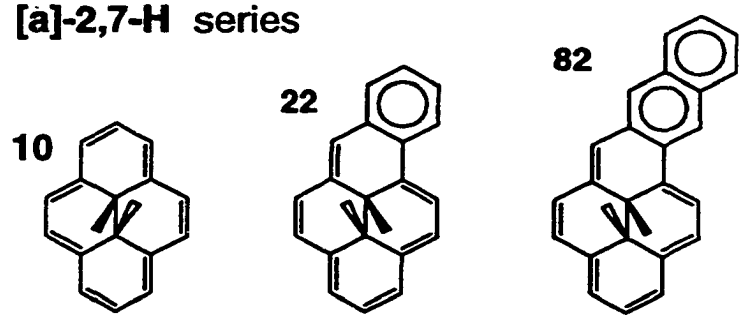

The chemical shift difference between **10** and **22** was $\Delta\delta = 2.63$ ppm, while for **10** and **82** the difference was $\Delta\delta$ = -0.44-(-4.25 ppm) = 3.81 ppm. Thus the relative aromaticity of the 2,3-naphtho system would be

RA(2,3-naphthalene) = 3.81 ppm/2.63 ppm = 1.45

If we let $\Delta\delta$(Ar[a]) be the change in the chemical shift of the internal methyl protons from **10** for arene [a]-annelated derivative of **10**, and if we let $\Delta\delta$(Bz[a]) be the change in the internal methyl protons from **10** for [a]-benz-annelated derivative of **10**, then in general the relative aromaticity of a system would be given by; $RA = \Delta\delta(Ar[a]) / \Delta\delta(Bz[a])$. (5)

Similarly, the relative aromaticity of an arenes could be derived from [e]-annelated derivatives of **10** by using an analogous equation;

$$RA = \Delta\delta(Ar[e]) / \Delta\delta(Bz[e]). \quad (6)$$

The relative aromaticities of some aromatics have been determined using the annelated derivatives of **10** shown below[44a]. The chemical shifts of the internal methyl protons of these arene annelated derivatives of **10** and the relative aromaticities derived for the arenes fused to **10** are given in Table 4 below.

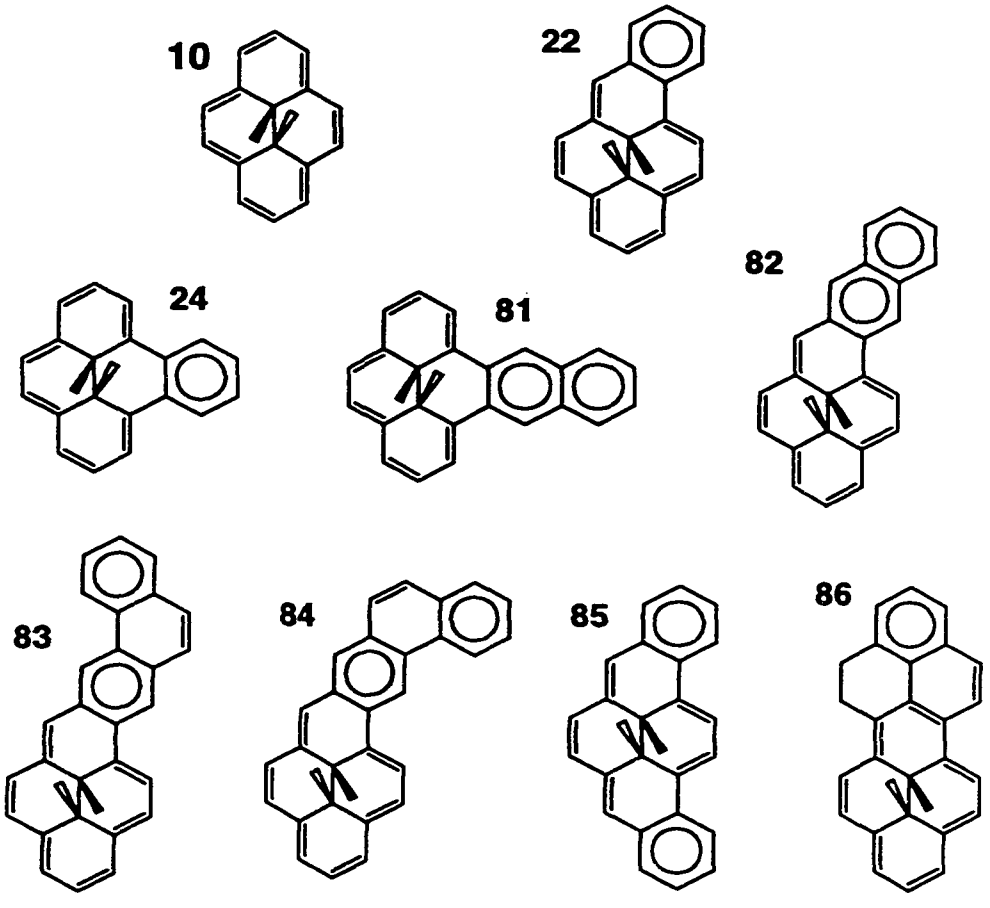

The question then would be, "Do such relative aromaticities relate to any other measures of aromaticity?"

It was found that for a number of [a]-annelated derivatives of **10** , the

relative aromaticities arising from simple calculation as in the example above correlated well with relative aromaticity calculated from Dewar resonance energies[45] (RE). In order to discuss this, we need to define relative aromaticities of annelating fragments in a systematic way. For this, Relative Bond Localizing Energy has been defined, and is explained below.

3.1.3 Relative Bond Localization Energy (RBLE)

In the quantitative studies [44a] which showed relation between the chemical shift of the internal methyl ^1H resonances and the Dewar resonance energy of the annelated fragments, resonance energies were converted to Relative Bond Localization Energy, (RBLE). RBLE was defined[44a] as the difference between the resonance energy of the π delocalized annuleno fragment and the resonance energy of the π localized anneleno fragment of two respective contributing Kekule structures, relative to benzene. In these, DMDHP had π localization in the former, and π delocalization in the latter. In the second structure, with delocalized DMDHP, any portion of the annelating fragment which could be figured as delocalized, was taken as such, when this did not interfere with delocalization of DMDHP. Illustration follows.

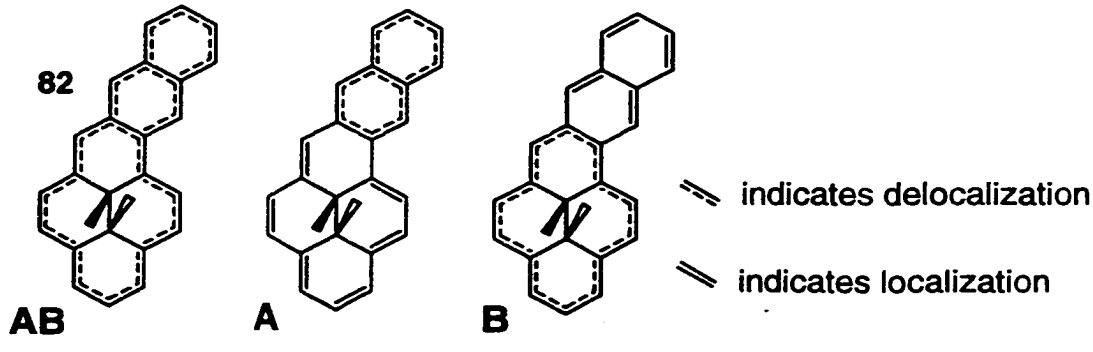

For example, in **A** and **B** above, the annelating fragment is naphthalene. Structure **82** has resonance contributors **a**, **b** and **c**, below.

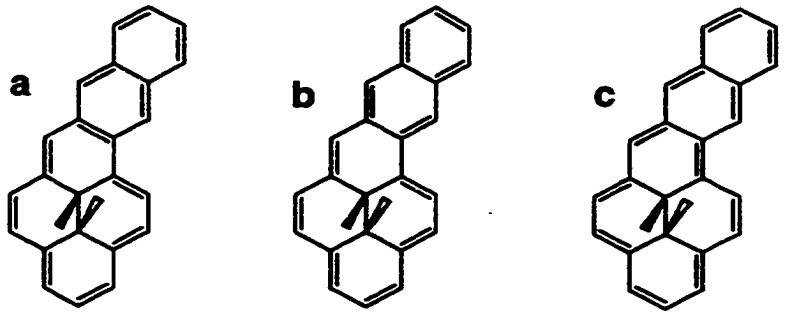

Structure **A** derives from **a** and **b**, while structure **B** derives from **a** and **c**.

The RBLE of the 2,3-naphthaleno fragment is

[RE(naphthalene) - RE(localized 2,3-naphthalene in **c**)] / RE(benzene) =

[1.323 eV - 0 eV] / 0.869 eV = 1.522

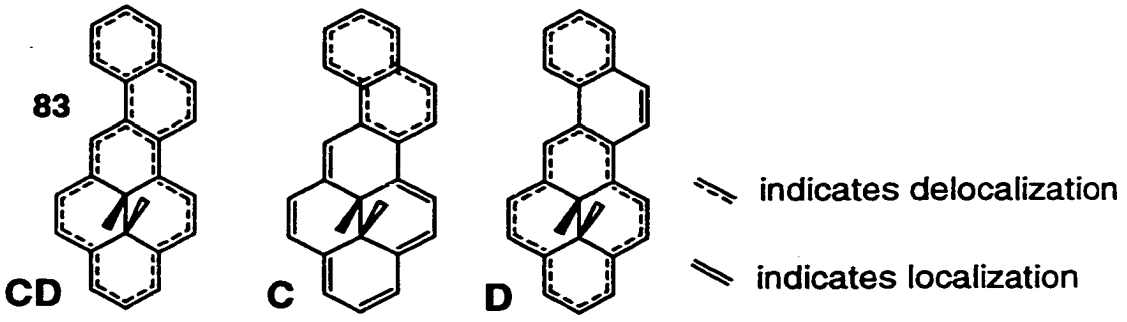

Compound **83** has contributors **C** and **D**. Structures **C** and **D** derive from localized contributors analogous to those for **82**. The RBLE of 1,2-naphthalene is calculated on the next page. Note: The value of RE(localized 1,2-naphthalene) in **D** is taken as ~ RE(benzene) = 0.869 eV.

[RE(naphthalene) - RE(localized 1,2-naphthalene in **D**)] / RE(benzene) =

[1.323 eV - 0.869 eV] / 0.869 eV = 0.522

The general RBLE equation would thus be;

(7) RBLE = [RE(annelating fragment) - RE(of fragment in the localized structure)] / [RE(benzene)]

Table 3. Resonance energies and RBLEs of selected aromatics.

Arene	RE/(eV)[45]	fusion bond	residual arene	RBLE
benzene	0.869	any	none	1.00
naphthalene	1.323	1 - 2	benzene	0.52
		2 - 3	none	1.52
anthracene	1.600	1 - 2	naphthalene	0.32
		2 - 3	none	1.84
phenanthrene	1.933	1 - 2	naphthalene	0.70
		2 - 3	benzene	1.22
		9 -10	biphenyl	0.27
tetracene	1.822	1 - 2	anthracene	0.26
		2 - 3	none	2.10

3.1.4 Experimental Aromaticity Scale.

By plotting RBLE (Table 3) as a function of the experimental values obtained for $\delta(Me_{internal})$ for compounds **29**, **53**, **57**and **59** (Table 2), we obtained a calibration curve, Figure 4. For smaller values of RBLE, the curve was approximately linear. For larger values of RBLE, $\delta(Me_{internal})$ converged on ~1 ppm. This was the value of $\delta(Me_{internal})$ for a fully localized system, a model of which is the dihydro derivative of **10**, shown below. The model had internal methyl protons at δ 0.97 [61] . ($\delta(Me_{internal})$ is also written as δ(Me).)

Dihydro derivative of **10.**

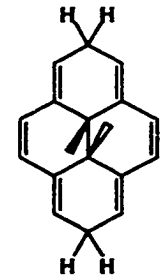

The linear equation through the data plotted in Figure 4 below was;

(8) $RBLE = [3.99 + \delta(Me)]/2.242$ $R = 0.997$.

Polynomial curve fitting shown in Figure 5 gave a better fitting relation;

(9) $RBLE = 1.834 + + 0.5806(\delta(Me)) + 0.03175(\delta(Me))^2$ $R = 0.99997$.

An empirical relation also fitted the data well, shown in Figure 6 below;

(10) $RBLE = 2.825 - [0.97 - \delta(Me)]^{0.643}$ $R > 0.99999$.

In practice, the aromaticity of a system could be estimated, once the appropriate annelated DMDHP was synthesized, by comparing the value of δ(Me) to the experimental scale (Figure 2) and reading off the RBLE value. The Dewar RE then would be back calculated by manipulation of the RBLE equation.

Table 4. δ(Me) for annelated DMDHPs and RBLEs of the annelating arenes

compound	annelating arene	δ(Me)	RA	RBLE
10		-4.25	0	0
22	benzene	-1.62	1.00	1.00
24	benzene	-1.85	1.00	1.00
81	2,3-naphthalene	-0.74	1.46	1.52
82	2,3-naphthalene	-0.44	1.45	1.52
83	2,3-phenanthrene	-0.90	1.27	1.22
84	2,3-phenanthrene	-0.88	1.28	1.22
85	2 x benzene	0.02	1.62	2.00
86	1,2-naphthalene	-2.78	0.56	0.52

Figure 4

RBLE plotted against internal methyl chemical shift for the [e]-2,7-Di-t-butyl series.

Linear curve fit

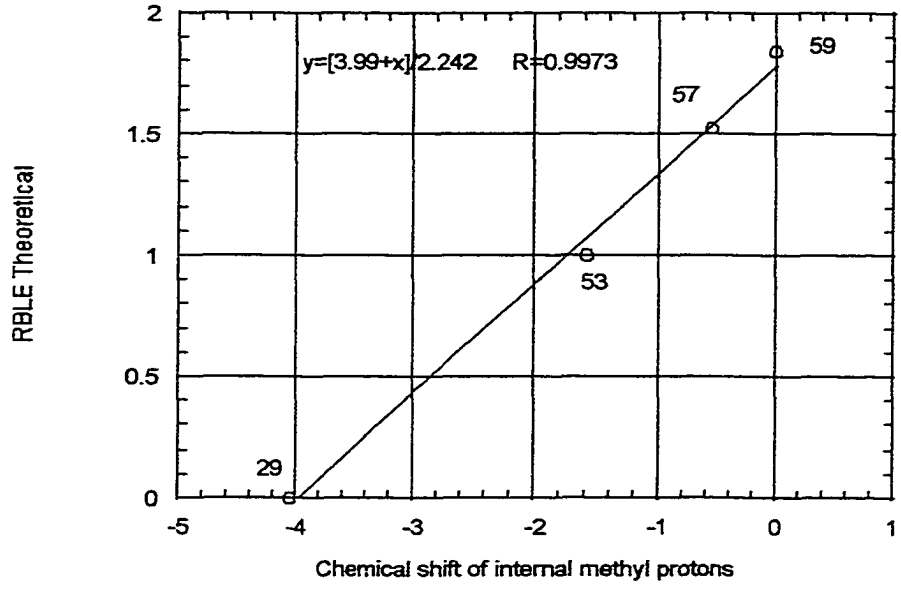

Figure 5

RBLE plotted against internal methyl chemical shift for [e]-2,7-Di-t-butyl series

polynomial curve fit

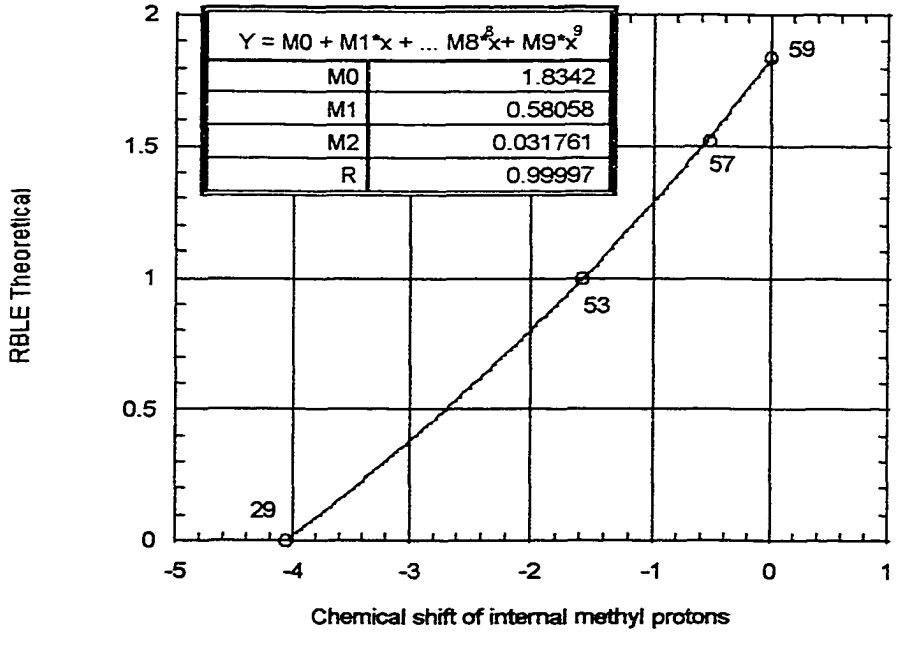

Figure 6

RBLE plotted against the internal methyl chemical shift for the [e]-2,7-Di-t-butyl series.

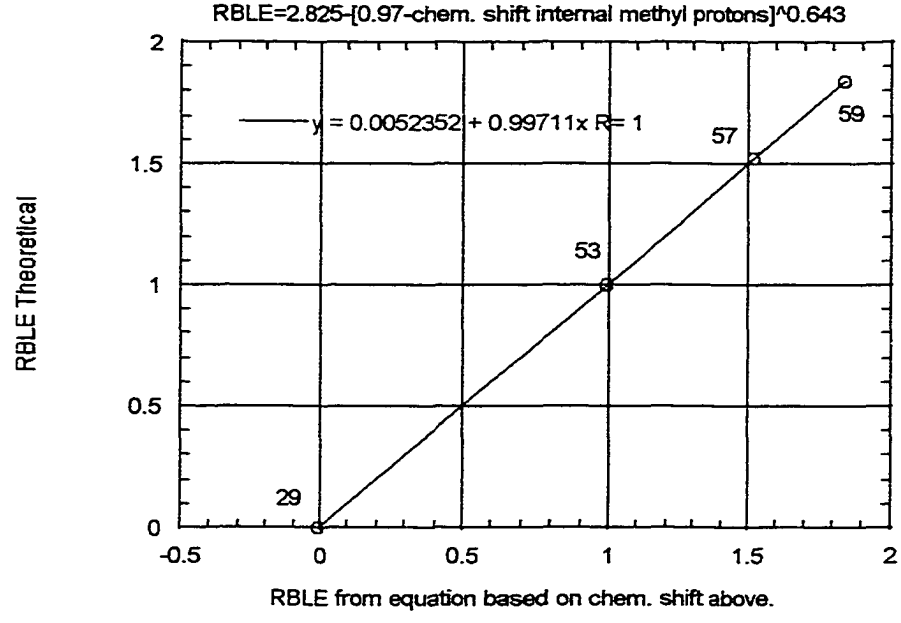

For comparison, the RBLE and δ(Me) values for some of the [a]-annelated DMDHP derivatives in Table 4 above were plotted, in Figures 7, 8 and 9 below. The results of curve fitting through the plots in Figures 7, 8 and 9, were equations (11), (12) and (13) below.

The linear equation best fitting the plot in Figure 7 was

(11) $$RBLE = [4.20 + \delta(Me)]/2.61 \qquad R = 0.996.$$

Polynomial curve fitting through the plot in Figure 8 gave;

(12) $$RBLE = 1.664 + 0.460[\delta(Me)] + 0.0163[\delta(Me)]^2 \quad R = 0.997.$$

An empirical relation between RBLE and δ(Me) was plotten in Figure 9;

(13) $RBLE = 2.82 - [0.97 - \delta(Me)]^{0.620}$ $R = 0.997$.

Comparing the experimental linear equations (8) and (11) for RBLE with the respective conceptual relations (6) and (5) for relative aromaticity (page 67), we found good agreement. For equations (6) and (5), respectively, the numerators would be $\Delta\delta(Ar[e]) = \delta(Me) - (-4.06\ ppm)$,

and $\Delta\delta(Ar[e]) = \delta(Me) - (-4.25\ ppm)$.

The numerators of equations (8) and (11) were [3.99 ppm + δ(Me)] and [4.20 ppm + δ(Me)] respectively. The denominators for equations (6) and (5) were

(6) $\Delta\delta(Bz[e]) = -1.58\ ppm - (-4.06\ ppm) = 2.48\ ppm$ and

(5) $\Delta\delta(Bz[a]) = -1.62\ ppm - (-4.25\ ppm) = 2.63\ ppm$.

The denominators found for equations (8) and (11) were 2.24 ppm and 2.61 ppm respectively.

Figure 7

RBLE plotted against internal methyl chemical shift for [a] annelated compounds

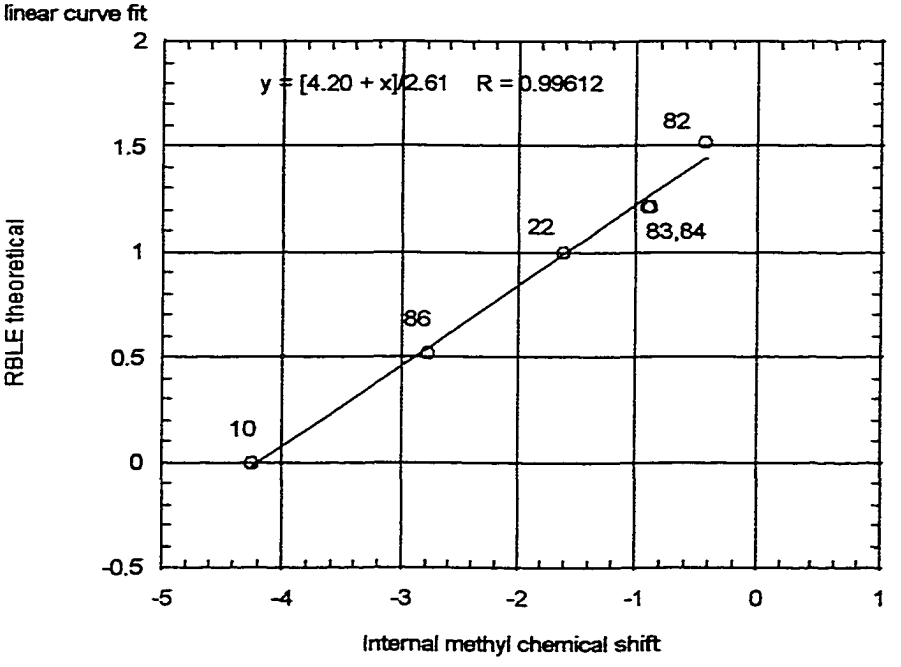

Figure 8

RBLE plotted against internal methyl chemical shift for [a] annelated compounds.

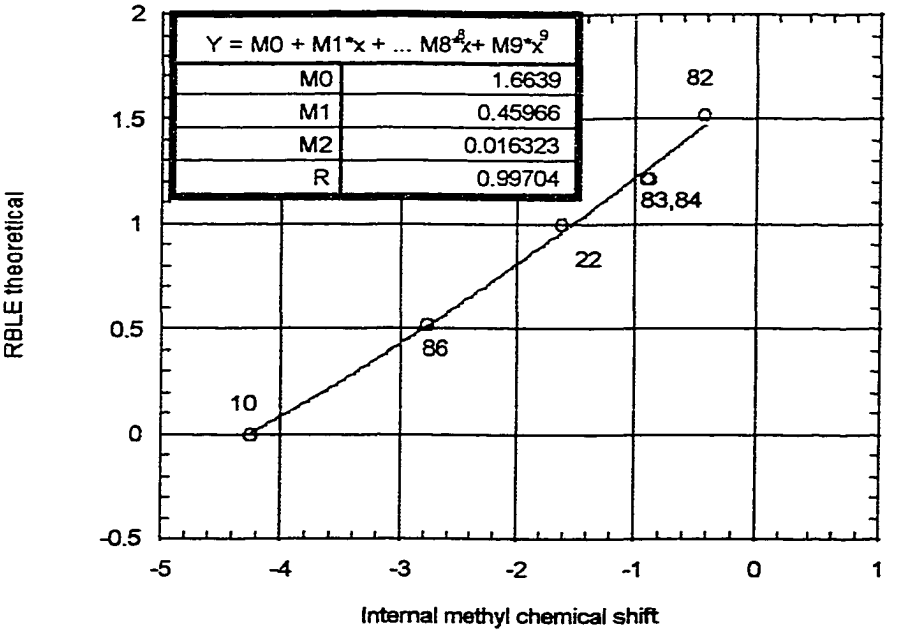

Figure 9

RBLE plotted against internal methyl chemical shift for [a] annelated compounds.

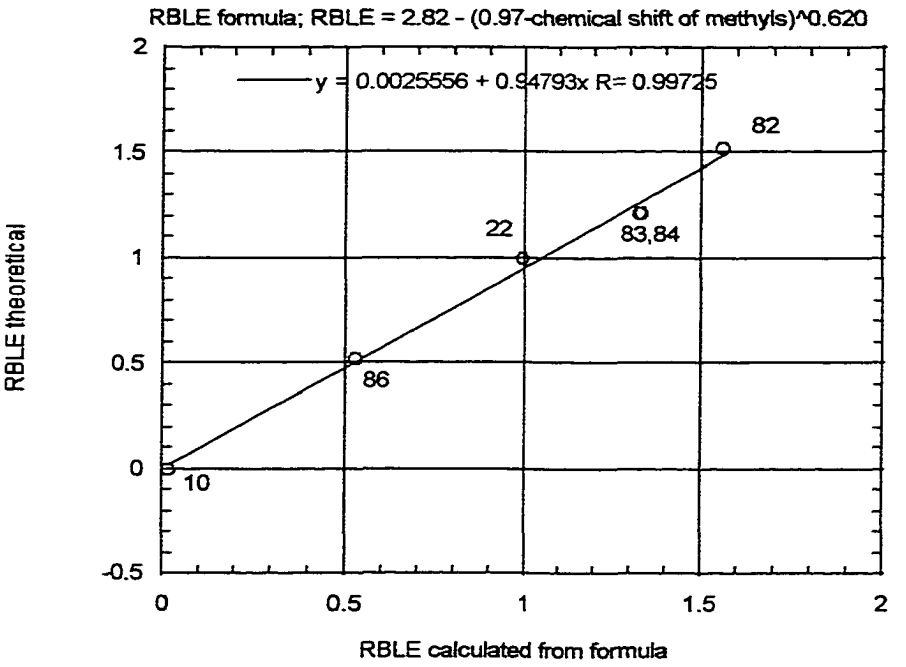

3.1.5 Strain effects

Annulene delocalization can also be affected by strain, and it would be natural to question whether our **[e]-2,7-Di-*t*-butyl** series shows π localization effects stemming from strain induced by annelation. Comparing the δ(Me) for the **[a]-2,7-H** and the **[e]-2,7-Di-*t*-butyl** series analogues, we see close agreement. Three series have been shown above on pages 66, 68 and 70. A fourth series, the **[e]-DiMe** series, is shown below.

Table 5

Chemical shifts of the internal methyl protons for some dihydropyrenes .

	Series			
	[a]-2,7-H[44a]	**[e]-2,7-H**[44a]	**[e]-2,7-Di-*t*-butyl**	**[e]-DiMe**[63]
non-annelated	δ -4.25 (**10**)	δ -4.25 (**10**)	δ -4.06 (**29**)	δ -4.25 (**10**)
benzannelated	δ -1.62 (**22**)	δ -1.85 (**24**)	δ -1.58 (**53**)	δ -0.78 (**45'**)
naphthannelated	δ -0.44 (**82**)	δ -0.74 (**84**)	δ -0.54 (**57**)	δ +0.72 (**46'**)
anthannelated			δ 0.004 (**59**)	δ +1.22 (**47'**)

[e]-DiMe series

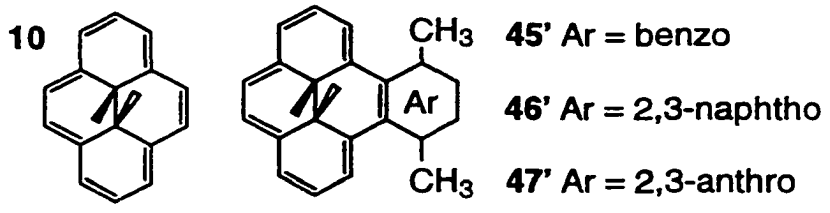

45' Ar = benzo

46' Ar = 2,3-naphtho

47' Ar = 2,3-anthro

The analogous [e]-annelated series **45', 46', 47'** was obtained by Lai and Chen[63], in which strain was definitely in evidence. Strain actually destabilized the DMDHP forms enough that the metacyclophanediene forms **45, 46, 47** (page 22)

were the thermally stable compounds. Photoisomerization allowed the proton NMR signals of the internal methyls of the DMDHP forms to be obtained. Inspection of the tabulated results reveals a large influence of strain on the proton NMR internal methyl signals.

3.1.6 Effects of annelation position and t-butyl substituents

In Table 5 above are chemical shifts for four analogous series. Plotting the internal methyl proton chemical shifts of respective series against other series brought out some points.

1) The plot in Figure 10 below of the **[e]-2,7-Di-*t*-butyl** series against the **[e]-2,7-H** series had slope 1.008, and a high correlation coefficient of 0.9997. This indicated that the influence of [e]-annelation was almost the same in the two series, with and with out the *t*-butyl groups, and that the influence of the *t*-butyl groups was constant. The *t*-butyls introduced a down field chemical shift of ~0.24 ppm.

2) The plot of the **[a]-2,7-H** series against the **[e]-2,7-H** shown in Figure 10 had a non unity slope, 1.09, with a high correlation coefficient of 0.99988. The effects of annelation in the [a] position were thus proportionately greater than in the [e] position. It appears that this effect was not due to increased strain in the **[e]-2,7-H** series. The **[e]-2,7-H** series had one more bay type strain interaction than the **[a]-2,7-H** series. Strain causes aromatic molecules to twist, perturbing the planarity of the system. This leads to lower π overlap and thus lower stabilization energy. If present in the **[e]-2,7-H** series, such strain induced

reduction in the π overlap would reduce ring current, and lead to larger down field internal methyl chemical shifts. Comparing the **[a]-2,7-H** and the **[e]-2,7-H** series as in Table 5 and Figure 10 shows that the reverse was true. The **[a]-2,7-H** series analogues were more down field than those of the **[e]-2,7-H** series.

3) The plot in Figure 11 below, of the **[e]-DiMe** series against the **[e]-2,7-Di-*t*-butyl** series indicated that the consistent strain effects in the **[e]-DiMe** series introduced a proportionate effect in chemical shift changes of 1.37 times those found for the **[e]-2,7-Di-*t*-butyl** series, with a correlation coefficient of 0.9991. The effect of strain on internal methyl chemical shifts as hypothesized in 2) above appeared to be present in the **[e]-DiMe** series. Each **[e]-DiMe** analogue internal methyl chemical shift was shifted ~1.37 times further down field from **10**, than the corresponding **[e]-2,7-Di-*t*-butyl** analogue internal methyl chemical shift from **29**. This relation was important because it provided clear evidence that the aromaticity of strained annelated fragments could be probed using [e]-fused DMDHPs. That is, for the **[e]-DiMe** series, the consistent strains introduced altered the sensitivity of the internal methyl chemical shifts to the resonance energies of the annelated fragments, but the linearity of response was maintained. Thus the use of [e]-annelated derivatives of **29** could be used to probe the aromaticities of other strained aromatics, with the provision that a series of derivatives be obtained, with the same types of strain interactions, throughout the series.

Figure 10

Internal methyl chemical shifts of respective series in table 5 plotted against [e]-2,7-H series internal methyl chemical shifts.

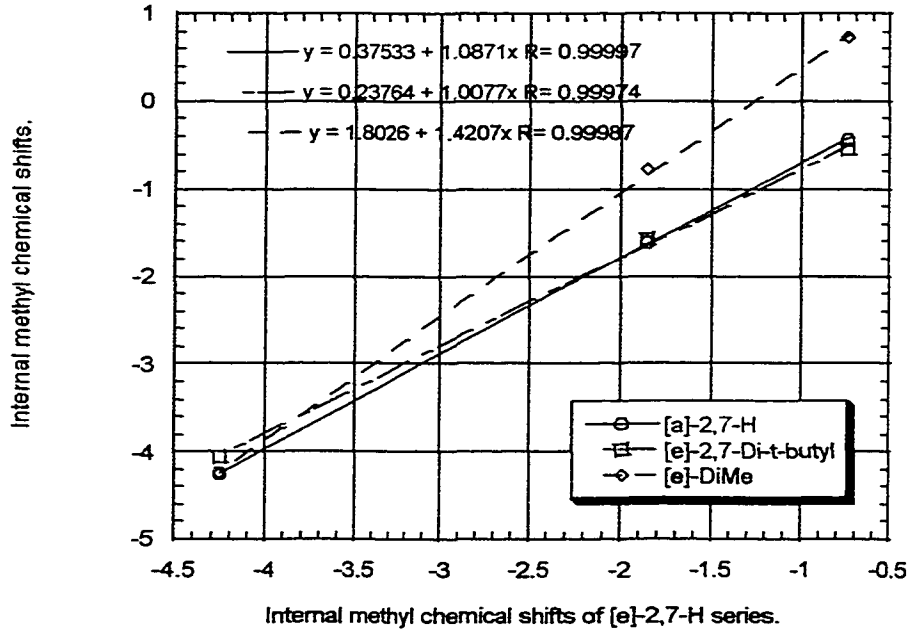

Figure 11

Internal methyl chemical shifts of respective series in table 5 plotted against the internal methyl chemical shifts of the [e]-2,7-Di-t-butyl series.

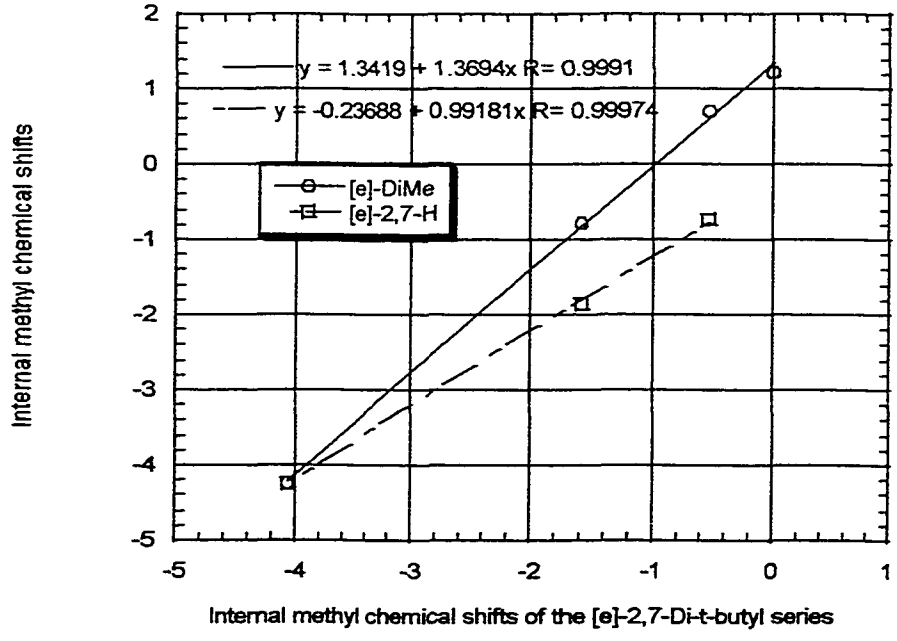

3.2 Photochromism

Introduction

DMDHP **10** and derivatives of DMDHP are intensely colored compounds. Colors displayed include greens, reds, purples and rarely blues. These colors depend on the visible light absorption patterns. DMDHP and its derivatives usually have four principle UV and visible absorption bands[60]. Two intense UV absorption bands occur in the 300 to 400 nm region, and two visible absorption bands of lesser intensity occur in the 400 to 800 nm region. Literature compound **29** followed the general pattern with absorptions at 340, 379, 476 and 645 nm [60]. The respective molar absorption coefficients[60] were 110000, 38000, 11000 and 810 $dm^3\ mol^{-1}\ cm^{-1}$.

Cyclophanedienes have absorption profiles deeper in the UV, as the chromophores are derivatives of benzene, with small amounts of conjugation. The cyclophanedienes range from colorless, to pale yellow.
Several intense absorptions usually occur in the 200 to 320 nm region [60]. The literature compound **29'**, (isomer of **29**), had absorptions at 220 and 240 nm, with molar absorption coefficients 36000 and 30000 $dm^3\ mol^{-1}\ cm^{-1}$ respectively[60].

One of the purposes of obtaining the series of annelated derivatives **53**, **57**, **59**, and **60** was to examine the effects of homologous annelation on the photoisomerizations and the properties of the photoisomers of the members of the series.

3.2.1 Benzannelated DMDHP 53

Benzannelated DMDHP **53** showed the four principle absorption bands characteristic of DMDHPs, and also some additional UV bands. Some red shifting from **29** was evident, as absorptions at 369, 388, 504, and 620 nm were found. Molar absorption coefficients were respectively 26400, 35000, 7000, and 400 $dm^3\ mol^{-1}\ cm^{-1}$. The additional UV bands were at 308 and 321 nm with molar absorption coefficients 24900 and 25500 $dm^3\ mol^{-1}\ cm^{-1}$ respectively. Irradiation of solutions of **53** with visible light caused rapid isomerization to **53'**. Figure 12 shows the absorption profiles of **53** and **53'**. The principle absorption of cyclophane **53'** was at 248 nm.

Proton NMR spectroscopy showed the conversion from **53** to **53'**. Figure 13 shows that conversion was virtually complete. For the purposes of NMR study, deuterio-toluene NMR solutions of 5 to 10 mg of **53**, chilled by ice water, irradiated with broad band light from a 250 W tungsten lamp, resulted in virtually complete conversion to **53'** in 5 to 10 minutes.

The bleaching process forming **53'** from **53** occurred rapidly irrespective of solvent deaeration. Photoisomerization occurred with broadband visible light, or with filtered light, using a 610 nm cut off filter. The return reaction of **53'** to **53** occurred on irradiation with 350 nm UV light. Return of **53'** to **53** was also effected by warming in solution. Thermal return reactions for the compounds studied are discussed further below.

Figure 12. The UV-visible absorption profiles of the isomers **53** and **53'** in cyclohexane.

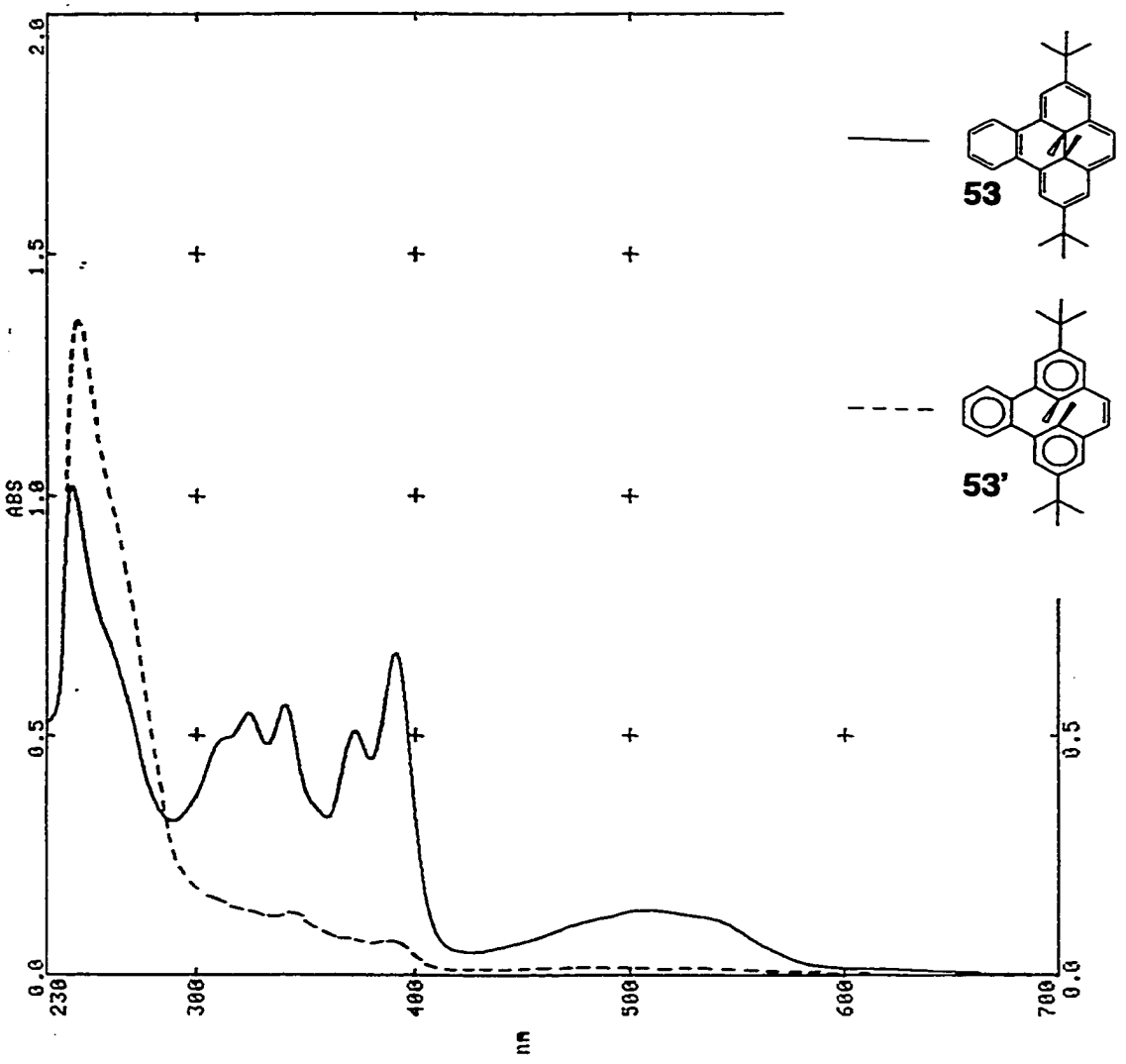

Figure 13. The parts of the proton NMR spectra of isomers **53** and **53'** in C_6D_6 showing the changes of the chemical shifts of the internal methyl and *t*-butyl proton resonances before (**53**) and after (**53'**) photoisomerization.

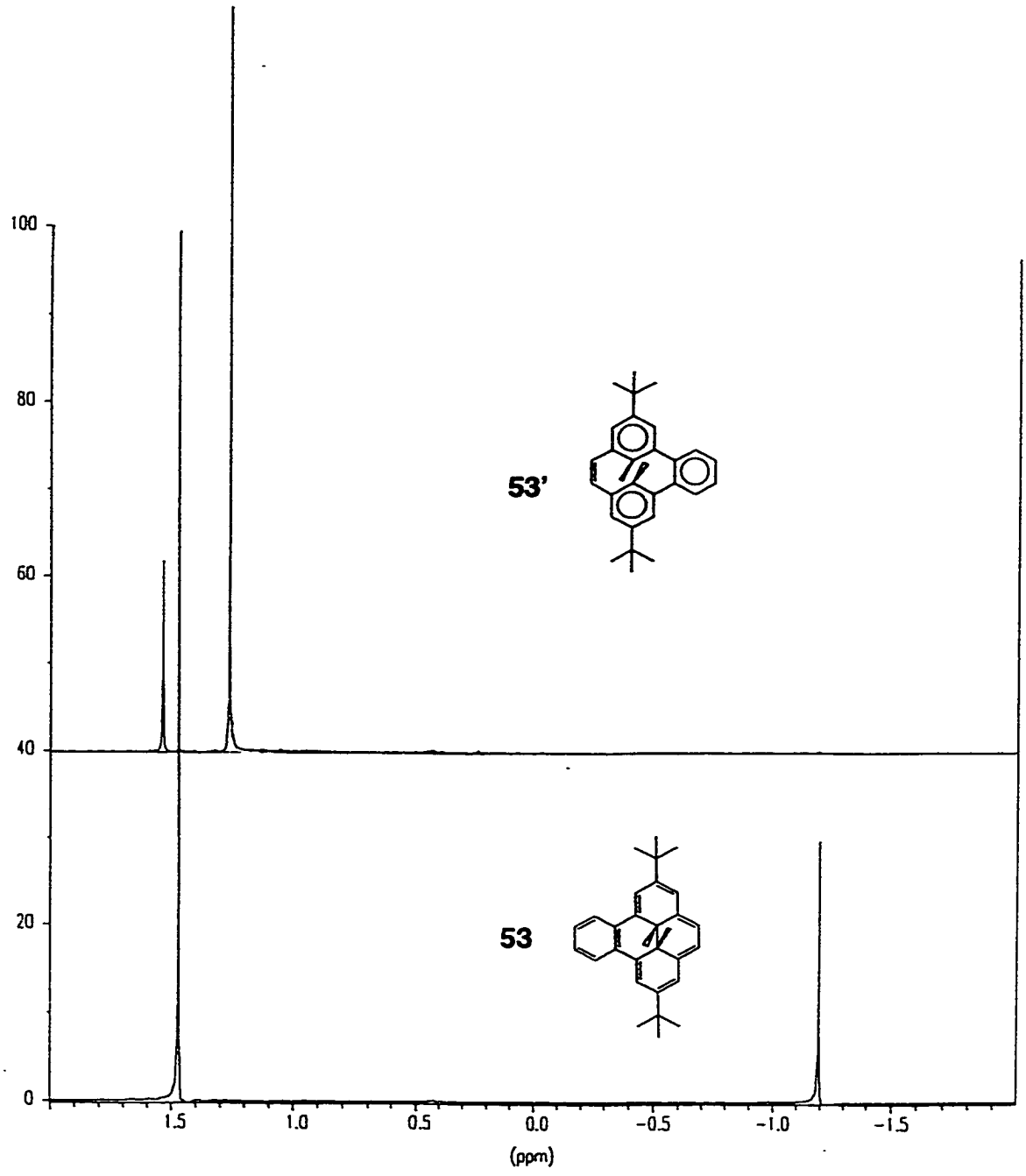

3.2.2 Naphthannelated DMDHP **57**

The naphtho[e]dimethyldihydropyrene **57** followed the pattern for DMDHPs, showing intense UV-visible absorptions, except that the longest wave band may have been over lapped by the larger visible band, which extended from 450 to 620 nm. Three UV-visible absorption bands were at 378, 398, and 553 nm. Molar absorption coefficients were respectively 31700, 41850, and 4200 $dm^3\ mol^{-1}\ cm^{-1}$. As would be expected, the UV-visible bands of **57** were red shifted from those of **53**. Additional UV bands also occurred at 262 and 321 nm with molar absorption coefficients 28500 and 25400 $dm^3\ mol^{-1}\ cm^{-1}$ respectively.

Compound **57** bleached rapidly in solution. Cyclophane **57'** had absorptions at 221, 251, and 269 nm, with molar absorption coefficients 46500, 43280 and 41480 $dm^3\ mol^{-1}\ cm^{-1}$ respectively. Proton NMR spectroscopy showed that virtually complete isomerization to **57'** was effected by broadband visible irradiation of deuterio-toluene solutions of **57**. For NMR studies, isomerizations were conducted using the same conditions as for **53** above, under which virtually complete conversion to **57'** occurred in 15 to 20 minutes. The internal methyl peak of **57**, at δ -0.06 in deuteriotoluene, disappeared and was replaced with a methyl peak at δ 1.60, after bleaching the NMR sample. The pyrene form **57** was reobtained by irradiating the bleached sample of **57'**, with 350 nm light, or by warming the solution. The thermal return reaction of **57'** to **57** was examined, and results are discussed further below.

3.2.3 Anthannelated DMDHP **59**

The anthro annelated DMDHP **59** was intensely green, and had UV-visible absorption bands at 393, 413, and 600 nm, red shifted from the analogous bands for **57**. Molar absorption coefficients were respectively 49700, 49500 and 4000 $dm^3\ mol^{-1}\ cm^{-1}$ for these bands. Additional absorptions were found at 225, 278, 304, and 325 nm, with molar absorption coefficients 45700, 45100, 49800, and 23000 $dm^3\ mol^{-1}\ cm^{-1}$.

Anthro annelated **59** was somewhat different than the benzo and naphtho analogues **53** and **57** above, in that photoisomerization was very slow. A deaerated NMR solution of **59** in deuterio-toluene irradiated under the same conditions as for **53** and **57** above resulted in ~75% conversion to **59'**, after 2 days. The proton NMR spectrum of the resulting solution showed that the internal methyl peak at δ 0.50 for **59** had decreased while a methyl peak at δ 1.63 for **59'** had grown in. The thermal reversion on **59'** to **59** was studied, and the results are discussed below.

3.2.4 Bis(dihydropyreno)chrysene **60**

The bis(dihydropyreno)chrysene **60** was intensely colored, appearing red in dilute solution, and almost black in crystalline form. Significant red shifting of the DMDHP UV bands was shown by **60**, with absorptions at 406 and 427. The visible absorptions were found at 527 and 576 nm. Molar absorption coefficients were respectively 70900, 132000, 10000 and 9600 $dm^3\ mol^{-1}\ cm^{-1}$, for these four

UV-visible bands. Additional bands occurred at 290 and 345 nm, with molar absorption coefficients 51600and 43400 $dm^3\ mol^{-1}\ cm^{-1}$ respectively.

The bis(dihydropyreno)chrysene **60** bleached in solution, on exposure to light. Solutions of ~5 mg **60** in deuterio-toluene for the purposes of NMR study, chilled by ice water and irradiated with broad band light from a 250 W tungsten lamp, resulted in almost complete conversion to **60"** in ~75 minutes. The internal methyl NMR signal at δ -0.22 for **60** disappeared and was replaced with methyl signals between δ 1.75 and 1.71 for **60"**, after the irradiation. See Figure 14. The structures of **60**, **60'** and **60"** appear in Figures 14 and 16 below.

The conversion of **60** to **60"** was also studied by UV-visible. The UV bands at 406 and 427 nm for a cyclohexane solution of **60** steadily decreased on exposure to light from a 600 nm cut off filter, using a 250W tungsten incandescent source. The resulting bleached solution of **60"** showed a principle absorption for the substituted chrysene, at 309 nm. The solution of **60"** was then exposed to sequential irradiation from a 350 nm source, to examine the return isomerization to **60**. The first UV bands to grow in were found to be at 394 and 416 nm, blue shifted from those of **60**. These new bands were ascribed to the third isomer **60'**. On continued exposure to 350 nm light, the new bands at 394 and 416 disappeared, and were replaced with the bands at 406 and 427, for **60**. The progress of the these isomerizations from **60** to **60"** and back to **60** as indicated by UV-visible absorption profiles can be seen in the Figure 15 and 16.

Figure 14. Photoisomerization of **60** to **60"** illustrated by proton NMR spectroscopy in C_7D_8.

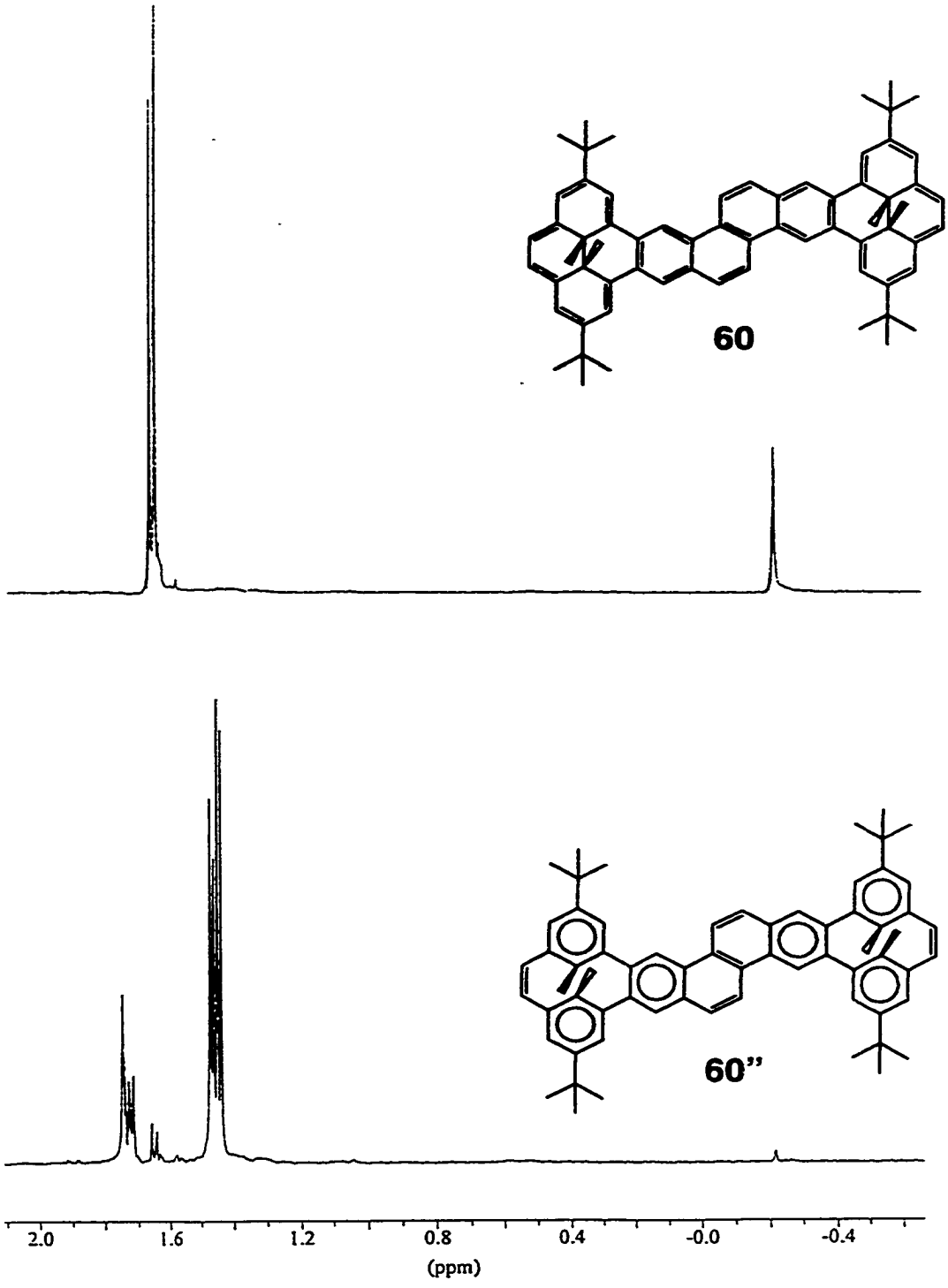

Figure 15. Photoisomerization of **60** to **60"** in C_6H_{12}, illustrated by the sequential decrease of the UV bands at 406 and 427 nm, with concomitant increase of the UV band at 311 nm.

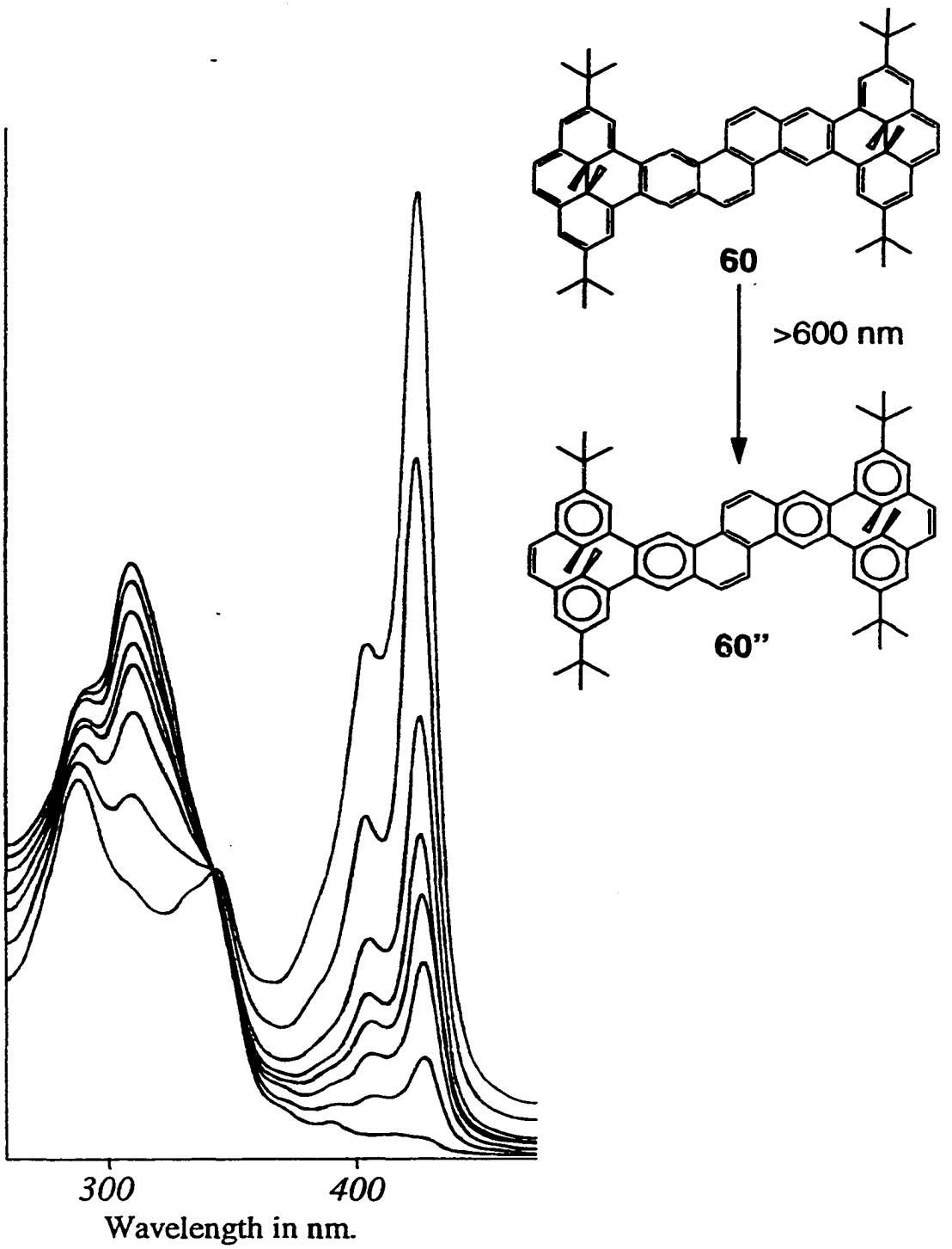

Figure 16. Return reaction of **60"** to **60'** to **60** in C_6H_{12}, stimulated by 350 nm UV light.

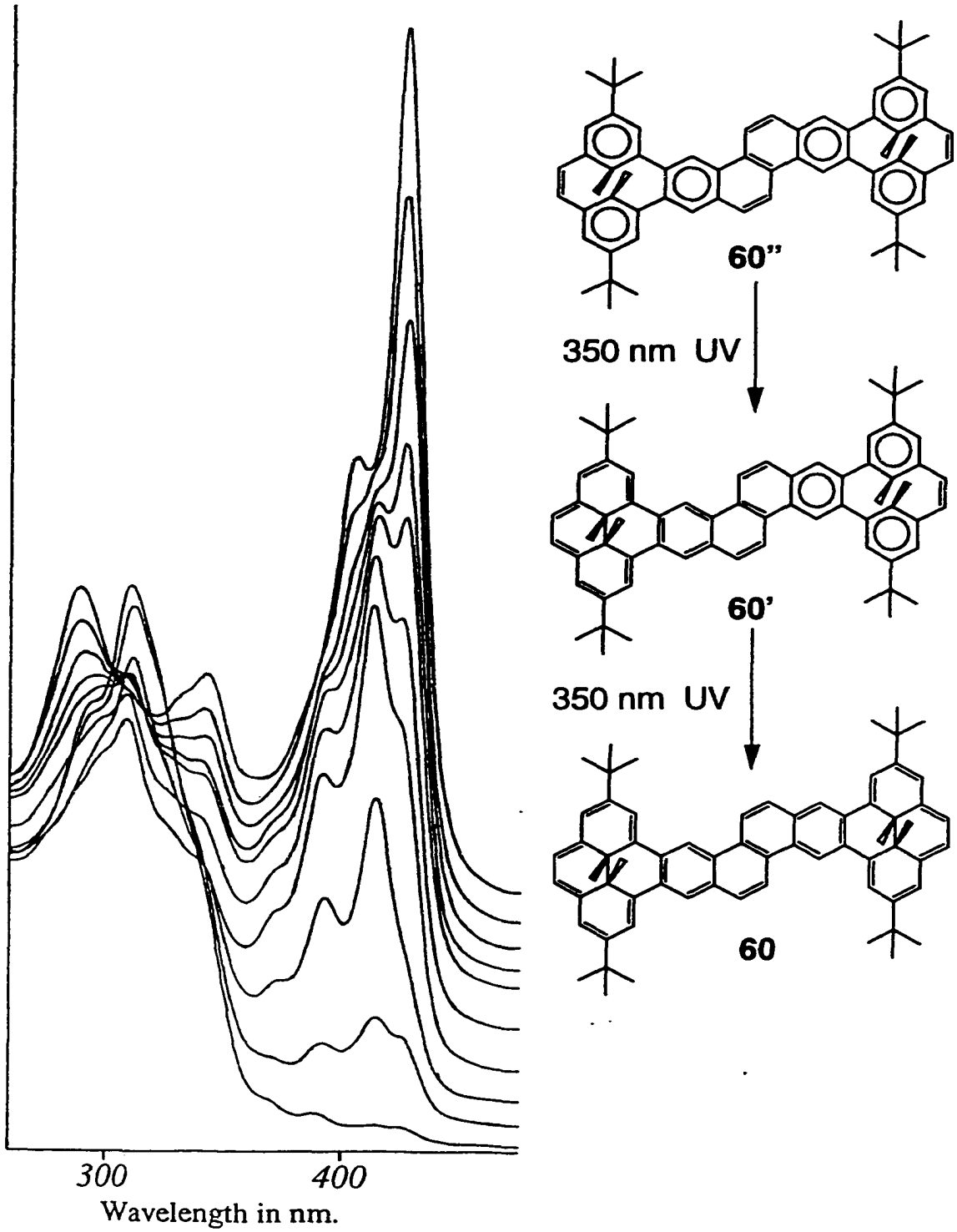

Proton NMR spectroscopy gave additional evidence for the third isomer, **60'**, in Figure 17. The internal methyl proton NMR peak for **60** was at δ -0.22, in deuterio-toluene. A new peak at δ -0.27 appeared during the thermal return of **60"** to **60**, and this new peak was ascribed to the isomer **60'**. Also, **60** showed two equal *t*-butyl proton NMR peaks, at δ 1.66 and 1.64. A new signal appeared at δ 1.62 in the thermal return, ascribed to **60'**, and the peaks at δ 1.66 and 1.64 were not equal. The new proton NMR signal at δ -0.27 which appeared for the thermal return of **60"** to **60** did not appear in the photoisomerization of **60** to **60"**.

The evidence from UV-visible and NMR experiments on the photoisomerization of **60** to **60"** appeared to indicate that **60** photoisomerized to **60"** with out passing through isomer **60'**. The fact that the near UV peaks for **60** diminished with out any shift in wave length, and the occurrence of an isosbestic point appeared to suggest that only two species, **60** and **60"**, were present during the photoisomerization of **60** to **60"**, see Figure 15. Proton NMR spectra taken during the course of the isomerization of **60** to **60"** did not show any new internal methyl signals. Evidence that **60'** could be obtained occurred in UV and NMR spectra obtained for the return of **60"** to **60**. Blue shifted near UV peaks at 394 and 416 nm occurred early in the UV induced return (Figure 16). These blue shifted peaks disappeared on further conversion, and were replaced by the absorption bands for **60** at 406 and 427 nm. The NMR spectrum of the thermal return of **60"** to **60** (Figure 17)showed a new peak at δ -0.27. This NMR peak at δ -0.27, and the UV peaks at 394 and 416 nm were taken as evidence for the third isomer, **60'**.

Figure 17. Proton NMR spectrum obtained in the thermal return of **60"** to **60**, in C_7D_8.

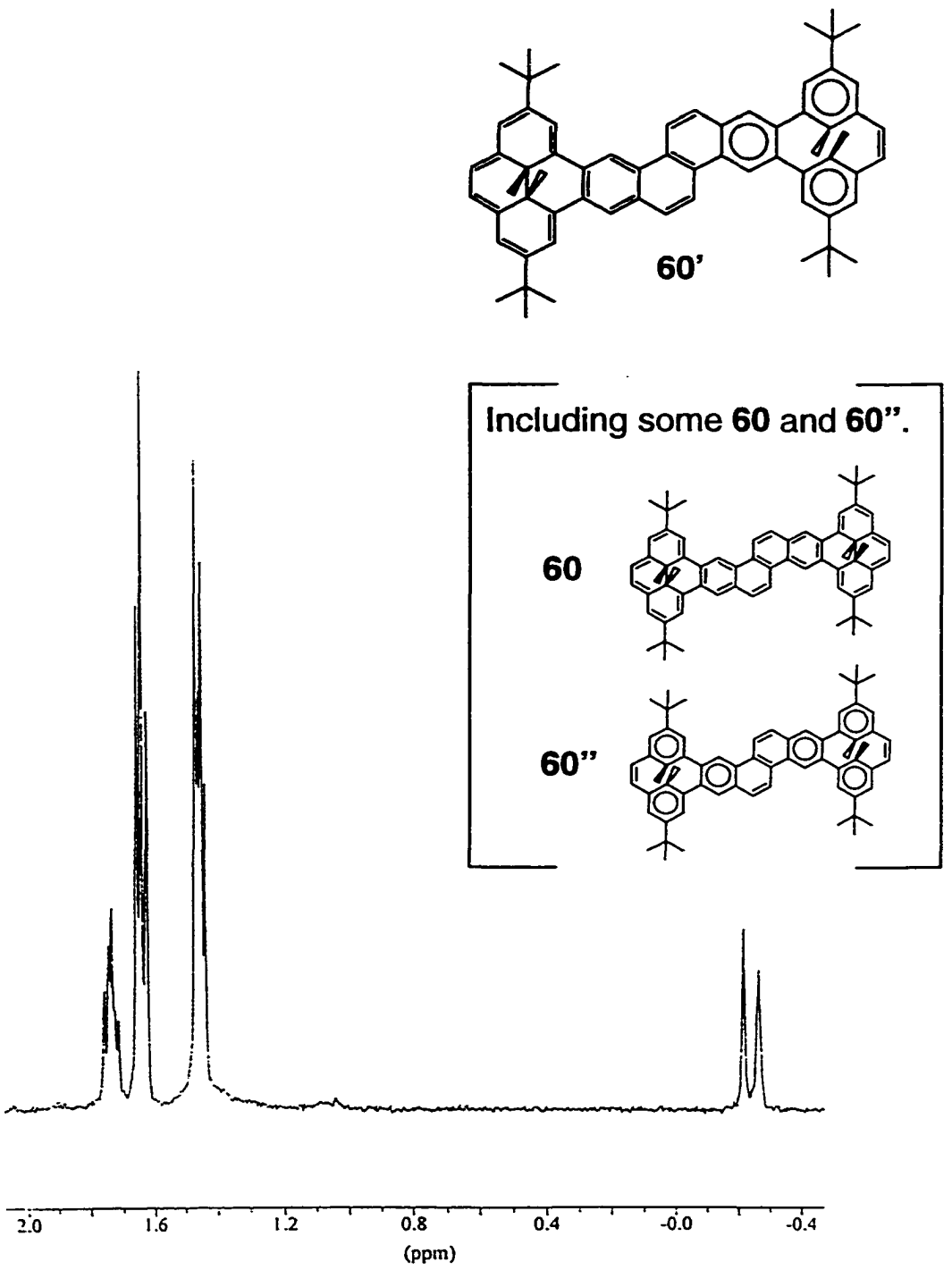

3.2.5 Three Position Photoswitch **68**

The mixed isomers of bis photoswitch **68** showed UV-visible characteristics of both component benzodihydropyrene and cyclophanediene fragments. Two near UV bands occurred at 390 and 408 nm, with molar absorption coefficients 29400 and 40500 $dm^3\ mol^{-1}\ cm^{-1}$ respectively. These were both red shifted from the corresponding peaks for benzodihydropyrene **53**, at 369 and 388 nm, by about 20 nm. Other bands for the mixed isomers of **68** were found at 520 and 640 (shoulder) nm, 4900 and 650 $dm^3\ mol^{-1}\ cm^{-1}$ respectively, also red shifted from **53**. Strong cyclophanediene absorptions occurred at 250 and 280 nm, with molar absorption coefficients 56800 and 52300 $dm^3\ mol^{-1}\ cm^{-1}$. Also, an absorption was found at 354 nm, with extinction coefficient 19900 $dm^3\ mol^{-1}\ cm^{-1}$.

Isomerization of **68** to **68'** occurred rapidly on irradiation with visible light, broad band, or filtered by a 600 nm cut off filter. Photoisomerization was accompanied by bleaching. The UV-visible absorption profiles of **68** and **68'** are presented in Figure 18.

Two isomers of **68** were found to exist. One isomer called **68a** was obtained on deoxygenation of the single isomer precursor **67** obtained by careful chromatography of the mixed isomers of **67** obtained by synthesis. A mixture of isomers, **68a** and **68b**, was obtained by deoxygenation after less rigorous purification of **67**. In deuterio-chloroform, for **68a**, the internal methyl proton signal was found at δ -1.37, while the internal methyl signal for the cyclophanediene was found at δ 1.18. The second isomer, **68b**, showed

Figure 18. UV-visible spectra of **68** and **68'** (mixed isomers), in C_6H_{12}.

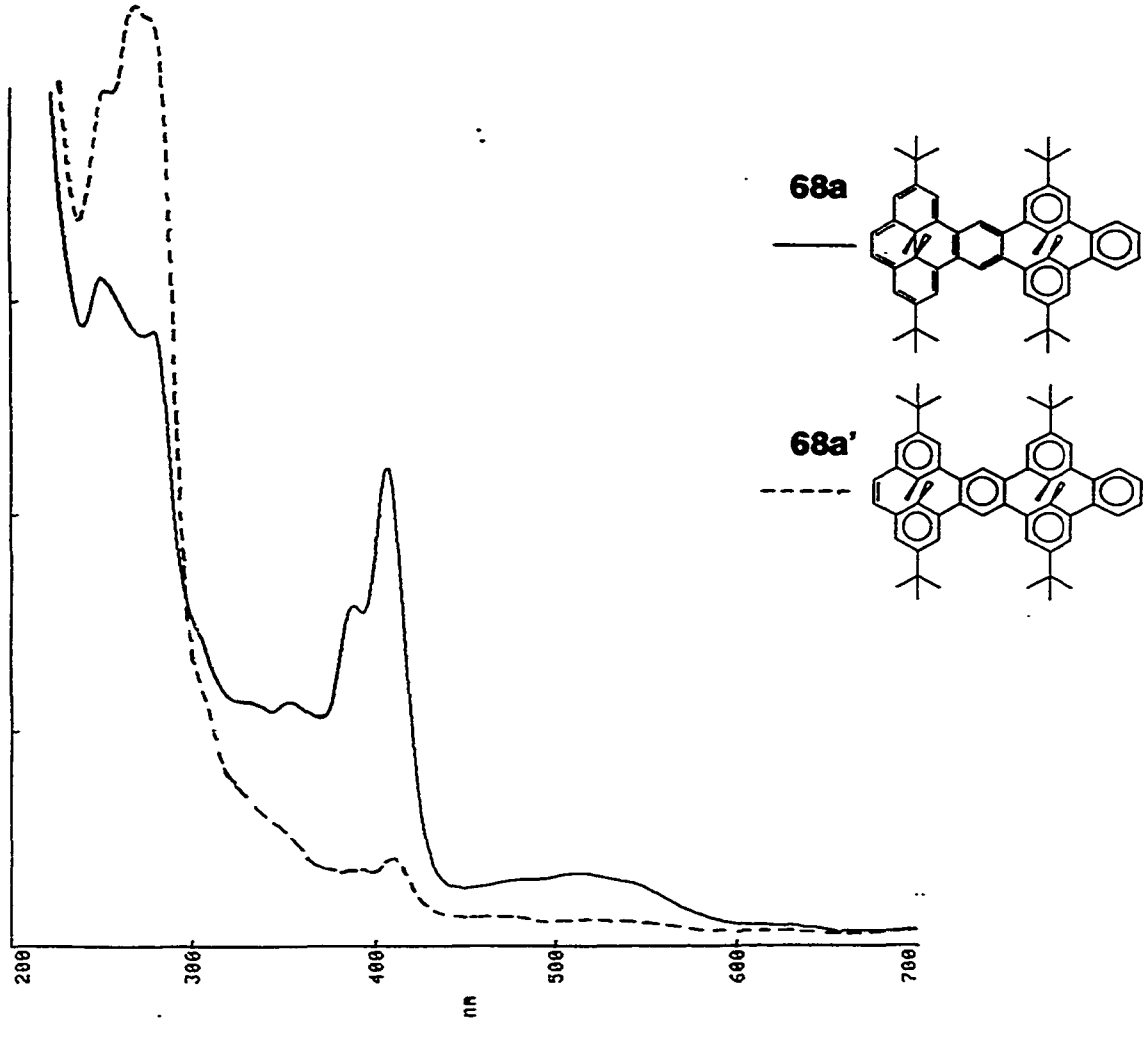

corresponding signals at δ -1.67 and 1.32, as calculated by subtraction of the spectrum of **68a** from that of the mixed isomers of **68**.

NMR Studies on the photoisomerization of **68** were conducted in deuterio-toluene on **68a**, in which the pyrene internal methyl proton resonance occurred at δ -1.01, while the cyclophanediene internal methyl protons were at δ 1.64. On photoisomerization to **68a'**, the internal methyl signals were found at δ 1.78 and 1.58. The results of the investigation on the thermal return of **68'** to **68** are discussed further below.

Compound **68** had a third possible photoisomer, **68"**, with two dihydropyrene fragments. To study the possibility of obtaining **68"**, laser flash photolysis (LFP) was selected, as it was anticipated that the thermal return of **68"** to **68** would be too rapid to study conveniently by other techniques. This rapid return of **68"** to **68** was anticipated because of the rapid return of **44'** to **44** as investigated by Yongsheng Chen[62].

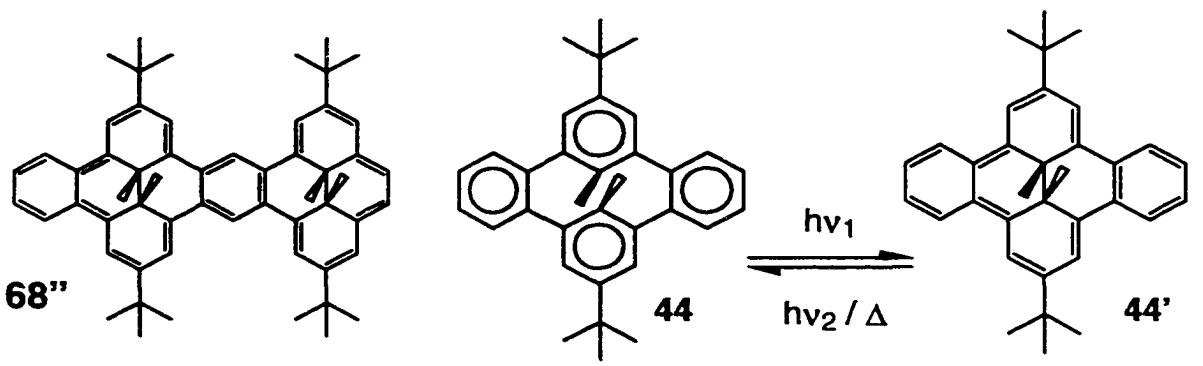

In the event, LFP study of a deaerated cyclohexane solution of mixed isomers **68** using laser excitation at 355 nm resulted in a transient spectrum

which showed bleaching of the 408 nm band of **68** and a large increase in absorption at 480 nm, for a transient species. The transient species was produced very rapidly, appearing promptly after the 10 ns laser pulse. The transient spectrum is below in Figure 19. The decay pattern of the transient was monitored at 480 nm. The decay pattern appeared to be first order, with a half life of ~0.10 s, at 20°C. The transient showed an absorbance change of ~+0.23 at 480 nm, while the 408 nm band of **68** had absorbance change of -0.055. This indicated that the extinction coefficient of the transient at 480 nm was significantly larger than the exinction coefficient of **68** at 408 nm. The UV-visible spectrum of the sample was reobtained after the LFP study, and found to be identical to that obtained before the LFP experiment.

The LFP data obtained were consistent for the photoisomerization of **68** to **68''**. Isomer **68''** would be expected to have UV-visible bands red shifted from those of **68**, from the more conjugated π framework of **68''**. The first order decay rate of **68''** to **68** would also be expected to be rapid, compared to thermal return rates for previously obtained systems as discussed in the introduction. An appropriate model system, **44** and **44'** had a half life of 3 minutes at -10°C[62]. The model would be expected to have a half life of about 2 seconds at 20 °C, based on the activation energy of ~20 kcal/mol[62]. Compound **68''** has more destabilizing interactions than **41** which would give it a shorter half life.

The only transient consistent with the LFP data was structure **68''**.

Figure 19. The transient spectrum obtained by LFP of **68a**, in cyclohexane.

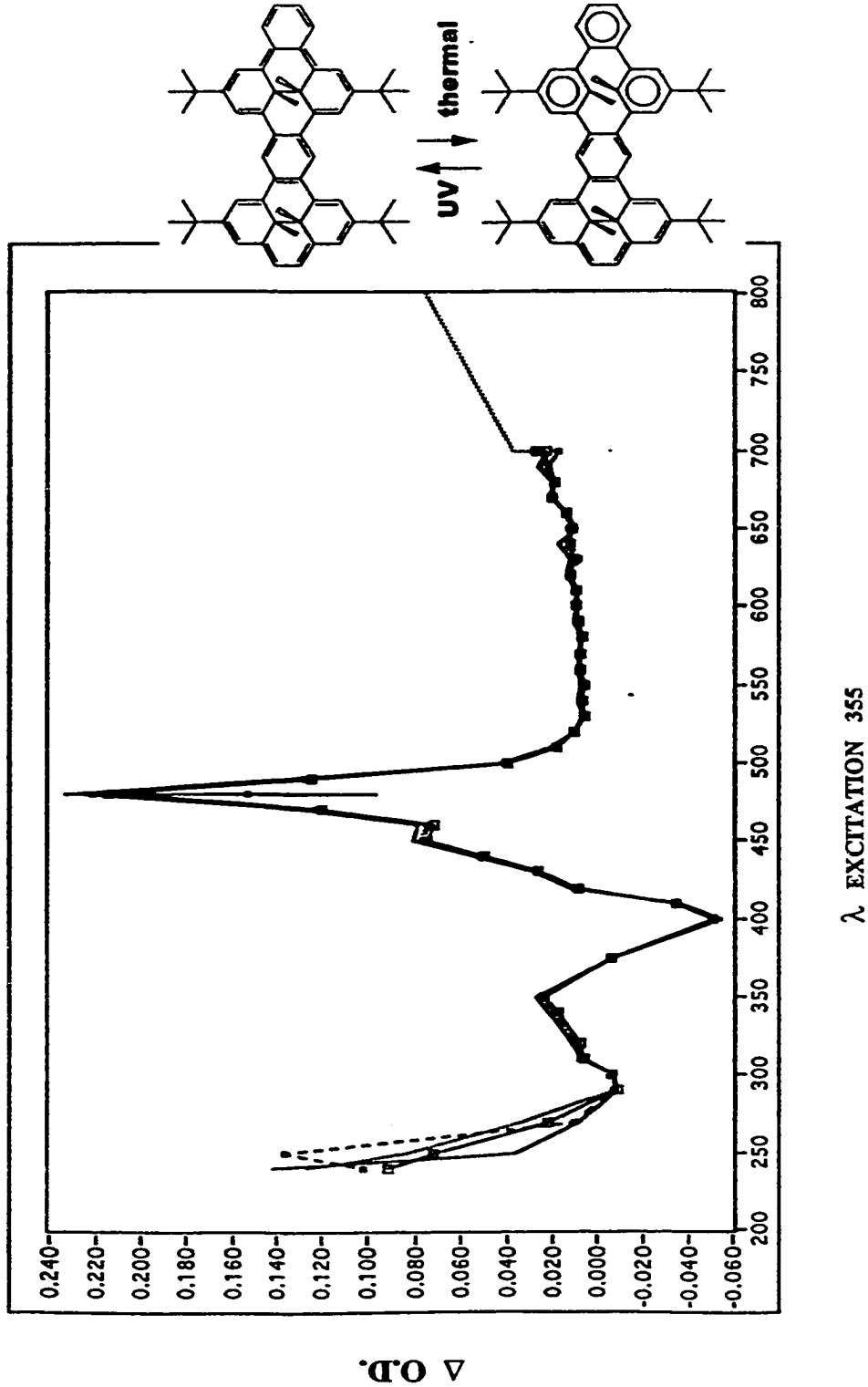

3.2.6 Furan **55**

The photochromism of furan annelated **55** was also tested. An NMR sample of 2 mg **55** in ~1 mL deaerated deuterio-toluene prepared as for other oxygen sensitive compounds (see section 5.1 p 124) was irradiated under the same conditions used for the other compounds. Complete isomerization of **55** to **55'** occurred in less than 5 minutes, as indicated by NMR spectroscopy. The thermal coloration reaction of **55'** is discussed below. Attempted coloration of **55'** with 350 nm UV light did show some isomerization to **55**, but additional small NMR peaks showed that some decomposition accompanied photoisomerization with UV. Photo-isomerization of **55** to **55'** with visible light appeared to be without significant side reactions, as the only detectable peaks in the NMR spectrum were assignable to **55'**.

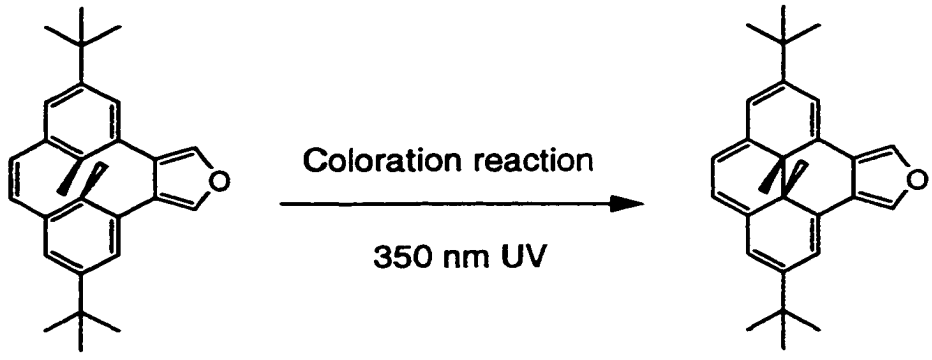

55' **55**

3.3 Thermal Coloration Studies

With the acene series **53, 57,** and **59** of annuleno derivatives of **29**, the influence of annelation on thermal coloration rates of the respective photoisomers **53'**, **57'**, and **59'** was examined. The coloration rates for the photoisomers of **29, 65, 60, 68a**, and **55** were also examined. The coloration reactions were the thermal return reactions of the metacyclophanediene (MCD) photoisomer forms to the highly colored dimethyldihydropyrene (DMDHP) forms as shown below. Such thermal return reactions have been found to follow first order kinetics[59], and the results obtained in this study were found to follow first order kinetics. For comparison, the reaction rates and the half lives of the thermal return reactions for the seven compounds at 46 °C are shown below in Table 6. Kinetic rates and half lives for the thermal return reactions for the seven compounds at the temperatures studied are found in Appendix 1. The results in Table 6 summarize some of the trends found in the kinetic results in Appendix 1.

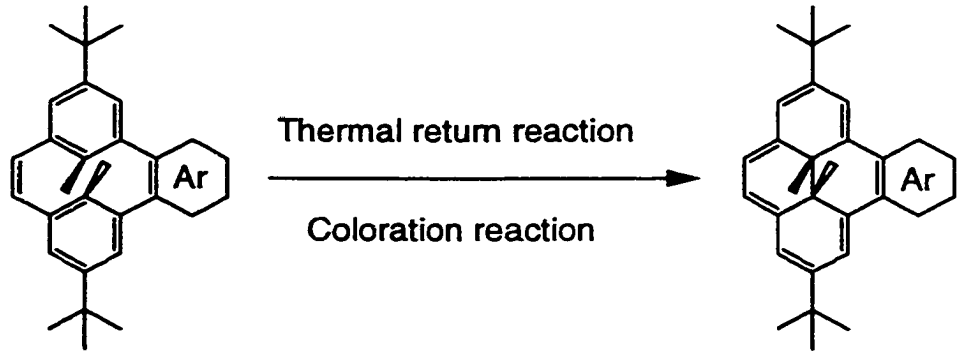

metacyclophanediene (MCD) form, colorless.

dimethyldihydropyrene (DMDHP) form, colored.

Table 6 Coloration rates at 46°C.

Coloration reaction	rate/(min^{-1}) at 46°C	$t_{1/2}$
53' to **53**	0.00200 ± 0.00005	5.75 h
57' to **57**	0.0101 ± 0.0003	1.15 h
59' to **59**	0.0344 ± 0.0009	0.33 h
29' to **29**	0.00610 ± 0.00012	1.88 h
65' to **65**	0.00124 ± 0.00003	9.50 h
60'' to **60**	0.0057 ± 0.0002	2.03 h
68a' to **68a**	0.00224 ± 0.00006	5.16 h
55' to **55**	0.000183 ± 0.000006	63.3 h

In the acene series **53'**, **57'** and **59'**, the return rate was slowest for the benzo derivative **53'**, and most rapid for the anthro derivative **59'**. This ordering was found at the other temperatures studied. The slowest coloration rate of the seven benzenoid annelated compounds studied at any single temperature was for the dibromide derivative of the benzo system, compound **65'**. The three benzannelated systems, **53'**, **68a'**, and **65'**, were consistently slower than the higher annelated compounds, **57'**, **60''**, and **59'**. Heteroannelated furan **55'** had the slowest coloration rate of all.

After obtaining the kinetic data for the coloration reactions, Arrhenius and Eyring plots were used to determine the activation parameters of the reactions [82]. The derived parameters are shown below in Table 7. The Arrhenius and Eyring plots are in Appendix 1. Included in Appendix 1 is a discussion of errors in the rates obtained, and the activation parameters.

Table 7.

Activation parameters derived from the kinetic results in Appendix 1.

reaction	E_{act}/(kcal/mol)/(kJ/mol)	$\Delta H^{\ddagger}$(kcal/mol)/(kj/mol)	$\Delta S^{\ddagger}$(cal/deg/mol)
29' to **29**	24.0 ±0.5 / 100.3 ±2.0	23.3 ± 0.5 / 97.5 ± 2.0	4.3 ± 1.0
65' to **65**	25.8 ±0.8 / 107.9 ±3.2	25.0 ± 0.8 / 104.4 ± 3.2	6.2 ± 1.3
53' to **53**	24.5 ±0.6 / 102.6 ±2.5	23.9 ± 0.6 / 99.9 ± 2.5	3.8 ± 1.0
57' to **57**	22.1 ±0.5 / 92.4 ±2.1	21.4 ± 0.5 / 89.6 ± 2.1	-0.7 ± 0.8
59' to **59**	19.1 ±1.2 / 79.8 ±5.0	18.4 ± 1.2 / 77.1 ± 5.0	-7.4 ± 3.0
60'' to **60**	24.3 ±0.6 / 101.7 ±2.6	22.6 ± 0.6 / 94.8 ± 2.6	5.1 ± 1.0
68a' to **68a**	24.1 ±0.8 / 100.8 ±3.2	23.4 ± 0.8 / 98.0 ± 3.2	2.9 ± 1.2
55' to **55**	26.1 ±0.6 / 109.9 ±2.5	25.2 ± 0.6 / 105.4 ± 2.5	-3.3 ± 0.9

3.3.1 The Acene series

In the simple acene series **53'**, **57'** and **59'**, it can be seen from Table 6 (and Appendix 1) that the rates of thermal return increase with each additional fused benzene ring. Thus coloration rates increased as the resonance energies of the annelated fragments increased. From Table 7 it can be seen that the effect of annelation was opposite on the activation energies and activation enthalpies. That is , as the resonance energies of the annelated fragments increased, the activation energies and enthalpies decreased. Resonance energies of annelated fragments normalized to RBLEs were found above to correlate well with the chemical shifts of the internal methyls (δ(Me)) of the annelated dihydropyrenes. Thus plots were constructed of the activation

enthalpies and energies respectively against the RBLEs of the annelated fragments, and the δ(Me)s of the dihydropyrene isomers. The plots are shown below in Figure 20 and 21.

It can be seen from the plot in Figure 20 that a modest correlation was found between the respective activation energies and enthalpies, and the chemical shifts of the internal methyls of the annelated dihydropyrene isomers. Figure 21 shows that the activation enthalpies and energies respectively decreased at a rates of 6.4 and 6.3 kcal/(unit RBLE). Since the resonance energy of benzene was 0.869 eV[45], the activation enthalpies and energies decreased at between 7.4 to 7.2 kcal/eV.

The dependence of the activation enthalpies and energies on the resonance energies of the annelated fragments found above parallels the situation reported by Irie for the dithienylethenes[51]. It was found that the thermal return rates of the photoisomers of several diarylethene systems was faster when the stabilization energies of the arenes was larger. Thiophene has one of the lowest resonance energies of arene systems, and the dithienylethene photo-systems based on thiophene have the slowest thermal return rates for the respective photoisomers. Both the dithienylethene and the [e]-annelated dimethyl-dihydropyrenes are related to the *cis*-stilbene to dihydrophenanthrene photo-system. One difference between diarylethene type photo-systems with varied arene stabilization energies, and the [e]-annelated

Figure 20

Activation energies and enthalpies for the thermal return reactions plotted against the chemical shifts of the internal methyls of the respective dihydropyrene forms.

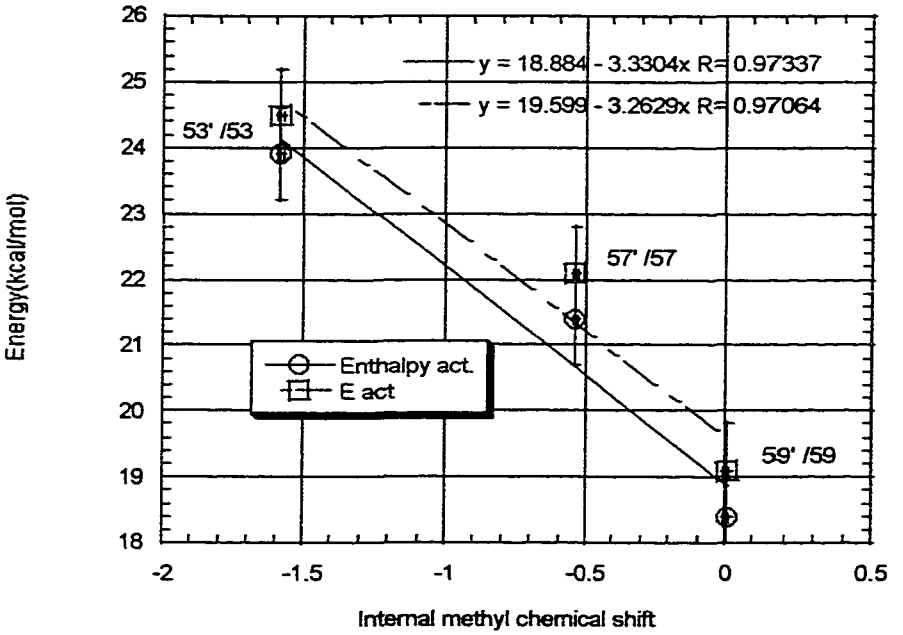

Figure 21

Activation energies and enthalpies for the the thermal return reactions plotted against the RBLEs of the respective annelated fragments for the acene series.

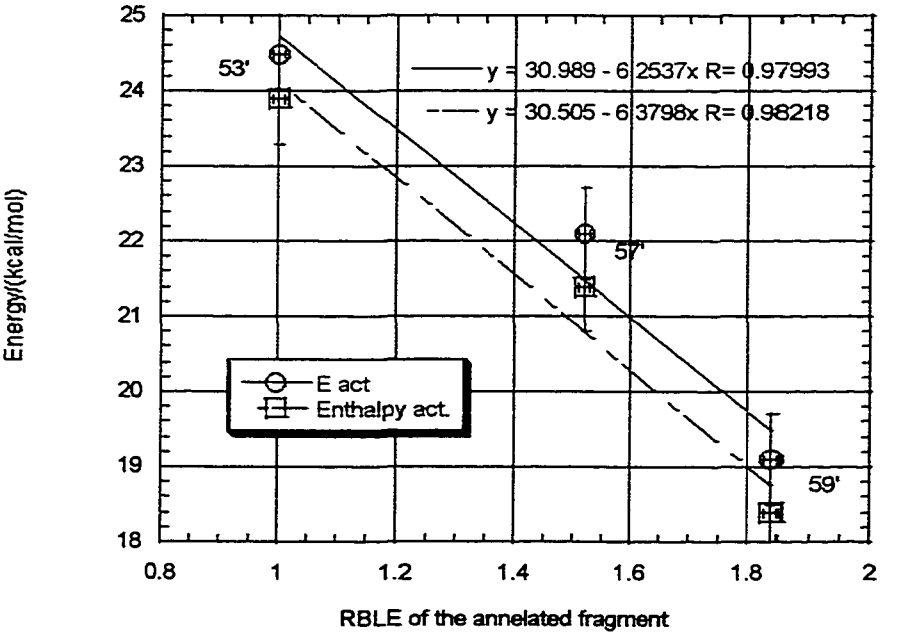

DMDHP photo-systems studied here was that the fragments with varied aromatic stabilization energies were located in different parts of the molecules. In the diarylethenes, the fragments with differing stabilization energies were directly involved in the electrocyclization reaction. In the [e]-annelated DMDHP derivatives studied here, the arene fragments varied did not themselves directly electrocyclize with another fragment.

Diarylethenes: Arene involved in electrocyclization varied.

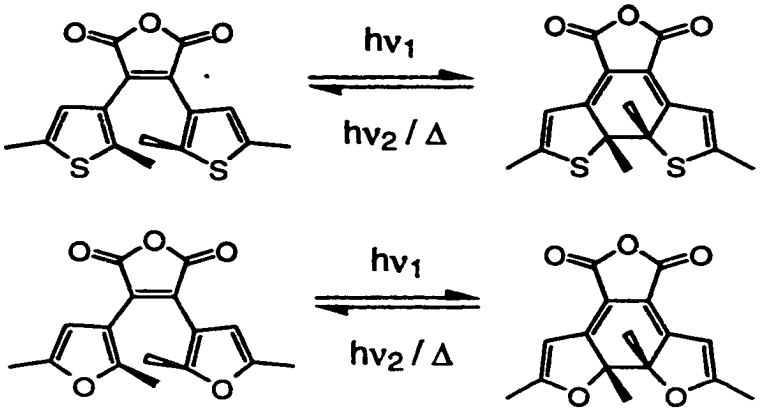

[e] annelated DMDHP derivatives:
arene varied not directly particitant in electrocyclization.

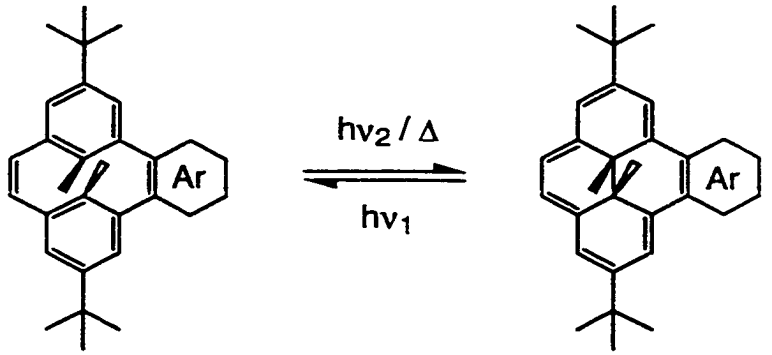

MCD form DMDHP form

Calculations of the energy differences between respective photoisomers of the acene series studied here showed small energy differences between the photoisomers. Calculated values of ΔH_f[83] for some of the compounds are shown below in Table 8. For example, the difference in the heats of formation for the benzo system **53'** and **53** was calculated to be ~1.5 kcal/mol. A similar low value was calculated for the naphtho system **57'** and **57**, ~1.1 kcal/mol. The differences in the transition state energies was larger than could be accounted for from differences in the ground state energies. Thus it appeared that some other effect was responsible for the coloration rate differences found in the acene series **53'**, **57'**, and **59'**.

The most likely origin of the coloration rate differences in the acene series was the stabilizing effect of resonance in the transition states. From Figure 21, the transition states energies and enthalpies decreased at a rate of ~7.3 kcal (~0.32 eV) for each eV of additional resonance energy of the annelated fragment. The MCD forms showed little resonance interaction between the ethene, the phenyl rings, and the respective annelated fragments, as evident from the UV-visible spectra. The DMDHP forms show large influences of resonance, as displayed by the intense UV-visible absorptions. One of the principle UV bands red shifted through the series **29**, **53**, **57**, to **59**, from respectively 379 to 388 to 398 to 413 nm. The transition state would probably have resonance interactions between the annelating fragment and the [14] annulene transition state, intermediate between the resonance in the DMDHP

and the MCD forms, because the transition state would not be expected to be as planar as the DMDHP form, nor as strained as the MCD form. Thus the transition state energies would experience different degrees of resonance stabilization relative to the ground state MCD forms, depending on the resonance energies of the respective annelated fragments. From this, anthro annelation would be expected to stabilize the transition state more than naphtho and benzo fragments. Benzannelation would be expected to stabilize the transition state the least amount of the three acenes. The observable consequences of the transition state stabilization by resonance interaction with the annelated fragments would be that the order of rates would be from fastest to slowest, anthro>naphtho>benzo, in the absence of any other effects.

Table 8 Activation Energies and ΔH_f for the coloration reactions to form the listed compounds from the respective photoisomers.

compound	E_{act}/(kcal/mol)	ΔH_f (kcal/mol)[83]
10	22.2[60]	3.36
10	23.2[59]	3.36
29	21.7[60]	2.27
24	25.1[61b]	
81	25.2[61d]	
29	24.0	2.27
53	24.5	1.47
57	22.1	1.12
59	19.1	0.96

3.3.2 The isomerization of metacyclophanediene **29'** to DMDHP **29**

In light of the results obtained above for the acene series, the coloration of **29'** to **29** would appear incongruous. The coloration of **29'** to **29** was only slightly slower than for **57'** to **57**, and the activation energy was similar to that for **53'** to **53**. The fact that **29'** and **29** lacked the additional annelation made the cases fundamentally different. In the **29'** system, two phenyl rings were bridged by two ethenes. In the acene series, two phenyl rings were bridged by an ethene, and an arene. Thus the cases had different strain interactions. An arene bridge would require more energy to distort, than an ethene.

3.3.3 Dibromide **65'** to **65**

Of the benzenoid annelated systems studied, the system with the largest activation energy and enthalpy and with the slowest thermal coloration rate, was for **65'**, the dibromide derivative of **53'**. The effect of the two bromines would be expected to raise the activation barrier for the thermal return, from the large van der Waals radius of bromine, ~2.0 A. The two bromines would sterically resist going into the more planar structure of the DMDHP form **65**, than the two hydrogens they replaced, in **53**. The bromines in **65** would have larger peri-type interactions with close by hydrogens, than would occur for the hydrocarbon **53**.

3.3.4 The coloration of **68a'** to **68**

The bis switch system, **68a'** to **68a** had coloration rates and activation parameters quite similar to the analogue system **53'** to **53**. The coloration reaction of **68a'** to **68a** was for the mono-benzannelated cyclophanediene portion of **68a'**, as was readily determined by the chemcal shifts fo the methyl groups. (The proton NMR spectrum of the dibenzo compound **44'** had internal methyl chemical shifts at δ -3.41, while **53** had δ(Me) at -1.58 ppm. Thus the product of coloration did not have a dibenzopyrene structure like **44'**. See pages 98 and 99 for structures.) The activation energy and enthalpy determined for **68a'** to **68a** were comparable to those for **53'** to **53**, within experimental error .

The coloration rates for **68a'** were slightly faster than those of **53'**. Thus the extra cyclophane portion of **68a'** had only a small effect on the coloration reaction. For a first approximation, the photoisomer system **68a'** to **68a** behaved as did the **53'** to **53** system. Also, the photoisomerization of **68a** to **68a'** was rapid, similar to that found for the photoisomerization of **53** to **53'**.

3.3.5 The bis(dihydropyreno)chrysene system

The final coloration reaction studied was for the bis pyrenochrysene system of **60''**, **60'**, and **60**. The coloration reaction of **60''** was complicated by the formation of a third isomer, **60'**. Since overlapping NMR signals occurred for the methyl proton signals used to determine rates, individual transformation rates could not be identified. Although the internal methyl signal of **60'** was distinct from that of **60** in the NMR spectrum, deconvolution of the

cyclophanediene methyl signals for **60''** and **60'** was not possible. Thus the apparant overall rate of coloration based on the sets of cyclophanediene methyls and the dihydropyrene methyls was determined.

Of the annelated systems studied, the coloration of **60''** to **60'** to **60** was most similar to that of the naphtho system **57'** to **57**. To understand the effect of the chrysene linker in **60''** on the thermal return reactions, it was useful to consider the effective RBLE of the chrysene linker in **60** and **60'**. The fact that **60** had symmetry about the central fusion between the two 1,2 fused naphthalenes in the chrysene linking the two attached dihydropyrenes, meant that the resonance energies to be used in the RBLE equation (7) (page 71) could not be unambiguously estimated. Thus the chemical shift of the internal methyl of **60** (δ -0.74, $CDCl_3$) provided an entry into the problem. The RBLE estimated for the chrysene linker in **60** from equation (10) was 1.41. The proton NMR spectrum showed that **60'** had δ(Me) ~0.05 ppm upfield from that of **60**. Thus the RBLE of the chrysene system would be 1.39 for **60'**.

Since the RBLE of 2,3 fused naphthalene was 1.52 (Table 3), it could be expected that each coloration from **60''** to **60'** to **60** would have rates similar to the naphtho system **57'** to **57**. Two isomerizations were involved, and so an overall rate from **60''** to **60** approximately half that of **57'** to **57** might be anticipated, as each step from **60''** to **60'** to **60** would occur at about the rate for **57'** to **57**. In the event, at 46°C, the rate for coloration of **57'** to **57** was found to be 0.0101 ± 0.0005 min^{-1}, while for **60''** to **60** overall was 0.0057 ± 0.0003 min^{-1}, close to half that for the naphtho system.

3.3.6 Furanometacyclophane 55' to 55

In light of the behavior noted above, that the activation energies and enthalpies decreased for the coloration reactions as the resonance energies of the annelating benzenoid fragments increased, it was of some interest to see that the coloration rates for furan **55'** were the slowest of all the compounds studied. Thus an attempt was made to correlate the free energies af activation for the colorations with the respective resonance energies of the annelating fragments. The free energies of activation ($\Delta G^{\ddagger}$) at 60°C were calculated from the activation parameters in Table 9, according to

(14) $$\Delta G^{\ddagger} = \Delta H^{\ddagger} - T\Delta S^{\ddagger}.$$

The free energies of activation calculated at 46°C and 70°C were within 0.1 kcal/mol of the values calculated at 60°C (333 °K).

Table 9 Free energies of activation, and resonance energies.

compound	$\Delta G^{\ddagger}$/(kcal/mol) at 60°C	RE/eV[45,84]	exp{-RE/eV}
55'	26.3 ± 0.6	0.187	0.829
53'	22.6 ± 0.6	0.869	0.419
57'	21.6 ± 0.5	1.323	0.266
59'	20.9 ± 1.2	1.600	0.202

From a plot of $\Delta G^{\ddagger}$ against RE (Figure 22), it appeared that there was an inverse exponential relation between $\Delta G^{\ddagger}$ and RE. A plot of $\Delta G^{\ddagger}$ against exp(-RE) was made, which showed significant correlation (Figure 23). The relationship derived from Figure 23 was

(16) $\Delta G^{\ddagger} = ([8.52\exp\{-RE/eV\}] + 19.20)$ kcal/mol $\quad R = 0.9986$

In the limit, for RE = 0, $\Delta G^{\ddagger} = 27.7$ kcal/mol. At the other extreme, for exp(-RE/eV) = 0, $\Delta G^{\ddagger} = 19.2$ kcal/mol.

Figure 22

Plot of the free energy of activation against Resonance Energy of the annelating fragment.

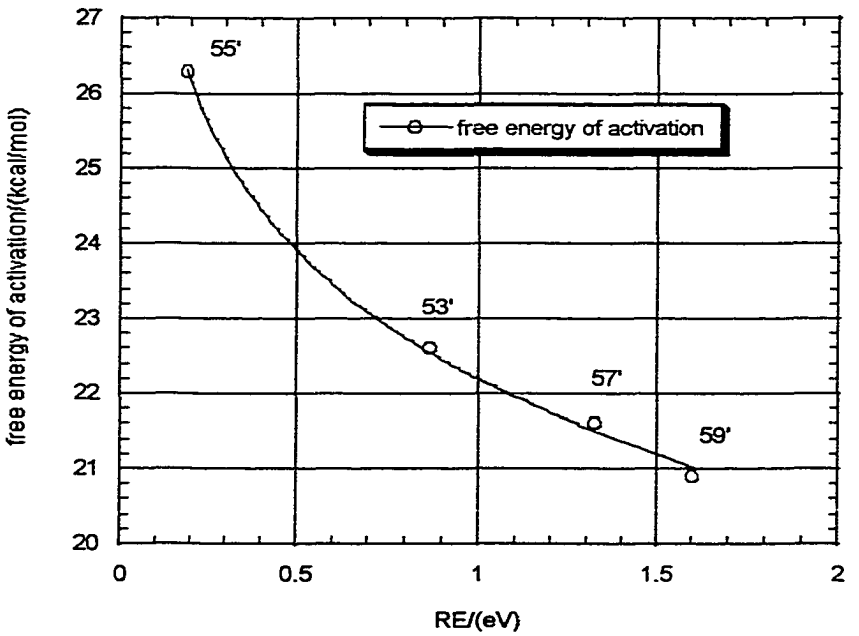

Figure 23

Plot of the free energy of activation against exp{-RE/eV} for the annelating fragments.

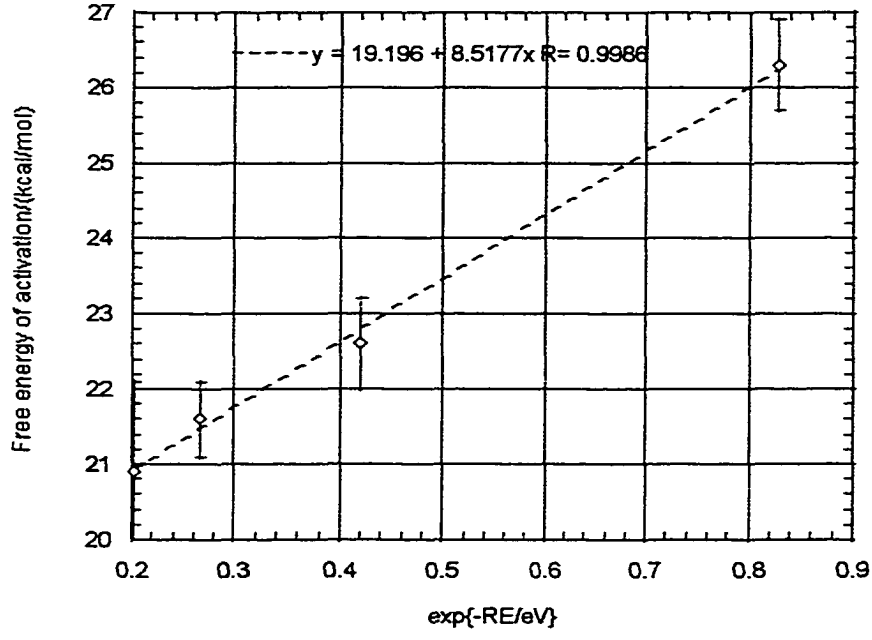

The relation between $\Delta G^{\ddagger}$ and exp(-RE/eV) would appear to help discriminate bond localizing effects from resonance effects. The annelating furan in **55** had the greatest effect on δ (Me) of all the [e]-fused DMDHP compounds studied here, but furan has the lowest RE of all the annelating fragments, 0.187 eV[84]. In contrast, the annelating anthro fragment in **59** also had a very large effect on δ(Me) but anthracene has the largest resonance energy of the annelating fragments studied here, 1.600 eV. Thus for arbitrary annelating fragments, it would be difficult to tell from δ(Me) alone what the resonance energy of the fragment would be. Differentiation of bond localizing effects from

resonance effects for arbitrary fragments may be possible with the relation of $\Delta G^{\ddagger}$ to exp(-RE) found above for coloration reactions.

Other factors may influence the changes observed in rates for different annelating fragments. It was suggested above that differences in the ΔH_f between MCD and DMDHP forms were not responsible for the rate differences and transition state energy differences through the series of colorations examined. When an MCD form isomerized to a DMDHP form, the annelating fragment would lose some of its aromaticity. This loss would vary through the series. The furan in **55'** would lose only little aromaticity, while the benzo in **53'** would lose somewhat more aromaticity on coloration. The isomerization process would be affected according to the Hammond postulate, by such ground state differences. The effects would be counter to the transition state stabilization effects. The anthro fragment would lose the most aromaticity on coloration of **59'**, and the furan in **55'** would lose the least aromaticity on coloration. It would appear that the transition state effects were more important than the ground state effects.

For heteroannelating fragments, such as the furan in **55'**, an additional factor would be the symmetry of fusion. That is, the [c]-fused furan in **55'** would have a different affect on the transition state for coloration than a [b]-fused furan. This is because molecular orbitals of furan of different energies would interact at the transition state for [b] and [c]-fusion.

It would be very interesting to see the effect on activation parameters of annelating DMDHP with various heterocycles of low resonance energies, and with different fusion positions. An experimental method of estimating resonance energies for benzenoid aromatics, heterocycles, and other aromatics would be of some value. Increasing the stability of the systems to oxygen would also be very useful. The significance of resonance interactions at the transition states might have interesting consequences for systems with antiaromatic interactions. The activation barriers might be raised above the 27.7 kcal/mol value estimated for annelating fragments with no resonance energy.

3.4 Future work

Several interesting derivatives of DMDHP **29** could be pursued, as a result of this work. The utility of **55** for synthesizing [e]-annelated dihydropyrenes could be explored using such aryne synthons as 1-bromonaphthalene, 4-bromophenanthrene, or 1-bromopyrene. The targets of such syntheses would be useful for investigating strain effects using the NMR probe capabilities of DMDHP. Also, such targets would help to investigate strain effects for the coloration reactions of the respective MCD forms of the product DMDHPs.

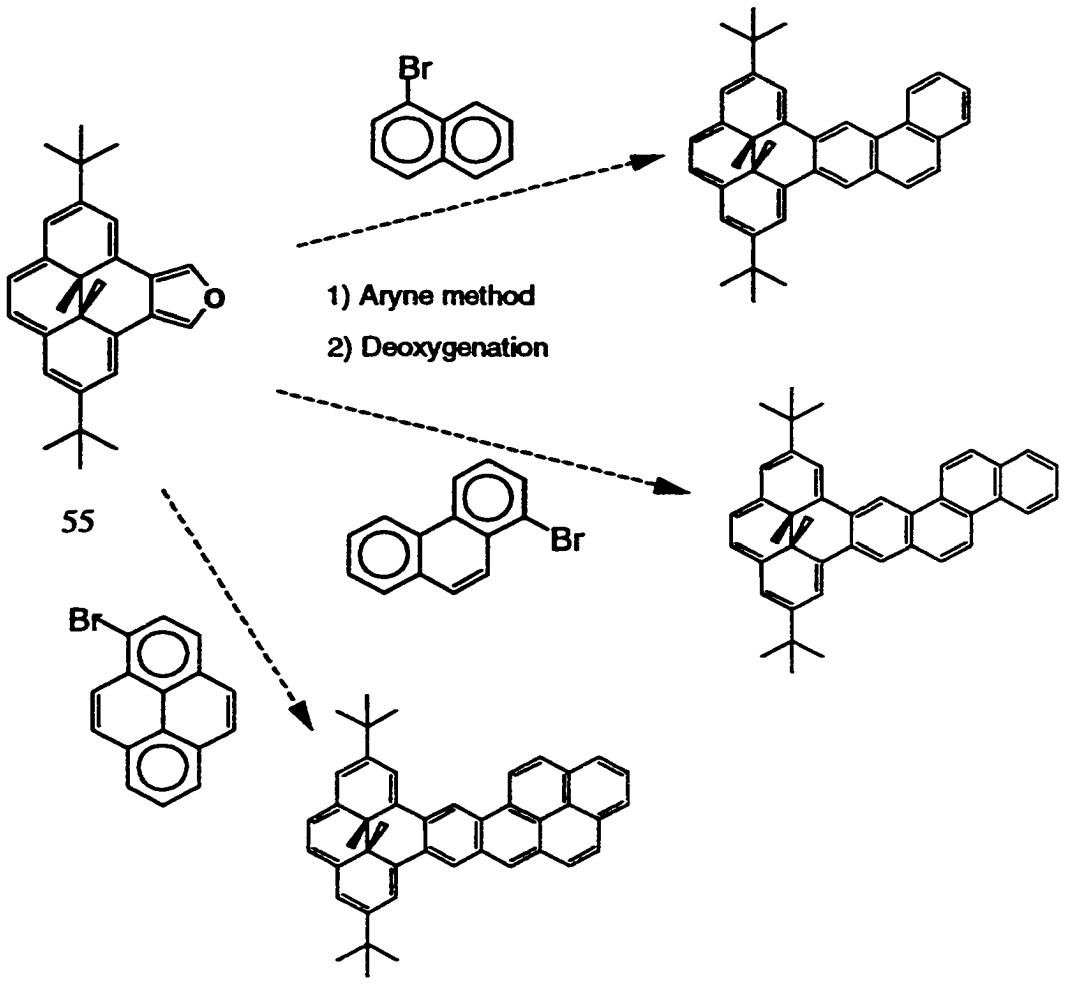

A challenging area would be the synthesis of [e]-annelated heterocyclic derivatives of **29**. The purpose of this would be two fold. The NMR properties would be of interest as aromaticity and bond localization effects would occur. A second property of interest would be the potential photochromic properties of such molecules. In view of the extremely slow thermal coloration rates displayed by **55**, fusion of **29** with heterocycles with strong bond localizing properties and low aromaticity might provide other photochromic molecules with slow coloration

rates. Deactivating heterocycles would be of useful, to help stabilize the products against oxidation. The triazole analogue of **55** would be interesting. Also of interest would be thiophene, pyrrole, imidazole, thiazole, and pyridazine derivatives.

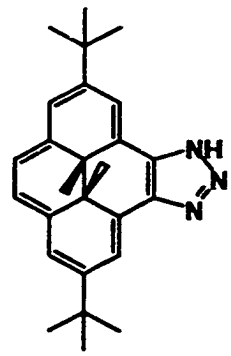

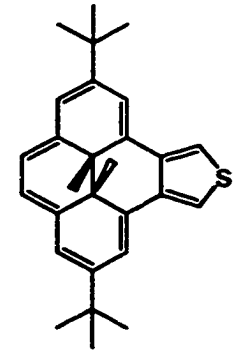

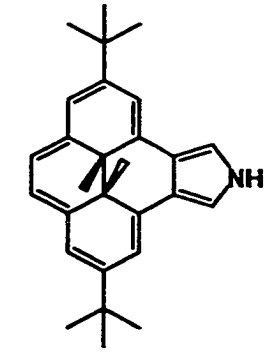

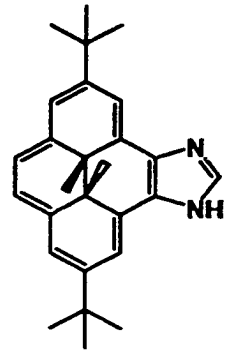

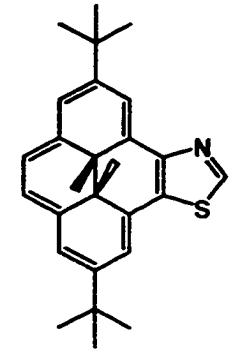

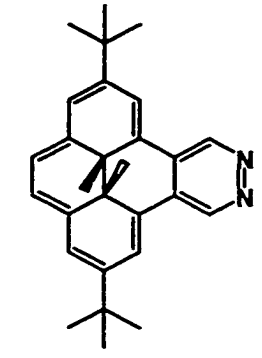

Chapter four Conclusions

4.1 Synthesis

Two complementary synthons useful for the systematic construction of [e]-annelated DMDHPs have been synthesized. Mono-bromination of DMDHP **34** using NBS in DMF/DCM provided the aryne synthon **50**. The aryne-furan Diels-Alder reaction of **50** with furan gave adduct **52**. Deoxygenation of **52** with $Fe_2(CO)_9$ gave the benzo[e]pyrene **53**. Reaction of **52** with tetrazine **54** provided the isoarenefuran **55**. Each of these reactions proceeded reliably in >86% yield, demonstrating the efficiency of the strategy. Both **50** and **55** have been used in aryne-furan reactions to form DMDHP fused derivatives.

Applying the aryne method to bromide **50** and naphthodifuran **62** gave bis dihydropyrene adducts **63** as a mixture of isomers. Deoxygenation of **63** with $Fe_2(CO)_9$ gave the bis(dihydropyreno)chrysene **60** as mixed isomers. Thus we have shown that the aryne-furan method can be used to form bis(dihydropyreno) derivatives from DMDHP **34**.

Applying the aryne-furan strategy to furan **55** using benzyne, 2,3-naphthalyne, and the 4,5-benzopyryne from **65**, we have synthesized [e] fused furan adducts **56**, **58**, and **67**. These compounds gave the 2,3-naphtho, 2,3-anthro, and the metacyclophane derivatives **57**, **59**, and **68**, after deoxygenation using $Fe_2(CO)_9$. This demonstrated that a complementary aryne-furan strategy using **55** can be used to generate [e]-annelated DMDHPs.

4.2 Photochromism

The [e]-annelated DMDHPs obtained were photochromic. Reversible, repeatable photoswitching of the DMDHP forms to the MCD forms was demonstrated for **53**, **57**, **59**, **65**, **60**, and **68**, in solution. Isoarenefuran **55** also proved to be photochromic, though repeatability was not investigated because of the reactivity of **55**. Kinetic studies showed that the activation energies and enthalpies for the thermal return reactions for the benzo, naphtho, and anthro MCD forms **53'**, **57'** and **59'** decreased through the series. A correlation was found for the change in activation energies and enthalpies with the resonance energies of the annelating fragments. This suggested that resonance stabilization of the transition states by the annelating fragments was responsible. Support for this came from the coloration of **55'** to **55** which was an order of magnitude slower than the coloration of **53'** to **53** at the same temperature. The annelating fragment in **55** , furan, has a much lower resonance stabilization energy than does benzene. Thus we have discovered a trend which may be useful in the design of photo-switches based on DMDHP.

The complex multiple state systems **60** and **68** were each shown to have three isomers. The bis(dihydropyreno)chrysene system **60** appeared to isomerize to the bis(metacyclophano)chrysene **60''** without passing through the third isomer, **60'**. Evidence for the dihydropyreno-metacyclophano-chrysene **60'** appeared during the thermal and UV induced returns of **60''** to **60**. The

metacyclophane-dihydropyrene **68** isomerized with visible light to a bis metacyclophane **68'**. The coloration rate of **68'** to **68** was similar to the analogous reaction of **53'** to **53**. The third isomer, **68''**, was produced by UV irradiation of **68**. The construction of these two systems, **60** and **68**, demonstrated that multiple state systems based on the DMDHP and MCD interconversion could be synthesized from **34**.

4.3 NMR Properties

Analysis of the proton NMR properties of the external (H^4) and internal methyl protons of the [e]-annelated DMDHPs obtained showed that δ(Me) and δ(H^4) were strongly correlated. A strong correlation was also found between the δ(Me)s and the relative resonance energies of the annelating fragments for the benzo, naphtho, and anthro derivatives **53**, **57**, and **59**. These results demonstrated that the NMR and aromaticity probe behavior of the DMDHP nucleus were operative in [e]-annelated DMDHPs, complementing previous findings for the [a]-annelated analogues.

Comparison of δ(Me) for the series **34**, **53**, **57**, and **59** with δ(Me) for the **[e]-DiMe** series showed that the effects of additional strain did not impair the linearity of response of δ(Me) as a function of the aromaticity of the annelating fragment, though sensitivity was altered. Thus for systems with consistent strains, DMDHP could be used to estimate aromaticity.

Chapter five Experimental

5.1 Instrumentation

Melting points were determined on a Reichert 7905 melting point apparatus integrated to an Omega Engineering Model 199 Chromel-alumel thermocouple. Infrared spectra, calibrated with polystyrene, were recorded on a Bruker IFS25 FT-IR spectrometer and only the major fingerprint bands are reported. UV-Visible spectra were recorded on a Cary 5 UV-VIS-NIR spectrometer using cyclohexane as solvent. Proton NMR spectra were recorded on a Bruker AMX 360 (360 MHz) spectrometer, or a Bruker AC 300 (300MHz) spectrometer, in $CDCl_3$ (unless otherwise specified), using the solvent residual peak for calibration (7.240 ppm for $CHCl_3$). Carbon NMR spectra were recorded on a Bruker AMX 360 (90.6 MHz), using the solvent peak at 77.0 ppm for calibration. Mass spectra were recorded on a Finnigan 3300 gas chromatography-mass spectroscopy system using methane as a carrier gas for chemical ionization. Exact mass measurements were done on a Kratos Concept-H instrument using perfluorokerosene as the standard. Elemental analyses were performed by Canadian Microanalytical Services Ltd., Vancouver, B.C. All the solvents used in reactions were purified and distilled according to standard procedures[85]. All evaporations were carried out under reduced pressure on a rotary evaporator, or by using an oil pump and dry ice condenser. Silica gel, 60 mesh or 60 mesh silica gel, refers to Merck silica gel, 60-200 mesh. Alumina refers to Aldrich aluminum oxide, activated, neutral, Brockmann I, standard grade, ~150 mesh.

Solutions of oxygen sensitive compounds for NMR spectroscopy were prepared by dissolving the compound in the minimum amount of deuterated solvent, filtration through alumina deactivated with 5% water, rinsing the alumina

with sufficient deuterated solvent to make up the correct volume for the spectrometer, and by bubbling argon through the filtrate in the NMR tube for 5 to 10 minutes. The tubes were then carefully capped under argon, and the spectra obtained. NMR spectra of photoisomerizable compounds were obtained using 5 mm amber NMR tubes. Where NMR assignments are made, these were on the basis of 2D COSY/NOESY experiments for protons, and HETCORR/HMQCB experiments for carbon. Expanded data sets (with computer iteration for AA'XX' systems) were used to obtain coupling constant data.

Laser flash photolysis (LFP) was conducted using a YAG laser (Spectra Physics GCR-12) at 355 nm with pulse energies ~40 mJ/pulse, with repetition rate 1 Hz. Transient spectra were obtained using a xenon lamp (150 W, Oriel housing model 66057, PTI power supply, model LPS-220) connected to a pulser (custom built, University of Victoria) synchronized with the laser pulses. A photomultiplier (Hamamatsu R446) coupled with a monochromator (CVI Digikrom 240) and a baseline compensation unit was used to monitor the transient absorption spectra. The operating system is detailed in reference 86. Samples for LFP were dissolved in cyclohexane in 7 mm fluorescence cells, adjusted for absorbance ~0.1 at λ_{max}, and deaerated 10 min with nitrogen and capped. Temperature was maintained at 20 ± 1°C.

Photoisomerizations for thermal return kinetic studies were performed using broadband irradiation from a 250 W tungsten incandescent lamp at a distance of 8 cm from the sample, with an ice bath and pyrex filter. All DMDHP compounds studied also photoisomerized to MCD forms using a 600 nm cut off filter, placing the filter in the ice bath between lamp and sample.

5.2 Synthesis

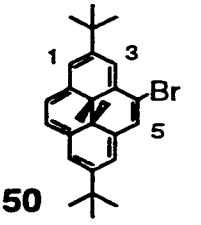

50

4-Bromo-2,7-di-*t*-butyl-*trans*-10b,10c-dimethyl-10b,10c-dihydropyrene 50

NBS (260 mg, 1.459 mmol) in dry DMF (40 mL) was added dropwise with stirring to a solution of DMDHP **29** (500 mg, 1.452 mmol) in dry CH_2Cl_2 (200 mL) cooled in a dry ice/acetone bath, under argon. After the addition was complete, the cooling bath was removed, and the reaction mixture was allowed to warm to room temperature. After stirring 1 hour at room temperature, the mixture was poured into a 1 L separatory funnel with hexanes (300 mL) and the mixture was extracted with water (8x100 mL). The green organic phase was dried ($MgSO_4$), filtered and evaporated. The green solid obtained was taken up in the minimum amount of hexanes/ CH_2Cl_2 (6:1) and filtered through silica gel (60 mesh, deactivated, 5% water), eluting with the same solvent. The green solution was evaporated to yield 600 mg of green crystals. This product contains approximately 94 % **50**, + ~3% **29**, +~3% **52**, and thus the yield of **50** was 92%. A portion was recrystallized from cyclohexane as intense green crystals, mp 189 - 191°C; ^1H NMR ($CDCl_3$, 360 MHz) δ 8.80 (d, J = 1.24 Hz, 1H, H-3), 8.64

(s,1H, H-5), 8.54 - 8.53 (m, 2H, H-1,6), 8.47 (br s,1H, H-8), 8.455 (AB, J = 8.10 Hz, 1H, H-9 or 10), 8.456 (AB, 1H, H-9 or 10), 1.70 (s, 9H, $-C(CH_3)_3$), 1.66 (s, 9H, $-C(CH_3)_3$), -3.93 (s, 3H, CH_3), -3.95 (s, 3H, CH_3);

^{13}C NMR ($CDCl_3$, 90.6 MHz) δ 146.9, 137.3, 137.0, 131.6, 126.0, 123.6, 123.5, 122.7, 121.8, 121.3, 121.1, 120.3, 115.6, 36.3, 36.0, 32.1, 31.95, 31.86, 29.7, 14.7, 13.9; UV (cyclohexane) λ_{max} (ε_{max}) nm 206 (23,300), 343 (96,400), 384 (44,600), 480 (10,200), 650 (1240); IR (KBr) 1590, 1460, 1380, 1360, 1340, 1226, 875, 780, 668 cm^{-1}; CI MS *m/z* 423 (MH+); Anal. Calc'd for $C_{26}H_{31}Br$: C, 73.75; H 7.38. Found: C, 73.60; H, 7.32.

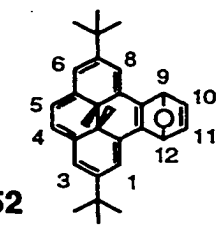

52

2,7-di-*t*-butyl-9,12,12c,12d-tetrahydro-*trans*-12c,12d-dimethyl-9,12-epoxybenzo[e]pyrene 52

Bromopyrene **50** (1.113 g, 2.677 mmol) was dissolved in dry THF (40 mL) in an oven dried round bottom flask (500 mL, 2 neck) with large oval magnetic stir bar, under argon. Dry furan (16 mL) was syringed in, and then sodium amide (4.9 g, 126 mmol) and potassium t-butoxide (~15 mg) were added. The mixture was stirred for 22 h. Hexane (60 mL) was then added, and the mixture allowed

to settle. The dark green mixture was filtered by decanting carefully into a glass frit vacuum filtration assembly containing layered silica gel (60 mesh deactivated with 5% water, 2 cm depth) with Celite (5 cm) on top. The filtrate was collected in a round bottom flask (500 mL). The reaction mixture solids were rinsed into the filtration assembly carefully with THF/hexane (1:1). Care was taken to avoid mixing the layers of silica gel and Celite. The solids were then carefully rinsed with more THF/hexane (1:1) (~120 mL), until the filtrate stream was diminished in color. The filtrate was then evaporated, and the dark green solid obtained was rinsed with hexane (4x4 mL). The solid was then air dried to yield **52** (890 mg, 81%) as a dark green microcrystalline solid.

The material obtained was suitable for preparative purposes. Purity was >95%.

A portion was further purified by chromatography (silica gel, 60 mesh, deactivated with 5% water; eluant, hexane/ethyl acetate, 6:1), and gave green crystals, mp (dec) 189 - 193°C; ^{1}H NMR (d_8 THF, 360 MHz) δ 8.20 - 8.18 (m, 4H, H-1,3,6,8), 8.108 (AB, J = 8.6 Hz, 1H, H-4 or 5), 8.111 (AB, 1H, H-4 or 5), 7.12 (dd, J = 1.9 Hz, J = 5.5 Hz, 1H, H-10 or 11), 6.99 (dd, J = 1.8 Hz, J = 5.5 Hz, J = 0.3 Hz, 1H, H-10 or 11), 6.49 (d, J = 1.8 Hz, 1H, H-9 or 12), 6.46 (dd, J = 1.9 Hz, J = 0.6 Hz, 1H, H-9 or 12), 1.62 (s, 9H, -$C(CH_3)_3$), 1.615 (s, 9H, -$C(CH_3)_3$), -3.18 (s, 3H, CH_3), -3.42 (s, 3H, CH_3); ^{13}C NMR (d_8 THF, 90.6 MHz) δ 145.8, 145.5, 141.0, 140.7, 138.2, 138.0, 137.9, 137.4, 128.3, 127.9, 125.22, 125.19, 122.10, 122.06, 115.7, 115.4, 81.6, 81.3, 36.4, 33.9, 33.0, 31.7, 17.0, 14.5; UV (cyclohexane) λ_{max} (ε_{max}) nm 268 (2,930), 361 (18,600), 380

(8,580), 411 (1520), 444 (1,470), 462 (1,520), 635(100); IR (KBr) 1622, 1559, 1475, 1457, 1359, 1343, 1263, 1210, 1033, 995, 882, 854,691, 674, 648 cm^{-1}; CI *m/z* 411 (MH+); Anal. Calc'd for $C_{30}H_{34}O$: C, 87.76; H 8.35. Found: C, 87.58; H, 8.43.

The product **52** was not stable in $CHCl_3$ nor in $CDCl_3$, hence C_6D_6 was used for NMR spectral purity checks. For analogues, d_8 THF is recommended for HMR and CMR, to avoid spectral overlap in aromatic regions. For the title compound and analogues, hexane washes of the obtained (chromatographed) solids is recommended as some deoxygenation usually occurs on evaporation/concentration.

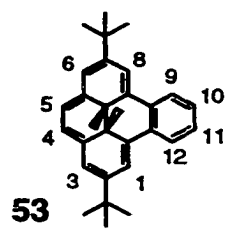

53

2,7-Di-*t*-butyl-*trans*-12c,12d-dimethyl-12c,12d-dihydrobenzo[e]pyrene 53

Adduct **52** (405 mg, 0.986 mmol) and $Fe_2(CO)_9$ (509 mg, 1.42 mmol) in benzene (35 mL) were refluxed in the dark, with stirring, under argon, for 2 hr. After cooling to room temperature, the mixture was filtered through silica gel (60 mesh, deactivated with 5% water, 10 cm column), and the column was rinsed with benzene (50 mL). The intense red solution was evaporated in vacuo, in the dark. Benzene (100 mL) was added to the solid, and the solution was re-

evaporated in the dark in vacuo. The solid red residue was chromatographed over silica gel (60 mesh, deactivated with 5% water) using hexanes/CH_2Cl_2 (6:1) as eluant. The first 70% of the red band was collected and the solvent removed to yield **53** (344 mg, 88%). A portion was recrystallized from cyclohexane to yield intense red crystals mp 172°C sharp; ^{1}H NMR ($CDCl_3$, 360 MHz) δ 8.767 (AA'XX', $J_{9,10}$ = 8.36 Hz, $J_{9,11}$ = 1.27 Hz, $J_{9,12}$ = 0.63 Hz, 2H, H-9,12), 8.28 (d, J = 1.05 Hz, 2H, H-1,8), 7.605 (AA'XX', $J_{10,11}$ = 6.94 Hz, $J_{10,12}$ = 1.27 Hz, 2H, H-10,11), 7.35 (d, J = 1.02, 2H, H-3,6), 7.135 (s, 2H, H-4,5), 1.49 (s, 18H, $C(CH_3)_3$), -1.58 (s, 6H, CH_3); ^{13}C NMR ($CDCl_3$, 90.6 MHz) δ 144.3, 138.3,134.6, 129.2, 125.5, 124.4, 120.9, 119.6, 116.9, 35.3, 35.1, 30.6, 17.3;

UV (cyclohexane) λ_{max} (ε_{max}) nm 308 (24,900), 321 (25,500), 338 (27,800), 369 (26,400), 388 (35,000), 504, (7000), 620 (400); IR (KBr) 1616, 1472, 1444, 1365, 1334, 1264, 1227, 872, 752, 634 cm^{-1}; CI MS *m/z* 394 (M+), 395(MH+); Anal. Calc'd for $C_{30}H_{34}$: C, 91.32; H 8.68. Found: C, 90.9; H, 8.7. HRMS, calc'd for $C_{30}H_{34}$ (M+); 394.2660. Found; 394.2661.

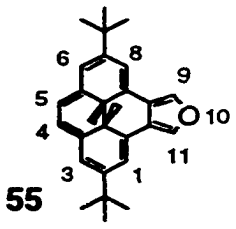

55

Di-*t*-butyl-*trans*-11c,11d-dimethyl-11c,11d-dihydropyreno[4,5-c]furan 55

Adduct **52** (403 mg, 0.981 mmol) was stirred with 3,6-di-2-pyridyl-1,2,4,5-tetrazine[72] (300 mg, 1.27 mmol) in dry THF (20 mL) in the dark, under argon for 2 hr. The solvent was then removed in vacuo and the residue taken up in hexanes/ CH_2Cl_2 (6:1) and filtered through alumina (deactivated with 5% water, 2.5 cm). The intense purple band was collected and evaporated in the dark in vacuo to **55** (340 mg, 90%) as intense purple crystals, mp (dec) 170 - 174 °C; ^{1}H NMR (d_8 THF, 360 MHz) δ 8.32 (d, J = 0.43 Hz, 2H, H-9,11), 7.12 (d, J = 1.43 Hz, 2H, H-1,8), 6.45 (d, J = 1.40 Hz, 2H, H-3,6), 6.21 (s, 2H, H-4,5), 1.28 (s, 18H, $C(CH_3)_3$), 0.17 (s, 6H, CH_3); ^{13}C NMR (d_8 THF, 90.6 MHz) δ 145.3, 140.3, 138.4(C-9,11), 131.8, 121.9(C-3,6), 121.3, 119.7(C-4,5), 117.9(C-1,8), 40.9, 35.3, 30.0($C(CH_3)_3$), 20.5 (CH_3); UV (cyclohexane) λ_{max} (ε_{max}) nm 232 (12,500), 291 (32,900), 350 (22,200), 367 (25,700), 525, (5760); IR (KBr) 1636, 1477, 1459, 1438, 1360, 1229, 1156, 1051, 881, 871, 765, 670, 638 cm^{-1}; CI MS *m/z* 384 (M+), 385(MH+); Anal. Calc'd for $C_{28}H_{32}O$: C, 87.45; H 8.39. Found: C, 87.75; H, 8.38.

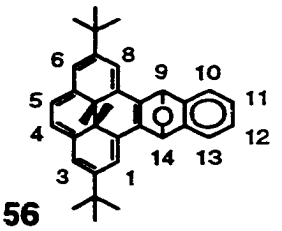

56

2,7-Di-*t*-butyl-*trans*-14c,14d-dimethyl-9,14-epoxy-14c,14d-dihydrodibenzo[de,qr]naphthacene 56

A solution of **55** (250mg, 0.650 mmol) and 1,2-dibromobenzene (1.70 g, 7.21 mmol) in dry toluene (6 mL) was cooled to -50°C under argon in the dark. Then butyllithium (1.3 mL x 2.5 M ^{n}Butyllithium in hexanes) was added dropwise in by syringe, with stirring. The mixture was stirred in the dark at temperatures between -50°C and -40°C for 15 minutes, at which time the reaction was quenched with methanol (3 mL).

(During the course of the reaction, the mixture turns from intense purple through shades of red brown to green brown, finally becoming green at about 15 minutes.) The volatiles were then removed in vacuo. The residue was taken up in benzene (30 mL) and washed with water (3x100 mL). The green organic phase was separated and evaporated. The solid residue was rinsed with pentane (5x4 mL) and dried to leave dark green crystalline **56** (254 mg, 85 %), mp (dec) 203 - 209°C; ^{1}H NMR (d_8 THF, 360 MHz) δ 8.483 - 8.479 (m, 2H, H-1,8), 8.366(d, J = 1.3 Hz, 1H, H-3 or 6), 8.346(d, J = 1.3 Hz, 1H, H-3 or 6), 8.247 (AB, J = 8.60 Hz, 1H, H-4 or 5) 8.248 (AB, 1H, H-4 or 5), 7.50 - 7.48

(m(ABXY), 1H, H-10 or 13), 7.41 - 7.38 (m(ABXY), 1H, H-10 or 13), 6.99 (s, 1H, H-9 or 14), 6.98(s,1H, H-9 or 14), 6.93 - 6.86 (m(ABXY), 2H, H-11,12), 1.68(s, 9H, $C(CH_3)_3$), 1.67(s, 9H, $C(CH_3)_3$), -3.49(s, 3H, CH_3), -4.14(s, 3H, CH_3); ^{13}C NMR (d_8 THF, 90.6 MHz) δ 149.5, 149.1, 146.3, 146.0, 138.5, 138.3, 138.0, 137.95, 128.2, 127.7, 126.2, 126.1, 125.1, 125.0, 122.2, 122.1, 120.3, 120.0, 116.4, 115.7, 82.5, 82.1, 36.5, 33.6, 32.0, 31.4, 16.3, 14.1; IR (KBr) 1618, 1458, 1343, 1264, 983, 885, 864, 750, 653, 634 cm^{-1}; CI MS *m/z* 461(MH+); Anal. Calc'd for $C_{34}H_{36}O$: C, 88.65; H 7.88. Found: C, 87.78; H, 7.83.

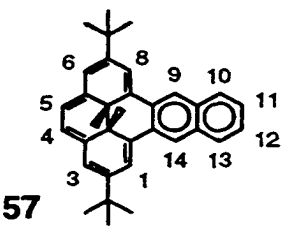

57

2,7-Di-*t*-butyl-*trans*-14c,14d-dimethyl-14c,14d-dihydrodibenzo[de,qr]naphthacene 57

Adduct **56** (200 mg, 0.450 mmol) was refluxed with $Fe_2(CO)_9$ (260 mg 0.715 mmol) in benzene (30 mL), with stirring under argon in the dark for 2 hr. After cooling to room temperature, the mixture was filtered through silica gel (60 mesh, deactivated with 5% water, 10 cm column), and the silica gel column was rinsed with benzene (60 mL). The intense purple solution was evaporated in the dark. Benzene (100 mL) was added to the solid, and this was evaporated. The

purple solid residue was chromatographed over silica gel (60 mesh, deactivated with 5% water) using hexanes/ CH_2Cl_2 (6:1) as eluant. The first ~70% of the mobile purple band was collected and evaporated to yield **57** (150 mg, 75%). (More **57** was contained in the tail of the purple band. Content, ~ 20 mg, ~10%) A portion was crystallized from cyclohexane, to yield intense purple crystals, mp (dec) 172 - 174°C; ^{1}H NMR ($CDCl_3$, 360 MHz) δ 9.01(s, 2H, H-9,14), 8.076 (AA'XX', $J_{10,11}$ = 8.30 Hz, $J_{10,12}$ = 1.20 Hz, $J_{10,13}$ = 0.83 Hz, 2H, H-10,13), 8.00(d, J = 1.3 Hz, 2H, H-1,8), 7.530 (AA'XX', $J_{11,12}$ = 6.66 Hz, $J_{11,13}$ = 1.20 Hz, 2H, H-11,12), 6.90(d, 2H, J = 1.3 Hz, H-3,6), 6.66(s, 2H, H-4,5), 1.44 (s, 18H, $C(CH_3)_3$), -0.54 (s, 6H, CH_3); ^{13}C NMR ($CDCl_3$, 90.6 MHz) δ 144.6, 139.2, 135.7, 131.4, 128.7, 127.7, 125.6, 122.6, 121.1, 119.9, 117.6, 37.7, 35.1, 30.2, 19.2; UV (cyclohexane) λ_{max} (ε_{max}) nm 262 (28,500), 321 (25,400), 378 (31,700), 398 (41,850), 553, (4,200); IR (KBr) 1618, 1479, 1459, 1362, 1271, 1225, 883, 872, 746, 672 cm^{-1}; CI MS *m/z* 445(MH+); Anal. Calc'd for $C_{34}H_{36}$: C, 91.84; H 8.16. Found: C, 90.47 H, 8.30.

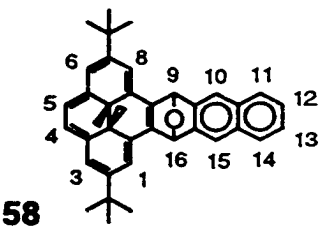

58

2,7-Di-*t*-butyl-*trans*-16c,16d-dimethyl-9,16-epoxy-16c,16d-dihydrodibenzo[av,ef]pentacene 58

A solution of **55** (75.0 mg, 0.195 mmol) and 2,3-dibromonaphthalene[74] (168 mg) in dry toluene (12 mL) was cooled to -45°C, with stirring under argon, in the dark. Butyllithium (1 mL x 2.5 M *n*-butyllithium in hexanes) was syringed in and the mixture stirred gently for 15 minutes, at which time methanol (3 mL) was syringed in to quench the reaction. The solvent was removed in vacuo. The residue was purified by chromatography (silica gel 60 mesh, deactivated with 5% water). Elution with hexane:benzene (2:1) removed faster moving colored impurities. The green product band separated into two bands. The second green band was collected. Evaporation of solvents, followed by rinsing the product with hexanes (4x4 mL) and drying, yielded **58** (45 mg, 0.088 mmol, 45%) as green crystalline solid, mp (dec) 207 - 211°C; ^{1}H NMR (d_8 THF, 360 MHz) δ 8.59 - 8.78 (m, 2H), 8.39 (d, J = 1.3 Hz, 1H), 8.37 (d, J = 1.3 Hz, 1H), 8.259 (AB, J = 8.52 Hz, 1H), 8.260 (AB, 1H), 7.86 (s, 1H), 7.73 (s, 1H), 7.68 - 7.60 (m(ABXY), 2H), 7.28 - 7.21 (m(ABXY), 2H), 7.10 (m, 2H), 1.674 (s, 9H, $C(CH_3)_3$), 1.666

(s, 9H, $C(CH_3)_3$), -3.62 (s, 3H, CH_3), -4.30 (s, 3H, CH_3); ^{13}C NMR (d_8 THF, 90.6 MHz) δ 146.53, 146.27, 146.12, 145.68, 138.28, 138.02, 137.95, 137.91, 133.44, 133.39, 128.84, 128.78, 128.26, 127.67, 126.25, 125.89, 125.12, 122.31, 122.20, 118.63, 118.16, 116.75, 116.03, 82.35, 81.90, 36.63, 33.36, 32.06, 31.12, 26.36, 16.02, 14.09; IR (KBr) 1616, 1446, 1345, 1263, 1043, 977, 877, 868, 833, 751, 654 cm^{-1}; LSIMS *m/z* 510 (M+), 511(MH+), (nice fragmentation pattern, loss of groups from MH+); HRMS. Calc'd for $C_{38}H_{38}O$: 510.2922. Found: 510.2924.

Inverse addition is also possible. This was done once after **55** decomposed on dissolution.

To a solution of 2,3-dibromonaphthalene (0.733 g, mmol) in dry toluene (20 mL) cooled to -40° was added Butyllithium (1.5 mL x 2.5 M ^{n}Butyllithium in hexanes) by syringe. **55** was promptly dissolved and transferred quantitatively in the minimum dry toluene to the reaction flask, by pipette. Methanol (2 mL) was added at 16 minutes. The flask was allowed to warm to room temperature, and all the solvents were evaporated using a vacuum pump. The crude product residue was purified as above.

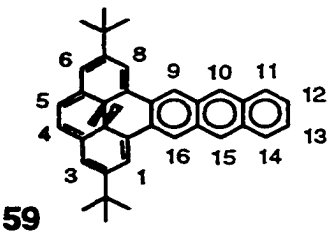

59

2,7-Di-*t*-butyl-*trans*-16c,16d-dimethyl-16c,16d-dihydrodibenzo[av,ef]pentacene 59

A mixture of **58** (45 mg, 0.088 mmol) was refluxed with $Fe_2(CO)_9$ (55 mg) in benzene (25 mL) for 1 hr., with stirring under argon, in the dark. After cooling, the mixture was filtered through silica gel (60 mesh, deactivated with 5% water) and the silica gel was rinsed through with benzene (50 mL). After evaporation of the solvent, the sample was purified by chromatography (silica gel, 60 mesh, deactivated with 5% water), using hexanes/CH_2Cl_2 (6:1) as eluant. The first ~70% of the greenish product band was separated. The solvent was evaporated to yield **59** (25 mg, 0.050 mmol, 57 %) as a green solid with purple lustre, mp (dec) 158 - 160°C; ^{1}H NMR ($CDCl_3$, 360 MHz) δ 9.08 (s, 2H, H-9,16), 8.68 (s, 2H, H-10,15), 8.065 (AA'XX', $J_{11,12}$ = 8.58 Hz, $J_{11,13}$ = 1.19 Hz, $J_{11,14}$ = 0.76 Hz, 2H, H-11,14), 7.85 (d, J = 1.3 Hz, 2H, H-1,8), 7.461 (AA'XX', $J_{12,13}$ = 6.47 Hz, $J_{12,14}$ = 1.19 Hz, 2H, H-12,13), 6.68 (d, J = 1.2 Hz, 2H, H-3,6), 6.43 (s, 2H, H-4,5), 1.41 (s, 18H, $C(CH_3)_3$), 0.004 (s, 6H, CH_3); ^{13}C NMR ($CDCl_3$, 90.6 MHz) δ 144.78, 139.74, 136.19, 131.65, 129.91, 128.95, 128.27 (C-11,14), 125.82 (C-10,15), 125.11 (C-12,13), 122.45 (C-9,16), 121.18 (C-4,5), 120.08 (C-3,6), 117.92 (C-1,8), 38.88, 35.01, 30.04 ($C(\underline{C}H_3)_3$), 20.20 ($\underline{C}H_3$);

UV (cyclohexane) λ_{max} (ε_{max}) nm 225 (45700), 278 (45100), 304 (49800), 325 (2300), 393 (49700), 413 (49500), 600 (4000); IR (KBr) 1625, 1444, 1363, 1276, 1226, 1139, 896, 873, 737, 751, 654 cm^{-1}; LSIMS *m/z* 494.2 (M+), 479.2(M+ - 15); HRMS. Calc'd for $C_{38}H_{38}$: 494.2973. Found: 494.2971.

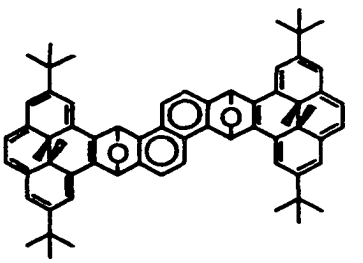

63

Isoarenefuran-aryne adduct 63

Isoarenefuran **62** was generated from **61** as described in the literature[75]. Bis(acetal) **61** (62 mg, 0.23 mmol) was added to 2 mmol LDA prepared in THF (20 mL), cooled with a dry ice/acetone bath. The mixture was allowed to warm to ~0°C for about 10 minutes to allow all the acetal **61** to dissolve, and to allow the isoarenefuran to form. The mixture was then cooled in the dry ice/acetone bath and reaction mixture was quenched with methanol (0.5 mL). The volatiles were then evaporated with an oil vacuum pump, using a cool water bath ~7 °C .

The product was than taken up with hexane/ethyl acetate (3.5:1) (10 mL), and filtered through a 4 cm column of alumina deactivated with 5% water, using the same mixed solvent (90 mL) to rinse through the colorless product. The solvents were then evaporated with an oil vacuum pump, using a cool water bath ~7°C and the product was dried for an additional hour under vacuum at room

temperature. The product **62** was obtained as colorless crystalline leaflets, yield 35 mg, 74%.

To the solid **62** obtained was added dry THF (10 mL), bromopyrene **50** (192 mg, 0.455 mmol), sodium amide (240 mg), and potassium t-butoxide (5 mg). The mixture was stirred under argon for 24 hr.

The reaction was quenched by cooling in an ice bath and slowly adding saturated aq. ammonium chloride(5 mL). The organics were separated and washed with $NH_4Cl_{(aq)}$ (5 mL), brine(2x5 mL), then separated, dried ($MgSO_4$), and evaporated. The aqueous layers were extracted with ether(2x15 mL). These organics were dried ($MgSO_4$) and evaporated with the previous product. The solid was rinsed with hexanes (4x4 mL) and dried to yield **63**(122 mg, 0.137 mmol, 81 %) as a green crystalline mixture of equal amounts of two isomers, mp (dec) 205 - 210°C; ^{1}H NMR (C_6D_6, 300 MHz) δ 8.6 - 8.0(m, 24 H), 7.75 - 7.55 (m, 4 H), 7.4 - 7.2(m, 8H), 6.95 - 6.83(m, 4H), 1.70 - 1.60(m, 8 x $C(CH_3)_3$), -2.89(s, 6H, CH_3, first isomer), -2.89(s, 3H, CH_3, second isomer), -2.95(s, 3H, CH_3, second isomer), -3.79(s, 6H, CH_3, first isomer), -3.79(s, 3H, CH_3, second isomer), -3.92(s, 3H, CH_3, second isomer); IR (KBr) 1616, 1464., 1361, 1345, 1260, 1213, (1147, 1115, 1087), 1037, 868, 670 cm^{-1}; LSIMS *m/z* 893.4 (MH+), 877.4 (M - 15); HRMS calculated for $C_{66}H_{69}O_2$ (MH+); 893.5297. Found; 893.5294

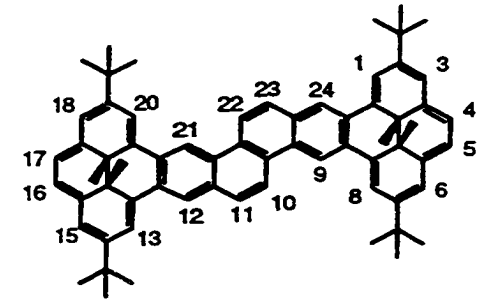

60

Bispyrenochrysene 60

A mixture of **63** (38 mg 0.0425 mmol, mixture of isomers), $Fe_2(CO)_9$ (140 mg), and benzene (15 mL) was refluxed with stirring under argon in the dark, for 2 hr. After cooling, the mixture was filtered through silica gel (60 mesh, deactivated with 5% water), and the silica gel column was rinsed with $CHCl_3$ (100 mL). The brown solution was evaporated. The residue was purified by chromatopraphy under argon (silica gel, 60 mesh, deactivated with 5% water), using hexanes/ CH_2Cl_2 (6:1) as eluant. The product band was collected and evaporated to yield **60** (30 mg, 0.0348 mmol, 82 %) as a mixture of isomers, mp (dec) >345°C; ^{1}H NMR (C_6D_6, 360 MHz) δ 10.35 (s, 2H, H-9,21), 9.39 (s, 2H, H-12,24), 9.18 (d, J = 9.0 Hz, 2H, H-10,22), 8.54 (unresolved d, 2H, H-8,20), 8.41 (unresolved d, 2H, H-1,13), 8.17 (d, J = 9.0 Hz, 2H, H-11,23), 7.25 - 7.20 (overlapping unresolved doublets, 4H, H-3,6,15,18), 6.91 - 6.89 (two overlapping unresolved AB, 4H, H-4,5,16,17), 1.45 (s, 18H), 1.44 (s, 18H), -0.29 (unresolved overlapping s, two isomers 12H); ^{1}H NMR ($CDCl_3$, 300 MHz) δ - 0.74 (unresolved s) , and 6.84(H-4,5,16,17); ^{13}C NMR (C_6D_6, 90.6 MHz) δ; 144.76, 139.58, 139.35, 136.57, 136.04, 131.05, [benzene peak 129 -127] ,

124.37, 122.04, 121.96, 121.77, 120.92, 120.90 , 119.31, 118.21, 118.14, 37.96, 35.30, 30.50, 30.44, 19.28; UV (cyclohexane) λ_{max} (ε_{max}) nm 290 (51,600), 345 (43,400), 406 (70,900), 427 (132,000), 527, (10,000); IR (KBr) 1626, 1477, 1362, 1228, 878, 869, 803, 671 cm^{-1}; LSIMS *m/z* 860.5 (M+), 815.4(M+ - 3 x 15); HRMS Calc'd for $C_{66}H_{68}$: 860.5321. Found: 860.5323. Note: NMR spectrum broadens on standing.

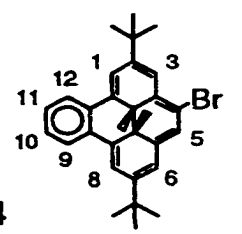

64

4-Bromo-2,7-di-*t*-butyl-*trans*-12c,12d-dimethyl-12c,12d-dihydrobenzo[e]pyrene 64

A solution of **53** (176 mg, 0.445 mmol) in dry CH_2Cl_2 (50 mL) under argon was cooled in an ice bath in the dark. A solution of NBS(79.9 mg, 0.449 mmol) in dry DMF(10 mL) was added slowly to the stirred cooled darkened solution of **53**. After addition, the cooling bath was removed, and the reaction mixture was allowed to warm to room temperature in the dark. After stirring at room temperature for an hour, the mixture was poured into hexanes (100 mL) in a separatory funnel. The organic layer was washed with water (8x50 mL), separated and evaporated. The red residue was taken up in the minimum

amount of hexane/DCM (6:1) and filtered through silica gel (60 mesh, deactivated with 5% water), eluting with the same solvent. Evaporation of the red eluate yielded **64** (193 mg, 92 %) as crystals. A sample was recrystallized from hexane to give intense red crystals, mp 178 - 179°C; ^{1}H NMR ($CDCl_3$, 360 MHz) δ 8.74 - 8.69 (m(ABXY), 2H, H-9,12), 8.26 (d, J = 0.9 Hz, 1H, H-1), 8.23 (d, J = 1.0 Hz, 1H, H-8), 7.63 (s, 1H, H-3), 7.63 - 7.59 (m(ABXY), 2H, H-10,11), 7.26 (s, 1H, H-6), 7.236 (s, 1H, H-5), 1.50 (s, 9H, $C(CH_3)_3$), 1.47 (s, 9H, $C(CH_3)_3$, -1.43 (s, 3H, CH_3), -1.44 (s, 3H, CH_3), [note $CHCl_3$ = 7.240]; ^{13}C NMR ($CDCl_3$, 90.6 MHz) δ 148.5, 146.8, 146.3, 139.6, 135.5, 135.3, 133.1, 129.2, 126.2, 124.7, 124.5, 118.7, 118.5, 117.3, 117.1, 114.1, 38.8, 35.8, 35.7, 35.5, 30.5, 17.8, 17.0; IR (KBr) 1617, 1603, 1552, 1476, 1368, 1361, 1256, 1117, 875, 753, 638 cm^{-1}; CI MS *m/z* 472 (M+ ^{79}Br), 474 (M+ ^{81}Br), 473 (MH+ ^{79}Br), 475 (MH+ ^{81}Br); Anal. Calc'd for $C_{30}H_{33}$ Br: C, 76.10; H 7.03. Found: C, 76.17; H, 6.94.

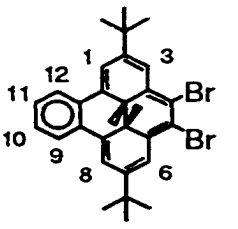

65

***trans*-4,5-Dibromo-2,7-di-*t*-butyl-12c,12d-dihydro-12c,12d-dimethylbenzo[e]pyrene 65**

A solution of vacuum dried **53** (285 mg, 0.721 mmol) in dry CH_2Cl_2 (200 mL) was prepared under argon in the dark, and cooled in an ice bath. NBS (vacuum dried, 257 mg, 1.44 mmol) in dry DMF (40 mL) was added slowly with stirring to the solution of **53**. after addition, the reaction mixture was allowed to warm to room temperature, and let stir for 2 hr. The reaction mixture was then poured into hexanes (280 mL) and was washed with water (8x200 mL). The organic phases were separated, dried and evaporated. The residue was purified by repeated chromatography (4x)[silica gel, 60 mesh, deactivated with 5% water, eluted with hexanes/ CH_2Cl_2 (9:1)], to yield **65** (191 mg, 48 %)

[repeated chromatography (4 x) to separate close moving colorless fluorescent compounds]

A sample was recrystallized from cyclohexane to give intense purple crystals, mp (dec) 187 - 189°C; ^{1}H NMR ($CDCl_3$, 360 MHz) δ 8.69 - 8.64 (AA'XX', 2H, H-9,12), 8.21 (d, J = 1.3 Hz, 2H, H-1,8), 7.73 (d, J = 1.3 Hz, 2H, H-3-6), 7.65 - 7.60 (AA'XX', 2H, H-10,11), 1.49 (s, 18H, $C(CH_3)_3$), -1.30 (s, 6H, CH_3);

^{13}C NMR ($CDCl_3$, 90.6 MHz) δ 148.7, 136.2, 135.7, 129.1, 126.7, 124.7, 120.2, 117.5, 117.0, 39.1, 35.9, 30.4, 17.3; IR (KBr) 1616, 1602, 1475, 1445, 1367, 1361, 1318, 1255, 1201, 1121, 1000, 959, 913, 866, 800, 754, 637, 610 cm^{-1}; CI MS *m/z* 553 (MH+ ^{79}Br, ^{81}Br), 551 (MH+ ^{79}Br, ^{79}Br), 555 (MH+ ^{81}Br, ^{81}Br); Anal. Calc'd for $C_{30}H_{32}Br_2$: C, 65.23; H, 5.84 . Found: C, 65.33; H, 5.89.

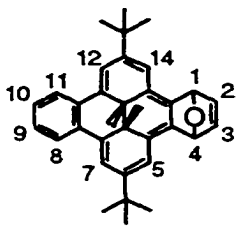

66

***trans*-6,13-Di-*t*-butyl-1,4,14b,14c-tetrahydro-14b,14c-dimethyl-1,4-epoxydibenzo[fg,op]naphthacene 66**

A solution of **65** (92 mg, 0.167 mmol) in dry toluene (20 mL) with dry furan (13 mL) was cooled to -40°C, with stirring under argon, in the dark. Then butyllithium (0.80 mL x 2.5 M *n*-butyllithium in hexanes) was added slowly by syringe, with stirring. After 15 minutes, methanol (3 mL) was added. The solvents were then removed in vacuo, below room temperature. The solid residue was taken up in benzene and purified by chromatography (deactivated neutral alumina, 5% water, eluted with benzene) to yield **66** (50 mg, 66%) as an orange microcrystalline solid, mp 212 - 213°C; ^1H NMR (d_8 THF, 360 MHz) δ 8.66 - 8.60 (m(ABXY), 2H, H-11,14), 8.08 and 8.06 (d, J = 1.3 Hz, 1H each, H-

1,10), 7.52 - 7.31 (m(ABXY), 2H, H-12,13) 7.24 and 7.22 (d, J = 1.3 Hz, 1H each, H-3,8), 6.83 and 6.72 (dd, J = 5.6, 1.8 Hz, 1H each, H-5,6); 6.03 and 5.99 (dd, J= 1.8, 0.7 Hz, 1H each, H-4,7), 1.468 (s, 9H, $C(CH_3)_3$), 1.464 (s, 9H, $C(CH_3)_3$), -0.98 (s, 3H, $-CH_3$), -1.20 (s, 3H, $-CH_3$); ^{13}C NMR (d_8 THF, 90.6 MHz) δ 144.85, 144.58, 138.80, 137.88, 136.40, 136.35, 135.16,134.77,130.67, 130.59, 129.02, 128.83, 128.58, 126.91, 125.34, 125.28, 117.64, 117.57, 115.62, 115.54, 80.22, 80.15, 39.18, 38.38, 35.97, 30.58, 19.98, 17.68;

IR (KBr) 1474, 1367, 1253, 1034, 875, 858, 752 cm^{-1}; CI MS *m/z* 461(MH+).

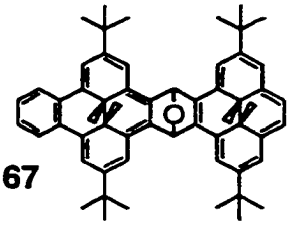

67

Isoarenefuran adduct 67

A solution of **55** (720 mg, 1.872 mmol) and **65** (298 mg, 0.539 mmol) was prepared in dry toluene (15 mL) in the dark under argon, and cooled to -40 °C. Butyllithium (1.6 mLx2.5 M ^{n}Butyllithium in hexanes) was then added slowly by syringe, with stirring. At 16 minutes, methanol (3 mL) was added. All the solvents were removed in vacuo below room temperature. The products were purified by chromatography (neutral alumina, deactivated with 5% water, eluted with hexanes/benzene 2:1) to yield **67** as an equal mixture of the two isomers (50

mg, 0.064 mmol, 12 %) as a golden (maple syrup like color) microcrystalline solid. A single isomer was obtained by further chromatography, yield, 20 mg. Crystallization of the single isomer from benzene gave dark crystals, mp 222 - 225°C; ^{1}H NMR (d_8 THF, 360 MHz) δ 8.82 (d, J = 1.3 Hz, 1H), 8.70 (d, J = 1.2 Hz, 1H), 8.66 - 8.62 (m(ABXY, 2H), 8.45 (br.s., 1H), 8.41 (br.s., 1H), 8.34 - 8.28 (AB, 2H), 8.16 (d, J = 1.3 Hz, 1H), 8.13 (d, 1H, J = 1.3 Hz), 7.92 (d, J = 1.2, 1H), 7.69 (d, J = 1.3, 1H), 7.50 (d, J = 0.6 Hz, 1H), 7.47 (br.s., 1H), 7.48 - 7.43 (m(ABXY, 2H), 1.76 (s, 9H, $C(CH_3)_3$), 1.71 (s, 9H, $C(CH_3)_3$), 1.60 (s, 9H, $C(CH_3)_3$), 1.53 (s, 9H, $C(CH_3)_3$), -1.04 (s, 3H, CH_3), -1.99 (s, 3H, CH_3), -3.60 (s, 3H, CH_3), -4.18 (s, 3H, CH_3); ^{1}H NMR (C_6D_6, 300 MHz) mixture of isomers, methyl groups; δ -0.63, -0.64, -1.67, -1.70, -3.17, -3.21, -3.87, -3.95, (3H each); ^{13}C NMR (d_8 THF, 90.6 MHz) δ 146.23, 146.14, 145.34, 145.14, 138.48, 137.80, 137.68, 137.60, 136.65, 136.59, 136.35, 136.16, 130.55, 130.40, 128.46, 127.94, 127.61, 127.21, 126.80, 126.78, 125.88, 125.31, 125.19, 125.01, 124.78, 122.07, 121.85, 117.57, 117.43, 117.13, 116.53, 116.16, 80.47, 80.27, 39.87, 36.90, 36.66, 36.61, 36.16, 36.06, 33.40, 32.16, 31.08, 30.87, 30.77, 30.71, 19.52, 17.53, 15.76, 14.62; IR (KBr) 1601, 1474, 1466, 1459, 1361, 1346, 1261, 1005, 888, 865, 754, 673, 651, 645 cm^{-1}; LSIMS *m/z* 776.4 (M+), 761.4 (M+ - 15), 731.4 [M+ - 3(15)]; HRMS Calc'd for $C_{58}H_{64}O$ 776.4957 Found: 776.4977

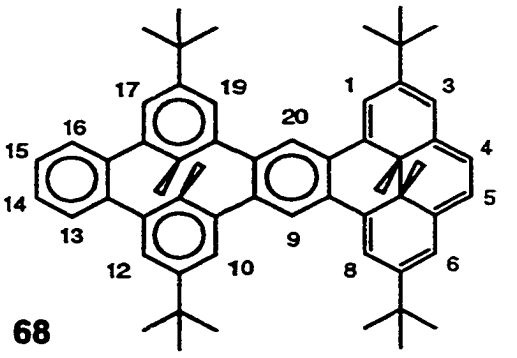

68

Bis switch 68

A mixture of the single isomer **67** from above (40 mg, 0.0 mmol) with $Fe_2(CO)_9$ (70 mg) was refluxed in benzene (30 mL) for 2 hr., with stirring under argon, in the dark. After cooling, the mixture was filtered under inert gas through silica gel (60 mesh, deactivated with 5% water). The silica gel was rinsed with benzene (50 mL). Evaporation of the solvent was accomplished in the dark, avoiding exposure to air. The sample was purified carefully under inert gas by chromatography (silica gel, 60 mesh, deactivated with 5% water), using hexanes/ CH_2Cl_2 (6:1) as eluant. The first ~70% of the red product band was collected. Evaporation of the solvent gave **68** (24 mg, 60 %) as an intense red solid. Crystallization from cyclohexane gave crystals with mp (dec) 170 - 175 °C; ^{1}H NMR ($CDCl_3$, 360 MHz) δ 8.94 (br. s, 2H, H-9,20), 8.32 (br. s, 2H, H-1,8), 7.80 - 7.74 (m[AA'XX'], 2H, H-13,16), 7.49 - 7.43 (m[AA'XX'], 2H, H-14,15), 7.38 (br. s., 2H, H-3,6), 7.16 (br. s., 2H, H-4,5), 7.08 (d, J = 2.1 Hz, 2H, H-10,19), 7.00 (d, J = 2.2 Hz, 2H, H-12,17), 1.50 (s, 18 H, $C(CH_3)_3$), 1.31 (s, 18 H, $C(CH_3)_3$), 1.18 (s, 6H, CH_3), -1.37 (s, 6H, CH_3); ^{13}C NMR ($CDCl_3$, 90.6 MHz) δ 150.29, 143.64, 142.06, 139.85, 139.80, 138.01, 128.73, 128.17,

120.97, 34.28, 31.45, 18.59. IR (KBr) 1615, 1596, 1464, 1362, 1264, 1225, 1201, 873, 756, 673, 644 cm^{-1}; LSIMS *m/z* 760.5(M+), 745.5(M+ - 15); HRMS. Calc'd for $C_{58}H_{64}$: 760.5008. Found: 760.5004.

When the mixture of isomers was used, almost identical material was obtained. The NMR spectrum of the second isomer was calculated by subtraction of the NMR spectrum of the first isomer from the NMR spectrum of the mixture of isomers.

^1H NMR, second isomer.($CDCl_3$, 300 MHz) δ 9.09 (br.s. 2H, H-9,20), 8.52 (br.s. 2H, H-1,8), 7.80 - 7.74 (m[AA'XX'], 2H, H-13,16), 7.49 - 7.43 (m[AA'XX'], 2H, H-14,15), 7.52 (br.s., 2H, H-3,6), 7.31 (br.s., 2H, H-4,5), 7.09 (d, J = 2.1 Hz, 2H, H-10,19), 7.01 (d, J = 2.2 Hz, 2H, H-12,17), 1.54 (s, 18 H, $C(CH_3)_3$), 1.32 (s, 18 H, $C(CH_3)_3$), 1.18 (s, 6H, CH_3), -1.67(s, 6H, CH_3).

Note: NMR spectrum broadens on standing.

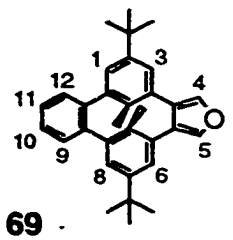

69

1,2-(3,4-Furano)-9,10-benzo[2.2]metacyclophane 69

Adduct **66** (38 mg, 0.083 mmol) was stirred with 3,6-di-2-pyridyl-1,2,4,5-tetrazine[72] **54** (48 mg, 0.20 mmol) in dry THF (20 mL) in the dark, under argon, for 12 hr. Next, the mixture was photolyzed in an ice bath using a 250 watt tungsten flood lamp, under argon for 0.5 h. The solvent was removed in vacuo. The residue was taken up with hexanes/benzene, 8:3 and filtered through alumina (4 cm, neutral, deactivated with 5% water). The solvent was removed in vacuo to give the cyclophanediene **69** (24 mg, 67%) as a colorless crystalline solid, mp 237 - 238°C; ^{1}H NMR ($CDCl_3$, 360 MHz) δ 7.73 (s, 2H, H-4,5), 7.75 - 7.70 (AA'XX', 2H, H-9,12), 7.46 - 7.41(AA'XX', 2H, H-10,11), 6.98 - 6.97(m, 4H, H-1,3,6,8), 1.28(s, 18H, $C(CH_3)_3$), 0.93 (s, 6H, CH_3); ^{13}C NMR ($CDCl_3$, 90.6 MHz) δ 150.11, 142.93, 140.17, 137.89, 137.46, 131.69, 130.18, 129.00, 128.49, 128.16, 127.45, 34.14, 31.38, 17.97; IR (KBr) 1465, 1362, 1236, 1046, 869, 794, 760 cm^{-1}; CI MS *m/z* 435 (MH+); Anal. Calc'd for $C_{32}H_{34}O$: C, 88.43; H 7.89. Found: C, 88.45; H, 7.99.

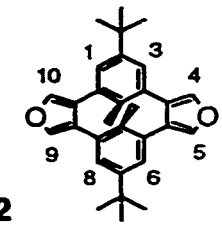

72

1,2:9,10-bis(3,4-Furano)[2.2]metacyclophane 72

DMDHP bis-furan adduct **71** [68b,c] (40 mg, 0.084 mmol) was stirred with 3,6-di-2-pyridyl-1,2,4,5-tetrazine[72] **54** (80 mg, 0.34 mmol) in dry THF (40 mL) for 12 h in the dark under argon. The resulting purple solution was photolyzed in an ice bath for 1.5 h, using a 250 watt tungsten incandescent flood lamp. After this, the solvent was removed in vacuo, the residue was taken up in hexanes/ CH_2Cl_2 (6:1), and passed through alumina (5 cm, neutral, deactivated with 5% water), under argon. The solvent was removed in vacuo to give the bis-furo-metacyclophanediene **72** (16 mg, 45%) as a colorless crystalline solid, mp 234°C (sublimes); (Solutions of **72** oxidize readily. It is best to deaerate such solutions. It is also best to the handle solid under inert gas.)

^{1}H NMR ($CDCl_3$, 360 MHz) δ 7.73 (s, 4H, H-4,5,9,10), 6.99 (s, 4H, H-1,3,6,8), 1.28 (s, 18H, $C(CH_3)_3$), 0.81 (s, 6H, CH_3); ^{13}C NMR ($CDCl_3$, 90.6 MHz) δ 149.94, 138.16, 137.42, 132.08, 129.44, 127.24, 34.09, 31.41, 17.81; IR (KBr) 1363, 1239, 1131, 1047, 877, 796, 760 cm^{-1}; CI MS *m/z* 425 (MH+); Anal. Calc'd for $C_{30}H_{32}O_2$: C, 84.87; H 7.60. Found: C, 84.80; H, 7.87.

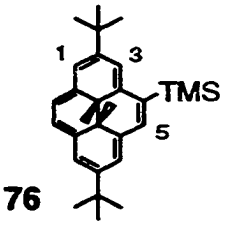

76

2,7-Di-*t*-butyl-4-trimethylsilyl-*trans*-10b,10c-dimethyl-10b,10c-dihydropyrene 76

Bromopyrene **50** (vacuum dried, 626 mg, 1.48 mmol) was dissolved in dry THF (120 mL) and cooled in a dry ice/acetone bath for 20 minutes. Butyllithium (4.0 mL x 2.5 M ^{n}Butyllithium in hexanes) was added dropwise by syringe. The initially green solution rapidly turned brown. The mixture was stirred for 7 minutes after addition. TMSCl (3.0 mL, 28 mmol, stored on CaH_2) was then carefully added by syringe. The reaction flask was allowed to warm to room temperature, and the reaction mixture gradually turned green. The mixture was stirred 0.5 h after warming. Hexanes (100 mL) was added and the whole transferred to a 1 L separatory funnel containing hexanes (100 mL) and water 50 mL). The organic phase was extracted with aq. $NaHCO_3$ (10%, 3x60 mL) and water (4x100 mL). The organic phase was evaporated to give a green solid (containing ~87 mole% TMSDHP **76** and ~13% **I**). The product was purified by chromatography (silica gel, 60 mesh, deactivated with 5% water, eluted with hexanes). The leading green band was collected as eight fractions, each evaporated separately and analyzed by NMR ($CDCl_3$). The fractions with over 96

mole% were summed to give **76** (292 mg, 47 %) as a bright green crystalline solid. The remaining fractions were evaporated and purified by similar chromatography to yield more **76** (186 mg, 0.446 mmol; total purified yield 478 mg, mmol, 78 %) The product **76** elutes before the side product **34**. A sample of **76** was crystallized from cyclohexane to give green crystals, mp 186 - 188 °C;

^{1}H NMR ($CDCl_3$, 360 MHz) δ 8.75(d, J = 1.0 Hz, 1H, H-3), 8.66 (s, 1H, H-5), 8.51 (s, 1H, H-6), 8.49 (br. s, 1H, H-8), 8.48 (br. s, 1H, H-1), 8.377 (AB, J = 7.7 Hz, 1H, H-9 or 10), 8.395(AB, 1H, H-9 or 10), 1.68 (s, 9H, $C(CH_3)_3$), 1.67 (s, 9H, $C(CH_3)_3$), 0.67 (s, 9H, $-Si(CH_3)_3$), -4.02 (s, 3H, CH_3), -4.05 (s, 3H, CH_3);

^{13}C NMR ($CDCl_3$, 90.6 MHz) δ 145.3, 145.2, 141.0, 138.5, 136.2, 135.7, 133.1, 129.5, 122.5, 122.3, 121.6, 121.2, 120.7, 120.1, 36.1, 35.9, 31.9, 30.3, 29.2, 14.6, 14.3, 1.04; IR (KBr) 1458, 1382, 1358, 1342, 1249, 1227, 874, 849, 835, 669 cm^{-1}; CI MS *m/z*, 417(MH+), 416 (M+); Anal. Calc'd for $C_{29}H_{40}Si$: C, 83.59; H 9.68. Found: C, 83.56; H, 9.65.

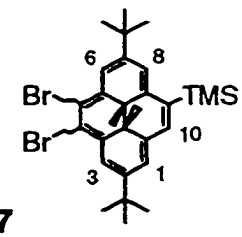

77

4,5-Dibromo-2,7-di-*t*-butyl-9-trimethylsilyl-*trans*-10b,10c-dimethyl-10b,10c-dihydropyrene 77

A solution of **76** (253 mg, 0.606 mmol) in dry CH_2Cl_2 (200 mL) (under argon in oven dried glassware with a magnetic stir bar), was cooled in an ice bath. A solution of NBS (334 mg, 1.88 mmol, 3.10 eq.) in dry DMF (40 mL) was added dropwise into the cooled solution of **76**. After addition, the ice bath was removed, and the mixture allowed to stir overnight (20 hr.). Next day, hexanes (200mL) was added and with rapid stirring, water (70 mL). After stirring for 2 minutes, the whole was transferred to a 1 L separatory funnel containing hexanes (100 mL) and water (100 mL). The organic phase was then extracted with water (8x150 mL), separated and evaporated. The solid residue was taken up in hexanes/ CH_2Cl_2 (1:1) and filtered through silica gel (60 mesh, deactivated with 5% water), eluting with the same solvent. The green eluate was evaporated to yield **77** (330 mg, 95%). Crystallization from cyclohexane gave green crystals, mp 203 - 206°C; ^{1}H NMR ($CDCl_3$, 360 MHz) δ 8.90(d, J = 1.1 Hz, 1H, H-6), 8.88(d, J = 1.3 Hz, 1H, H-3), 8.75(d, J = 0.9 Hz, 1H, H-8), 8.63(s, 1H, H-10), 8.50(br. s, 1H, H-1), 1.69(s, 9H, $C(CH_3)_3$), 1.68(s, 9H, $C(CH_3)_3$), 0.67(s, 9H,

-Si(CH_3)$_3$), -3.76 (s, 3H, CH_3), -3.78 (s, 3H, CH_3); ^{13}C NMR ($CDCl_3$, 90.6 MHz) δ 148.4, 148.3, 142.1, 137.0, 135.04, 134.98, 132.8. 131.2, 123.0, 122.9, 122.8, 122.3, 118.9, 118.7, 36.5, 36.3, 33.2, 32.1, 31.8, 14.5, 14.3, 0.92; IR (KBr) 1584, 1464, 1362, 1337, 1248, 965, 873, 848, 837, 749 cm^{-1}; CI MS *m/z* 575(MH+, ^{79}Br, ^{81}Br) (correct isotope pattern present), 503(MH+, ^{79}Br, ^{81}Br, -TMS), 495(MH+ -Br); Anal. Calc'd for $C_{29}H_{38}Br_2Si$; C, 60.63; H 6.67. Found: C, 61.72; H, 6.74. (Some mono-BrTMSDMDHP present)

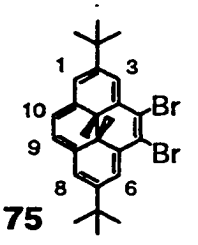

75

4,5-Dibromo-2,7-di-*t*-butyl-*trans*-10b,10c-dimethyl-10b,10c-dihydropyrene 75

A solution of **77** (93 mg, 0.162 mmol) in THF (20 mL) was refluxed with tetrabutylammonium fluoride (TBAF) (1.5 mL x 1.0 M TBAF in THF) under argon for 24 h. After cooling, the mixture was diluted with hexanes (100 mL) and extracted with water (4x100 mL). The organic phase was separated, dried ($MgSO_4$), filtered and evaporated. The residue was taken up in hexanes/ CH_2Cl_2

(6:1) and filtered through silica gel (60 mesh, deactivated with 5% water). The first band was collected and evaporated to yield **75** (68 mg, 84%) as green crystals. Recrystallization from cyclohexane gave crystals with mp 198 - 200 °C.

^{1}H NMR ($CDCl_3$, 360 MHz) δ 8.96(d, J =1.3 Hz, 2H, H-3,6), 8.54(d, J = 1.3 Hz, 2H, H-1,8), 8.45(s, 2H, H-9,10), 1.69 (s, 18H, $C(CH_3)_3$), -3.82 (s, 6H, CH_3);

^{13}C NMR ($CDCl_3$, 90.6 MHz) δ 148.3, 137.8, 133.2, 124.1, 123.2, 122.3, 119.2, 36.3, 32.1, 31.87, 14.24; IR(KBr) 1592, 1457, 1362, 1339, 1230, 1218, 1204, 1164, 1118, 965, 874, 794, 673 cm^{-1}; CI MS *m/z* 503(MH+, ^{79}Br, ^{81}Br)(correct isotope pattern present), 423(MH+ -Hbr); Anal. Calc'd for $C_{26}H_{30}Br_2$; C, 62.17; H 6.02. Found: C, 62.84; H, 5.97. (A small amount of bromopyrene **50** was present, ~3% by NMR.)

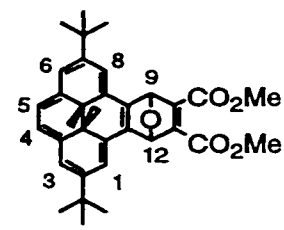

79

0,11-Dicarbomethoxy-2,7-di-*t*-butyl-9,12,12c,12d-tetrahydro-*trans*-12c,12d-dimethylbenzo[e]pyrene 79

To a stirred solution of furan **55** (340 mg, 0.88 mmol) in THF (25 mL) under argon in the dark, was added DMAD (280 mg, 1.97 mmol) by syringe. The mixture was stirred overnight (16 hr.). The solvent was then removed in vacuo, and the green crystalline solid was purified by chromatography (silica gel, 60

mesh, deactivated with 5% water), eluting with hexanes/ ethyl acetate (6:1). The green band was collected and evaporated to yield the adduct **79** yield, 420 mg, 0.80 mmol, 91 %. Recrystallization from methanol gave crystals with mp 206 - 207°C; ^{1}H NMR (d_8 THF, 360 MHz) δ 8.37 (d, 1H, J = 1.3 Hz), 8.34 (d, 1H, J = 1.3 Hz), 8.27 (d, 1H, J = 1.3 Hz), 8.25 (d, 1H, J = 1.3 Hz), 8.184 (AB, J = 8.7 Hz,1H, H-4 or 5), 8.187 (AB, 1H, H-4 or 5), 6.84 - 6.83 (m, 2H, H-9,10), 3.72 (s, 3H, -OCH_3), 3.67 (s, 3H, -OCH_3), 1.639, (s, 9H, C(CH_3)), 1.636 (s, 9H, C(CH_3)), -3.17 (s, 3H, CH_3), -3.52 (s, 3H, CH_3); ^{13}C NMR (d_8 THF, 90.6 MHz) d; 163.63, 149.63, 149.34, 146.90, 146.59, 138.75, 138.45, 133.98, 133.88, 130.58, 129.97, 125.58, 125.41, 122.34, 122.29, 116.88, 116.20, 52.06, 52.03, 36.47, 34.44, 32.84, 31.79, 17.02, 14.73; IR (KBr) 1747, 1722, 1622, 1437, 1322, 1300, 1242, 1202, 1110, 1066, 991, 905, 886, 864, 769, 664 cm^{-1}; CI MS *m/z* 527 (MH+); Anal. Calc'd for $C_{34}H_{38}O_5$: C, 77.54; H 7.27. Found: C,77.60; H, 6.96.

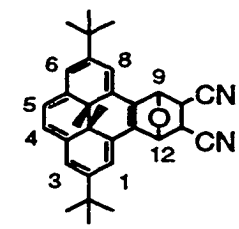

80

10,11-Dicyano-2,7-di-*t*-butyl-9,10,11,12,12c,12d-hexahydro-*trans*-12c,12d-dimethylbenzo[e]pyrene 80

To a stirred solution of furan **55** (700 mg, 1.84 mmol) in THF (50 mL) under argon in the dark, was added fumaronitrile (176 mg, 2.25 mmol). The

mixture was stirred overnight (18 hr.). The solvent was then removed in vacuo, and the solid green residue was left on an oil pump overnight to remove residual fumaronitrile. The solid was then purified by chromatography (silica gel, 60 mesh, deactivated with 5% water), eluting with hexanes/ CH_2Cl_2 (1:1) The green band was collected and evaporated to yield **80** as a mixture of isomers, 810 mg, 1.75 mmol, 95 %. Recrystallization from methanol gave green crystals with mp 195 - 206°C; ^{1}H NMR ($CDCl_3$, 360 MHz) δ 8.60 - 8.40 (m 6H), 6.77 - 6.71 (m, 2H), 3.95 - 3.88 (m, 1H), 3.20 - 3.10 (m, 1H), 1.70 1.67 (m, 18H), -3.90 - -4.10 (m,6H); ^{13}C NMR ($CDCl_3$, 90.6 MHz) δ 147.65, 147.53, 147.30, 147.22, 137.31, 137.10, 136.93, 136.85, 131.96, 131.22, 130.57, 129.51, 128.95, 128.10, 126.59, 125.58, 125.01, 124.96, 124.71, 124.62, 122.28, 122.18, 122.01, 118.95, 117.41, 116.77, 116.23, 116.12, 115.72, 115.44, 83.13, 82.88, 80.72, 80.10, 39.05, 38.62, 36.23, 32.14, 31.91, 31.83, 31.79, 29.02, 14.61, 14.53, 14.44, 13.97; IR (KBr) 2240, 1610, 1459, 1384, 1348, 1306, 1266, 1225, 1057, 959, 909, 876, 674, 652 cm^{-1}; CI MS *m/z* 463(MH+); Anal. Calc'd for $C_{32}H_{34}N_2O$: C, 83.12; H 7.41. Found: C, 82.88; H, 7.54.

References

1) Faraday, M.; *Phil. Trans. Roy. London* **1825**, 440 - 466.

2) a) Kekule, A. *Bull. Soc. Chim.* Paris **1865**, *1*, 98. b) Kekule, A. *Ann.* **1866**, *137*, 129 - 196. c) Kekule, A. *Lehrbuch der Organische Chemie*, Vol 2. Enk. Erlangen (1866).

3) Armit, J.W.; Robinson, R. *J. Chem. Soc.* **1925**, *127*, 1604-1618.

4) Huckel, E. *Z. Physik*, **1931**, *70*, 204 - 286, *ibid* **1931**, *72*, 310.

5) a) Pauling, L. *J. Chem. Phys.* **1936**, *4*, 673-677. b) Garratt, P.J. *Aromaticity*, Wiley, New York, 1986.

6) a) Evans, M.G.; Polanyi, M. *Trans. Faraday Soc.* **1938**, *34*, 11 -24.
b) Evans, M.G.; Warhurst, E. *ibid* **1938**, *34*, 614 - 624.
c) Evans, M.G. *ibid* **1939**, *35*, 824 -834.

7) a) Dewar, M.J.S. *Angew. Chem. Int. Ed. Engl.* **1971**, *10*, 761-776 .
b) Dewar, M.J.S. *The Molecular Orbital Theory of Organic Chemistry*, McGraw-Hill, New York, (1969).

8) a) Willstatter, R.; Waser, E. *Ber.* **1911**, *44*, 3424 - 3445.
b) Willstater, R.; Heidelberger, M. *Ber*, **1913**, *46*, 517 - 527.

9) Watts, L.; Fitzpatrick, J.D.; Pettit, R. *J. Am. Chem. Soc.* **1965**, *87*, 3252-3254.

10) Streitweiser, A., *Molecular Orbital Theory for Organic Chemists*; John Wiley & Sons, Inc.; New York; pp 117 - 135, *1961.*

11) a) Randic, M., *Chem. Phys. Lett.*, **1976**, *38*, 68 - 70. b) Randic, M., *J. Am. Chem. Soc.* **1977**, *99*, 444 - 448. c) Randic, M., *Tetrahedron*, **1977**, *33*, 1905 - 1912.

12) Minkin, V.J.; Glukhovtsev, M.N.; Simkin, B.Y. *Aromaticity and Antiaromaticity: Electronic and Structural Aspects*, Wiley, Inc. New York, (1994).

13) Sondheimer, F., *Acc. Chem. Res.*, **1972**, *5*, 81 - 91.

14) Nakagawa, M., *Pure Appl. Chem.*, **1975**, *44*, 885 - 924.

15) Boekelheide, V.; Phillips, J.B., *Proc. Natl. Acad. Sci. USA*, **1964**, *54*, 550.

16) a) Vogel, E.; Boll, W.A., *Angew. Chem. Int. Ed. Engl.* **1964**, *3*, 642 - 643. b) Mitchell, R.H. *Adv. Theor. Interesting Mol.* (JAI Press), **1989**, *1*, 135 - 199.

17) Schleyer, P.v.R.; Freeman, P.; Jiao, H.; Goldfuss, B. *Angew. Chem. Int. Ed. Engl.* **1995**, *34*, 337-340.

18) Bernardi, F.; Bottoni, A.; Venturini, A. *J. Mol. Struct. (Theochem.)* **1988**, *163*, 173.

19) a) Rosenstock, H.M.; Draxl, K.; Steiner, B.W.; Herron, J.T. *J. Phys. Chem.* Ref. data, Vol. 6. Suppl. 1. **1977**. b) Cohen, N.; Benson, S.W. *Chem. Rev.* **1993**, *93*, 2419-2438.

20) Rice, J.E.; Lee, T.J.; Remington, R.B.; Allen, W.D.; Clabo Jr, D.A.; Schaefer III, H.F. *J. Am. Chem. Soc.* **1987**, *109*, 2902-2909.

21) Pascal, P. *Ann. Chim. Phys.* **1910**, [8] *19*, 5.

22) Schleyer, P.v.R.; Jiao, H. *Pure Appl. Chem.*, **1996**, *68*, 209-218.

23) a) Pople, J.A., *J. Chem. Phys.*, **1956**, *24*, 1111 - 1116. b) Haigh, C.W.; Mallion, R.B., *Progress in NMR Spectroscopy*, **1980**, *13*, 303 - 344.

24) Boekelheide, V.; Phillips, J.B. *J. Am. Chem. Soc.*, **1967**, *89*, 1695-1704.

25) Mitchell, R.H.; Klopfenstein, C.E.; Boekelheide, V. *J. Am. Chem. Soc.*, **1969**, *91*, 4931-4932.

26) Haigh, C.W.; Mallion, R.B., *Mol. Phys.*, **1970**, *18*, 737 -750.

27) a) Laszlo, P.; Stang, P. *Organic Spectroscopy: Principles and Applications* Harper & Row, New York, N.Y. *1971.* b) Pouchert, C.J.; Behnke, J., *The Aldrich Library of ^{13}C and ^{1}H FT NMR Spectra*, Ed. 1; Vol. III; Aldrich Chemical Company, Milwaukee, *1993.*

28) Vogel, E.; Roth, H.D., *Angew. Chem. Int. Ed. Engl.*, **1964**, *3*, 228 - 229.

29) Schafer-Ridder, M.; Wagner, A.; Schwamborn, M.; Schreiner, H.; Devrout, E.; Vogel, E., *Angew. Chem. Int. Ed. Engl.*, **1978**, *17*, 853 -855.

30) Grimme, W.; Kanfhold, M.; Dettmeier, U.; Vogel,E., *Angew. Chem. Int. Ed. Engl.*, **1966**, *5*, 604 -605.

31) Vogel, E.; Konigshofen, H.; Mullen, K.; Oth, J.F.M., *Angew. Chem. Int. Ed. Engl.*, **1974**, *13*, 281 - 283.

32) Grasselli, J.G., *Atlas of Spectral data and Physical Constants for Organic Compounds*: CRC press, *1973*, p B460.

33) Oth, J.F.M., *Pure Appl. Chem.*, **1971**, *25*, 573 - 622.

34) Boekelheide, V.; Pepperdine, W., *J. Am. Chem. Soc.*, **1970**, *92*, 3684 - 3688

35) Huber, W.; Lex, J.; Meul, T.; Mullen, K., *Angew. Chem. Int. Ed. Engl.*, **1981**, *20*, 391 -292.

36) Breslow, R.; Groves, J., *J. Am. Chem. Soc.*, **1970**, *92*, 984 - 988.

37) Vogler, H., *J. Am. Chem. Soc.*, **1978**, *100*, 7464 - 7500.

38) Memory, J.D.; Wilson, N.K., *NMR of Aromatic Compounds*; John Wiley & Sons; New York; pp 30 - 33, *1982.*

39) a) Jiao, H.; Schleyer, P.v.R. *J. Chem. Soc. Faraday Trans.* **1994**, *90*, 1559-1567. b) Jiao, H.; Schleyer, P.v.R. *Angew. Chem. Int. Ed. Engl.* **1993**, *32*, 1760-1763. c) Herges, R.; Jiao, H.; Schleyer, P.v.R. *Angew. Chem. Int. Ed. Engl.* **1994**, *33*, 1376-1378. d) Jiao, H.; Schleyer, P.v.R. *Angew. Chem. Int. Ed. Engl.* **1995**, *34*, 334-337. e) Jiao, H.; Schleyer, P.v.R. *J. Am. Chem. Soc.*, **1996**, *118*, 6317-6318. f) Paquette, L.A.; Bauer, W.; Sivik, M.R.; Buhl, M.; Feigel, M.; Schleyer, P.v.r. *J. Am. Chem. Soc.* **1990**, *112*, 8776-8789. g) Buhl, M.; Thiele, W.; Jiao, H.; Schleyer, P.v.R.; Saunders. M.; Anet, F.A.L. *J. Am. Chem. Soc.* **1994**, *116*, 6005-6006.

40) Haddon, R.C. *J. Am. Chem. Soc.* **1979**, *101*, 1722-1728.

41) Schleyer, P.v.R.; Freeman, P.; Jiao, H.; Goldfuss, B. *Angew. Chem. Int. Ed. Engl.* **1995**, *34*, 332-334

42) Katritzky, A.R.; Karelson, M.; Sild, S.; Krygowski, T.M.; Jug. K. *J. Org. Chem.* **1998**, *63*, 5228-5231.

43) a) Aihara, J. *Bull. Chem. Soc. Jpn.* **1980**, *53*, 1163-1164. b) Verbruggen, A. *Bull. Soc. Chim. Belg.* **1982**, *91*, 865-868. c) Hess, B.A. Jr.; Schaad, L.J.; Agranat. F. *J. Am. Chem. Soc.* **1978**, *100*, 5268-5271.

44) a) Mitchell, R.H.; Iyer, V.S.; Khalifa, N.; Mahadevan, R.; Venugopalan, S.; Weerawarna, S.A.; Zhou, P., *J. Am. Chem. Soc.* **1995**, *117*, 1514-1532. b) Mitchell, R.H.; Venugopalan, S.; Zhou, P.; Dingle, T.W. *Tetrahedron Lett.* **1990**, *31*, 5281-5284.

45) Dewar, M.J.S.; de Llano, Carlos. *J. Am. Chem. Soc.* **1969**, *91*, 789-795.

46) Mitchell, R.H.; Khalifa, N.A.; Dingle, T.W. *J. Am. Chem. Soc.* **1991**, *113*, 6696-6697.

47) Mitchell, R.H.; Iyer, V.S. *J. Am. Chem. Soc.* **1996**, *118*, 2903-2906.

48) a) Mitchell, R.H.; Chen, Y.; Khalifa, N.; Zhou, P. *J. Am. Chem. Soc.* **1998**, *120*, 1785 - 1794. b) Mitchell, R.H.; Chen, Y. *Tetrahedron Lett.* **1996**, *37*, 6665-6668.

49) a) *Photochromism, Molecules and Systems* , (Eds.: Durr, H. and Bouas - Laurent, H.), Elsevier, Amsterdam, **1990**.
b) Brown, G.H., *Photochromism*, Wiley - Interscience, N.Y. **1971**.

50) a) Shinkai, S.; Manabe, O., *Topics Curr. Chem.* **1984**, *121*, 67 - 104.
b) Kumar, G.S.; Neckers, D.C., *Chem, Rev.* **1989**, *89*, 1915 - 1925.
c) Rau. H. in *Photochromism, Molecules and Systems* , (Eds.: Durr, H. and Bouas - Laurent, H.), Elsevier, Amsterdam, **1990**, chapter 4.
d) Balzani, V.; Scandola, F., *Supramolecular Photochemistry*, Horwood, Chichester, **1991**, chapter 7.

51) Irie, M., *Chem. Rev.* **2000**, *100*, 1685 - 1716.

52) a) Berkovic, G.; Krongauz, V.; Weiss, V., *Chem. Rev.* **2000**, *100*, 1741 - 1753 b) Willner,I.; Willner, B., *Bioelectrochemistry and Bioenergetics* **1997**, *42*, 43 - 57.

53) Hampp, N., *Chem. Rev.* **2000**, *100*, 1755 - 1776.

54) Yokoyama, Y., *Chem. Rev.* **2000**, *100*, 1717 - 1739.

55) a) Beyeler, A.; Belser, P.; De Cola, L. *Angew. Chem., Int. Ed. Engl.*, **1997**, *36*, 2779 - 2781. b) Tucker, J.H.R.; Bouas-Laurent, H.; Marsau, P.; Riley, S.W.; Desverhne, J.-P. *J.C.S. Chem. Commun.*, **1997**, 1165 - 1166.

56) Windsor, M.W. in *The Encyclopedia of Chemistry*, 2nd Ed., (Clark, G.L. editor in chief) Van Nostrand Reinhold Co. New York **1966**, pp 816 - 818.

57) Blattmann, H.R.; Heilbronner, E.; Molyneux, R.J.; Boekelheide, V., *J. Am. Chem. Soc.*, **1965**, *87*, 130 - 131.

58) Muskat, K.A.; Fischer, E., *J. Chem. Soc. (B)*, **1967**, 662 - 678.

59) Blattmann, H.R.; Schmidt, W., *Tetrahedron*, **1970**, *26*, 5885 - 5899.

60) Murakami, S.; Tsutsui, T.; Saito, S.; Yamato, T.; Tashiro, M., *Nippon Kagukukai Shi*, **1988**, 221 - 229.

61) a) Mitchell, R.H.; Carruthers, R.J.; Mazuch, L.; Dingle, T.W., *J. Am. Chem. Soc.*, **1982**, *104*, 2544 - 2551.
b) Mitchell, R.H.; Yan, J.S.H.; Dingle, T.W., *J. Am. Chem. Soc.*, **1982**, *104*, 2551 - 2559.
c) Mitchell, R.H.; Williams, R.V.; Dingle, T.W., *J. Am. Chem. Soc.*, **1982**, *104*, 2551 - 2559.
d) Mitchell, R.H.; Iyer, V.S.; Mahadevan, R.; Venugopalan, S.; Zhou, P., *J. Org. Chem.*, **1996**, *61*, 5116 - 5120.

62) Mitchell, R.H.; Chen, Y.-S., *Tetrahedron Lett.*, **1996**, *37*, 5239 - 5242.

63) a) Lai, Y.-H.; Chen, P.; Peck, T.-G. *Pure & Appl. Chem.*, **1993**, *65*, 81-87.
b) Chen, P. Ph.D. Thesis, National University of Singapore, 1992.

64) Mitchell, R.H.; Zhou, P., *Tetrahedron Lett.*, **1991**, *32*, 6319 - 6322.

65) Tashiro, M.; Yamato, T., *J. Am. Chem. Soc.* **1982**, *104*, 3701 - 3707.

66) Mitchell, R.H., *Heterocycles*, **1978**, *11*, 563 - 586.

67) Mitchell, R.H.; Yan, J.S.H., *Can. J. Chem.*, **1977**, *55*, 3347 - 3348.

68) a) Mitchell, R.H.; Chen, Y.; Zhang, J., *Org. Prep. Proc. Int.*, **1997**, *29*, 715 - 719.
b) Chen, Y.-S. Ph.D. Thesis, University of Victoria, 1997.

69) Wong, H.N.C.; Ng, T.K.; Wong, T.Y., *Heterocycles*, **1983**, *20*, 1815 - 18.

70) Best, W.M.; Collins, P.A.; McCulloch, R.K.; Wege, D. *Aust. J. Chem.* **1982**, *35*, 843 -

71) a) Warrener, R.N. *J. Am. Chem. Soc.* **1971**, *93*, 2346-2348.
b) Russell, R.A.; Marsden, D.E.; Sterns, M.; Warrener, R.N., *Aust. J. Chem.* **1981**, *34*, 1223-1234.

c) Moursounidinis, J.; Wege, D., *Aust. J. Chem.* **1988**, *41*, 235-249.
d) Mitchell, R.H.; Zhou, P., *Tetrahedron Lett.* **1992**, *32*, 6319-6322.

72) Geldard, J.F.; Lions, F., *J. Org, Chem.* **1965**, *30*, 318-319.

73) a) Wege, D., *Adv. Theor. Interesting Mol.* (JAI Press)**1998**, *4*, 1 - 52.
b) Rickborn, B. *Adv. Theor. Interesting Mol.* (JAI Press) **1989**, *1*, 1 - 134.

74) a) Danish, A.A.; Silverman, M.; Tajima, Y.A. *J. Am. Chem. Soc.*, **1954**, *76*, 6144 - 6150. b) Prill, E.A. *J. Am. Chem. Soc.*, **1947**, *69*, 62 - 63.

75) Yu, D.W.; Preuss, K.E.; Cassis, P.R.; Dejikhangsar, T.D.; Dibble, P.W., *Tetrahedron Lett.*, **1996**, *37*, 8845 - 8848.

76) a) Haley, M.M.; Kimball, D.B.; Mitchell, R.H.; Ward, T.R., *Paper 67*, ACS New Orleans Meeting, Aug. 22 - 26, 1999.
b) Sawada, T. Personal communication during study leave at the University of Victoria, Sept. 1999 - Aug. 2000.

77) Haddon, R.C., *Tetrahedron* **1972**, *28*, 3613-3633.

78) Shaik, S.; Shurki, A.; Danovich, D.; Hiberty, P.C., Theochem. *J. Mol. Struct.*, **1997**, *398*, 155 - 167.

79) Zhou, Z. *Int. Rev. in Phys. Chem.*, **1992**, *11*, 243 - 261.

80) Phillips, J.B.; Molyneux, R.J.; Sturm, E.; Boekelheide, V., *J. Am. Chem. Soc.*, **1967**, *89*, 1704 - 1709.

81) Memory, J.D. *J. Magn. Reson.*, **1977**, *73*, 241 - 244

82) Carey, F.A.; Sundberg, R.J., *Advanced Organic Chemistry, Part A: Structure and Mechanism.*, Third Ed., Plenum Press, New York (1990).

83) Hyperchem 4.5, from Hypercube, Inc., 419 Phillip Street, Waterloo, Ont. N2L 3X2, Canada

84) Dewar, M.J.S.; Trinajstic, N., *Theor. Chim. Acta.*, **1970**, *17*, 235 - 238.

85) Perrin, D.D.; Armarego, W.L.F., *Purification of Laboratory Chemicals*, 3rd edition, Pergamon Press, Great Britain, (1989).

86) Liao, Y.; Bohne, C., *J. Chem. Phys.*, **1996**, *100*, 734 - 743.

Appendix

Plots for the calculation of E_{act}, $\Delta H^{\ddagger}$,and $\Delta S^{\ddagger}$.

Consider the first order reaction:

$$-\ln(C_t) = kt + \text{Constant} \qquad (1)$$

where C_t = concentration of the reactant at time t, and k = rate constant. For the thermal return of a metacyclophanediene (MCD) form to a dihydropyrene (DHP) form, the concentration of the MCD will be

$$C_t = C_0[\text{MCD}/(\text{MCD}+\text{DHP})] \qquad (2)$$

where C_0 is the initial concentration of the MCD form.

That is, the concentration C_t will be a function of the mole fraction in the MCD form, assuming that only two interconvertible species are present.

Now $\ln(C_t) = \ln(C_0) + \ln[\text{MCD}/(\text{MCD}+\text{DHP})]$, and since $\ln(C_0)$ is constant, we can therefore derive k by plotting $\ln[\text{MCD}/(\text{MCD}+\text{DHP})]$ as a function of time, and k will be the slope of the function. Letting $x = [\text{MCD}/(\text{MCD}+\text{DHP})]$, we obtain

$$-\ln(x) = kt + \text{Constant}. \qquad (3)$$

This ratio [MCD/(MCD+DHP)] can be obtained from each NMR spectrum directly by integration of suitable peaks, such as the DHP internal methyl protons, and the MCD aryl methyl protons. Other signals may be used, as long as integration of signals is consistent. For example, the corresponding aryl protons of DHP and MCD may be selected. Different types of protons may not in general be selected on MCD and DHP, as integration is not consistent between protons of different

types, for example, *t*-butyl signals on one isomer may not be compared with internal methyl or aryl protons. The *t*-butyl signals are usually ~10% larger than expected.

The [MCD/(MCD+DHP)] ratios for compounds **29'**, **53'**, **57'**, **59'**, **60'**, **68a'**, and **65'** at suitable times were obtained, at three different temperature. The rate constants were then determined graphically, by using the relation (3) above.

From the values of k obtained, E_{act}, $\Delta H^{\ddagger}$,and $\Delta S^{\ddagger}$ were then determined graphically by using the Arrhenius and Eyring relations.

$$k = A\exp\{-E_{act}/RT\} \qquad (4) \qquad \text{(Arrhenius)}$$

From (4); $\ln(k) = -E_{act}/RT + \text{constant}$ (5)

Plotting ln(k) as a function of 1/T then allowed calculation of E_{act}.

$$k = (kT/h)\exp\{-(\Delta H^{\ddagger} - T\Delta S^{\ddagger})/RT\} \qquad (6) \qquad \text{(Eyring)}$$

$$k = 1.381 \times 10^{-23}\ J/^{\circ}K$$

$$h = 6.626 \times 10^{-34}\ J\ s$$

from which $\ln(k/T) = (1/T)(-\Delta H^{\ddagger}/R) + (\Delta S^{\ddagger}/R) - \ln(k/h)$.

Plotting ln(k/T) against (1/T) as the independent variable gives $(-\Delta H^{\ddagger}/R)$ as the slope, and $[(\Delta S^{\ddagger}/R) - 23.73]$ as the intercept of the vertical axis. Thus from the slope and the intercept, $\Delta H^{\ddagger}$ and $\Delta S^{\ddagger}$ may be obtained.

The error values in coloration rates were obtained by selecting the greater of the standard deviations from each plot, or the errors in the mole fractions (MCD)/(MCD + DHP) determined from NMR ratios. Errors in proton NMR ratios were determined by obtaining ten individual NMR spectra of a single sample of a

mixture of **55** and **55'** in deuterio-toluene. The system **55** and **55'** was chosen because of the extremely slow thermal return of **55'** to **55** at room temperature. The change in the ratio of **55'** to **55** was not detectable after 12 hours, by NMR. The NMR spectrometer used was a Bruker AC 300. The ten consecutive NMR spectra of 16 scans each required less than an hour to complete. Four NMR peaks in the aryl-H region were chosen and integrated. One peak was chosen from **55'**, and three peaks were chosen from **55.** The ratios of the integrations of the peaks for **55** to the peak for **55'** were formed, and the standard deviations of the ratios were calculated. The three standard deviations (σ values) were; 1) 0.46%, 2) 1.60%, and 3) 2.50%. The peak chosen as reference was the most isolated peak of **55'**, and the lowest σ value was found for the integration ratio of the corresponding proton of the isomer **55**. The σ value 2.50% results in an uncertainty (σ) in ln(x) of $\pm$ 0.025. Thus the σ value $\pm$ 0.025 was selected for the error bars for the plots for determining coloration rates for **29'**, **53'**, **57'**, **59'**, **65'**, **60''**, and **68a'**.

Table 10 Coloration reaction rates.

compound	T/(°K)	k/(min^{-1})	$t_{1/2}$
29'	319	0.00610 ± 0.00015	113 min.
	333	0.0300 ± 0.0008	22 min.
	343	0.086 ± 0.002	8 min
	(293		estimate 2.25 d.)
65'	319	0.00124 ± 0.00003	9.5 h.
	333	0.0063 ± 0.0002	1.8 h.
	343	0.0212 ± 0.0005	33 min.
	(293		est. 14 d.)
53'	319	0.00198 ± 0.00005	5.75 h.
	333	0.0095 ± 0.0002	1.2 h.
	343	0.0299 ± 0.0008	23 min.
	(293		est. 7.7 d.)
57'	319	0.0101 ± 0.0003	1.15 h.
	333	0.042 ± 0.001	16.5 min.
	343	0.117 ± 0.003	6 min.
	(293		est. 24 h.)
59'	319	0.0344 ± 0.0009	20 min.
	333	0.178 ± 0.005	5 min.
	343	0.27 ± 0.007	2.5 min.
	(293		est. 4.35 h.)
60''	319	0.0057 ± 0.0002	
	333.8	0.0297 ± 0.0008	
	343.6	0.090 ± 0.002	
68'	318	0.00224 ± 0.00006	
	333	0.0134 ± 0.0003	
	343	0.0356 ± 0.0009	
55'	319	0.000183 ± 0.000005	
	334	0.00108 ± 0.00003	
	343	0.00322 ± 0.00008	

Error in temperatures: ± 0.5°K.

Eyring plots for the thermal return reactions of the cyclophanediene photoisomers.

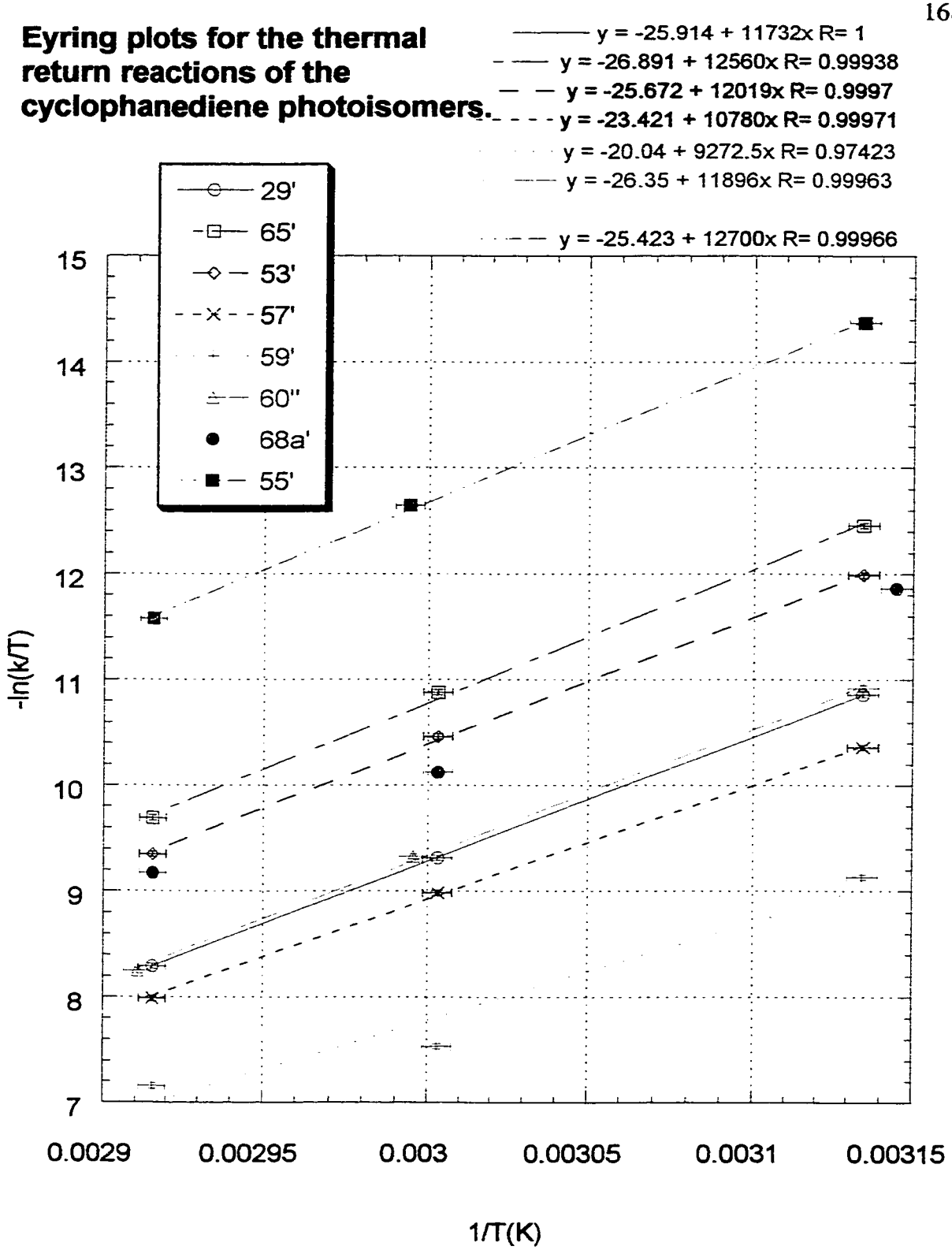

Arrhenius plots for the thermal return reactions of the cyclophanediene photoisomers.

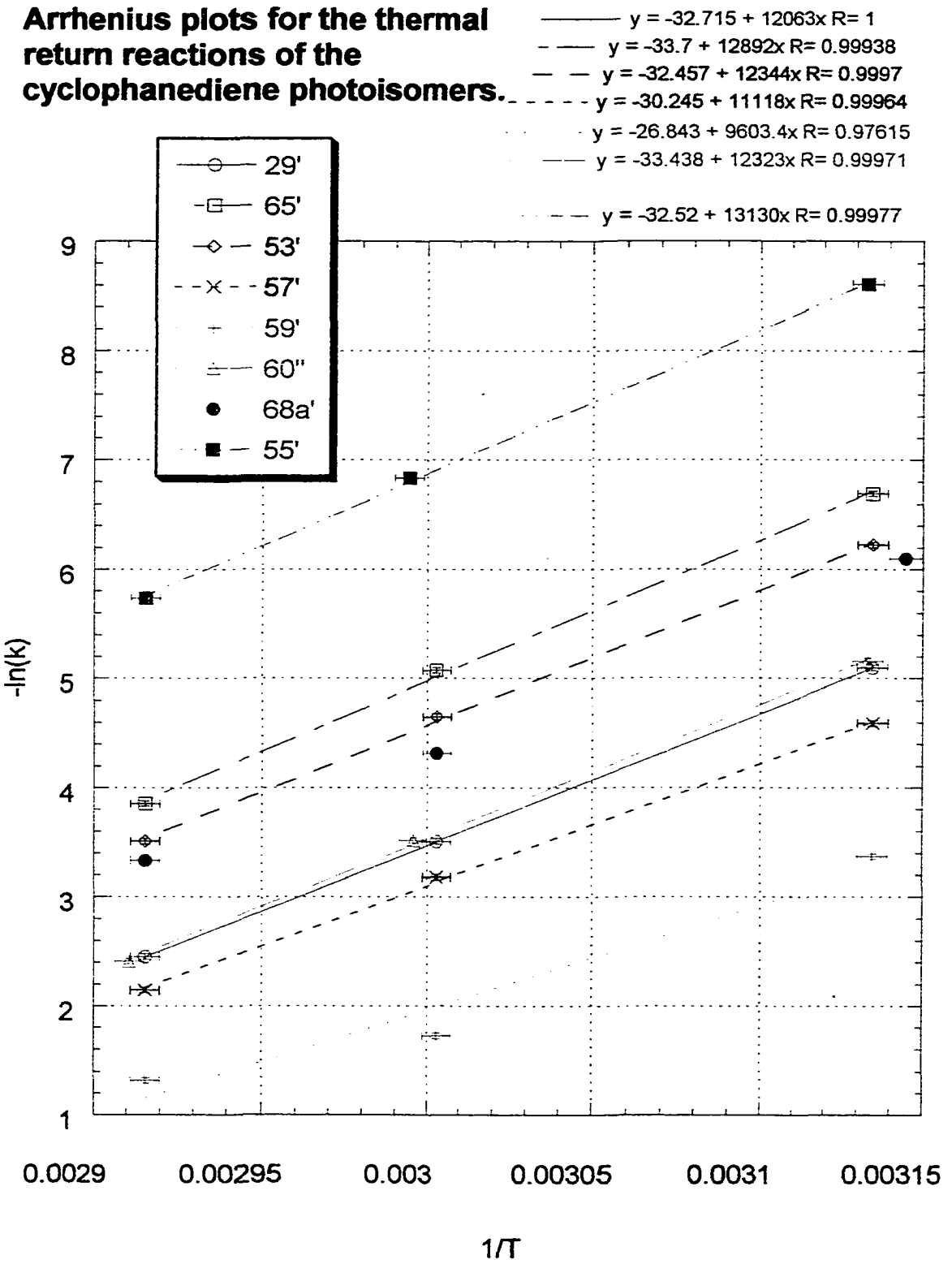

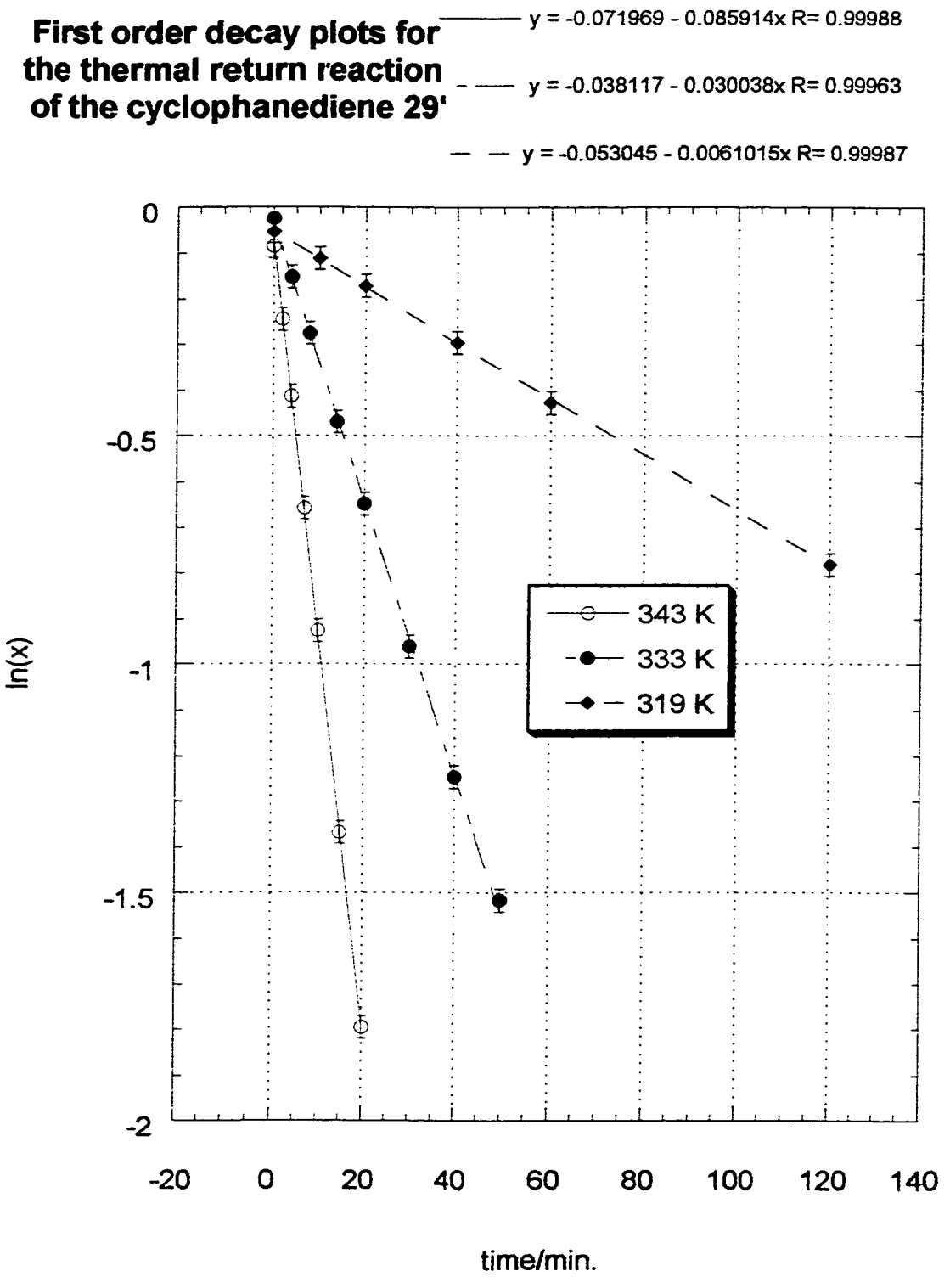
First order decay plots for the thermal return reaction of the cyclophanediene 29'
y = -0.071969 - 0.085914x R= 0.99988
y = -0.038117 - 0.030038x R= 0.99963
y = -0.053045 - 0.0061015x R= 0.99987
343 K
333 K
319 K
ln(x)
time/min.
0
-0.5
-1
-1.5
-2
-20
0
20
40
60
80
100
120
140

First order decay plots for the thermal return reaction of the cyclophanediene 65'

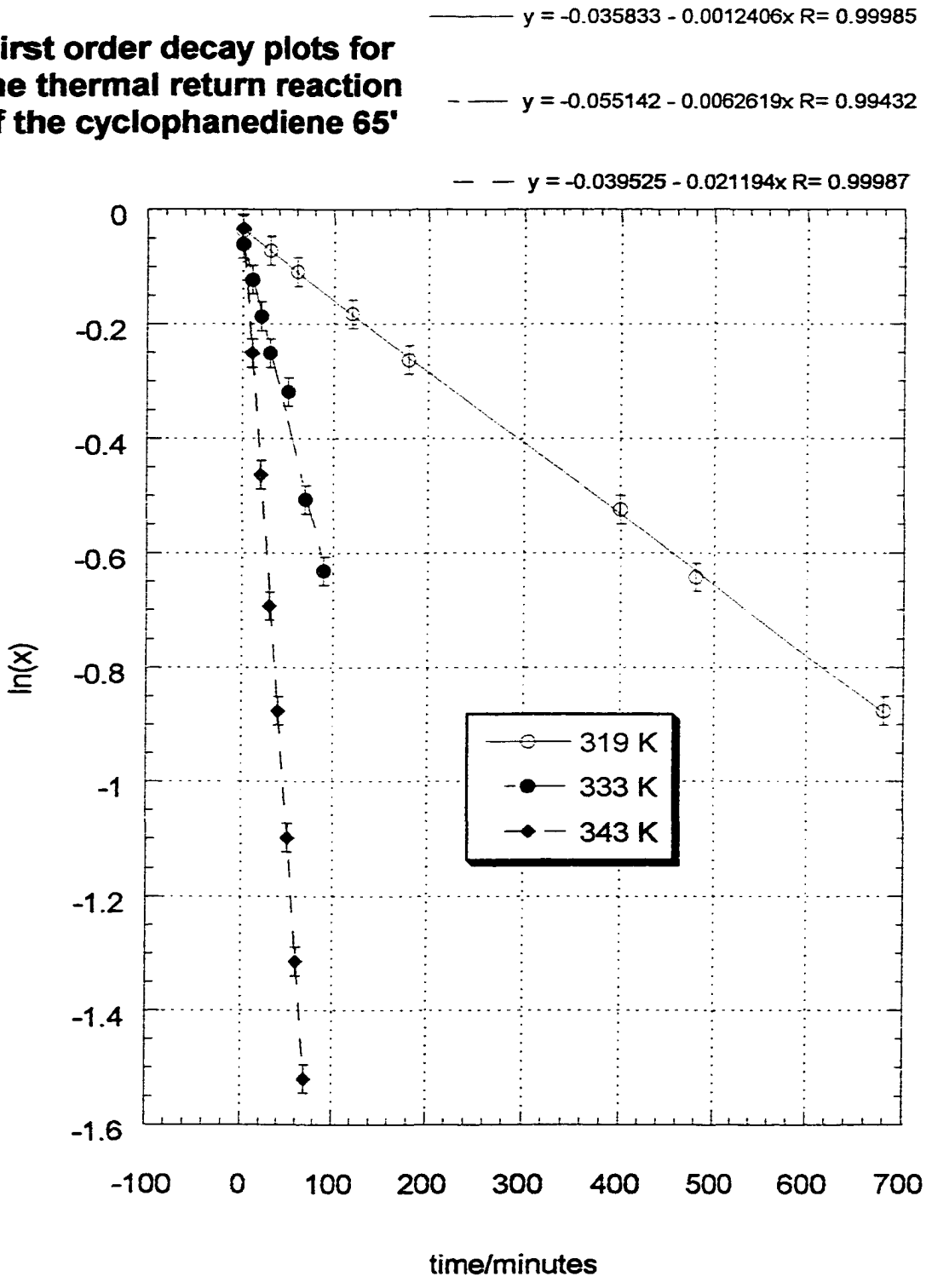

First order decay plots for the thermal return reaction of the cyclophanediene 53'

——— y = -0.00094678 - 0.00198x R= 0.9999

– – — y = -0.0048636 - 0.0095473x R= 0.99987

— — y = -0.0084667 - 0.029934x R= 0.9999

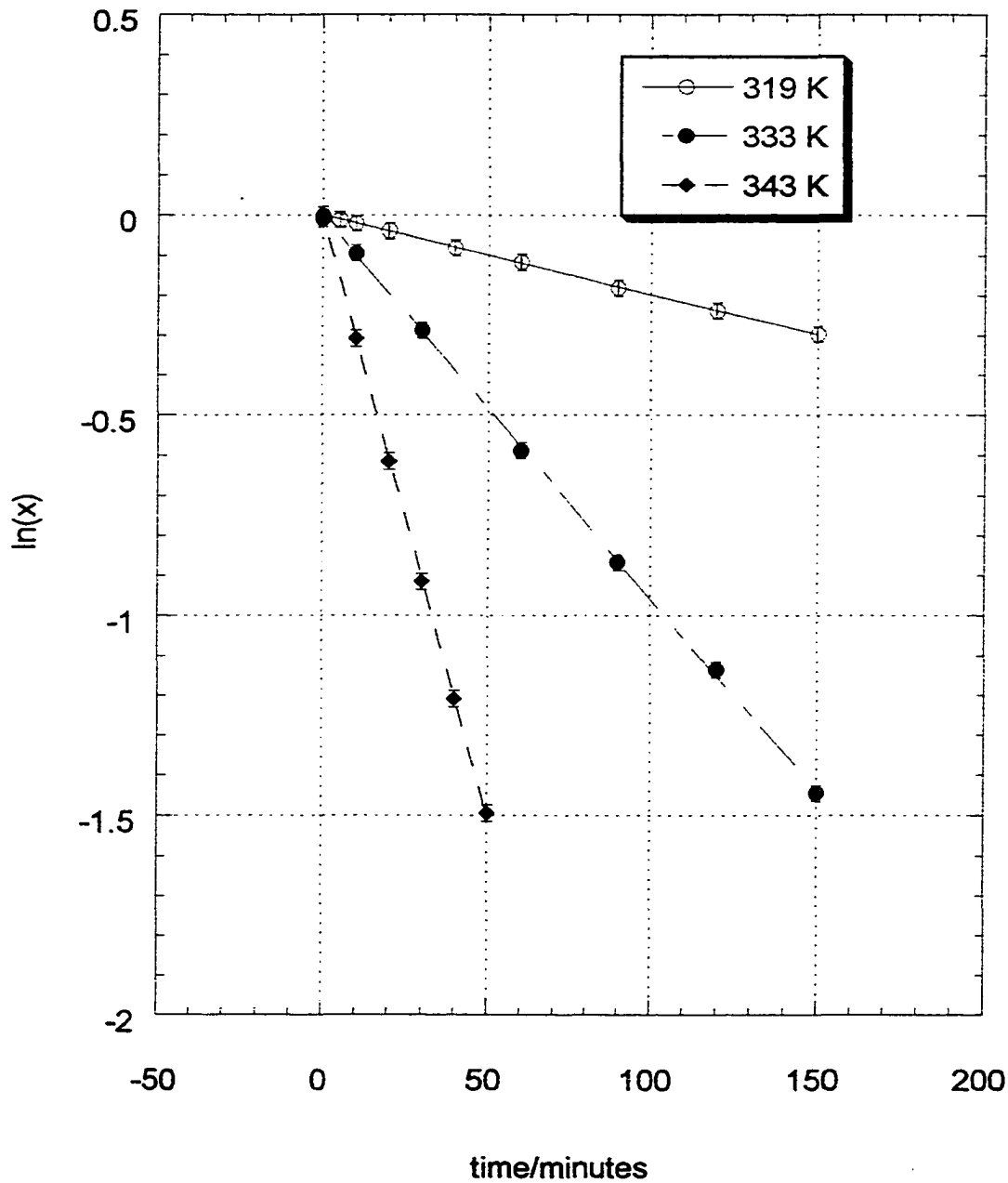

First order decay plots for the thermal return reaction of the cyclophanediene 57'

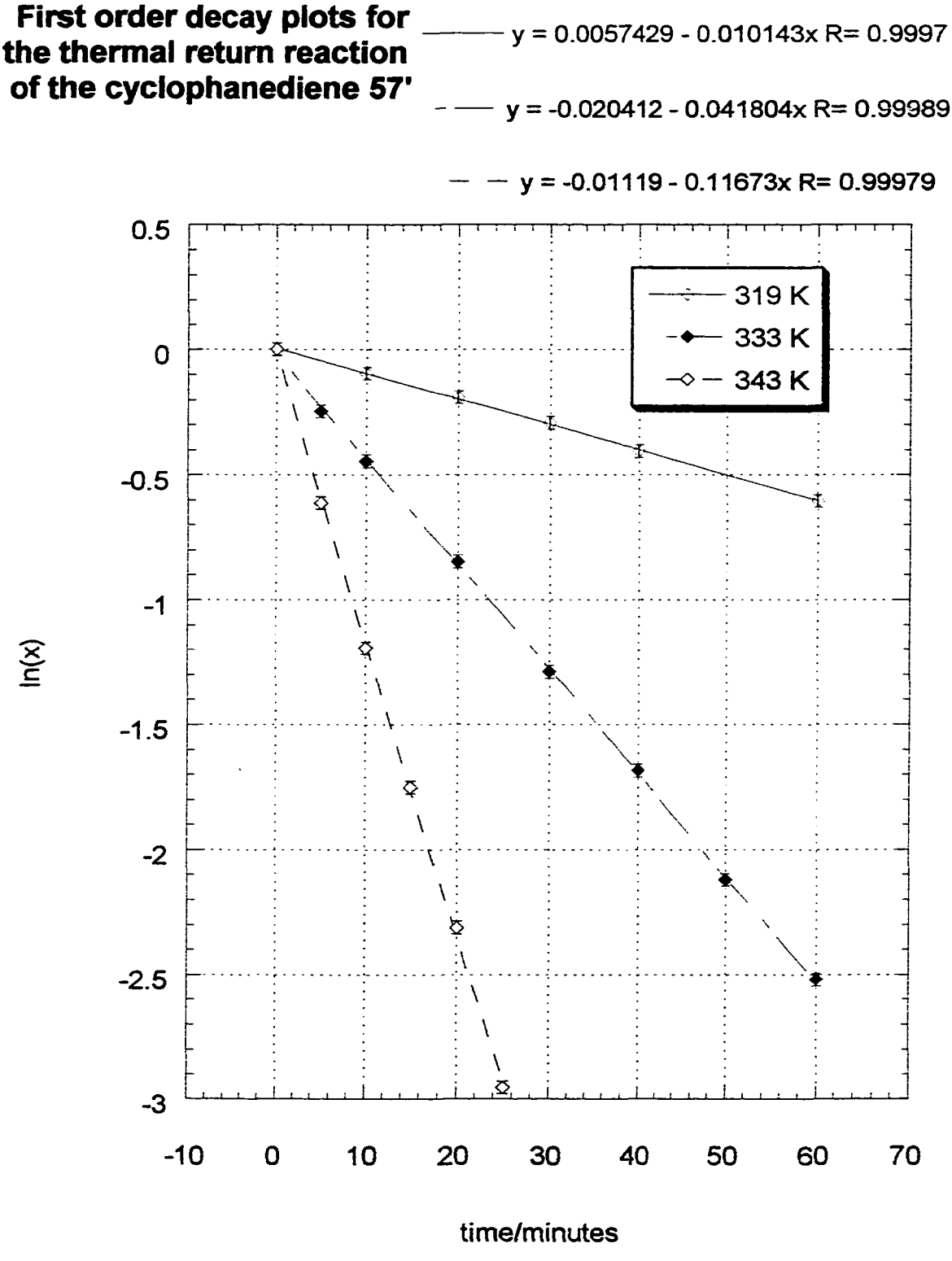

First order decay plots for the thermal return reaction of the cyclophanediene 59'.

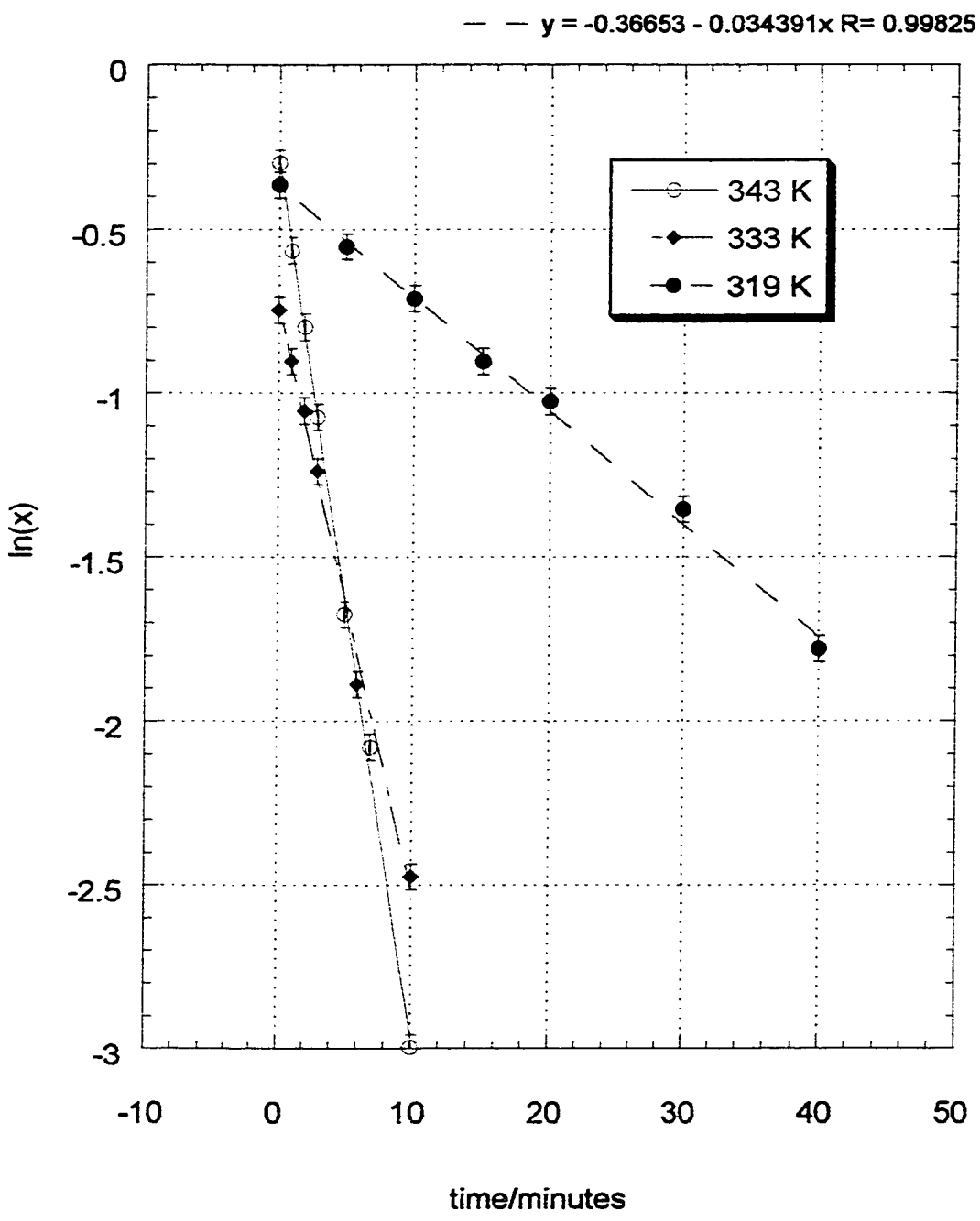

First order decay plots for the thermal return reaction of the cyclophanediene 60".

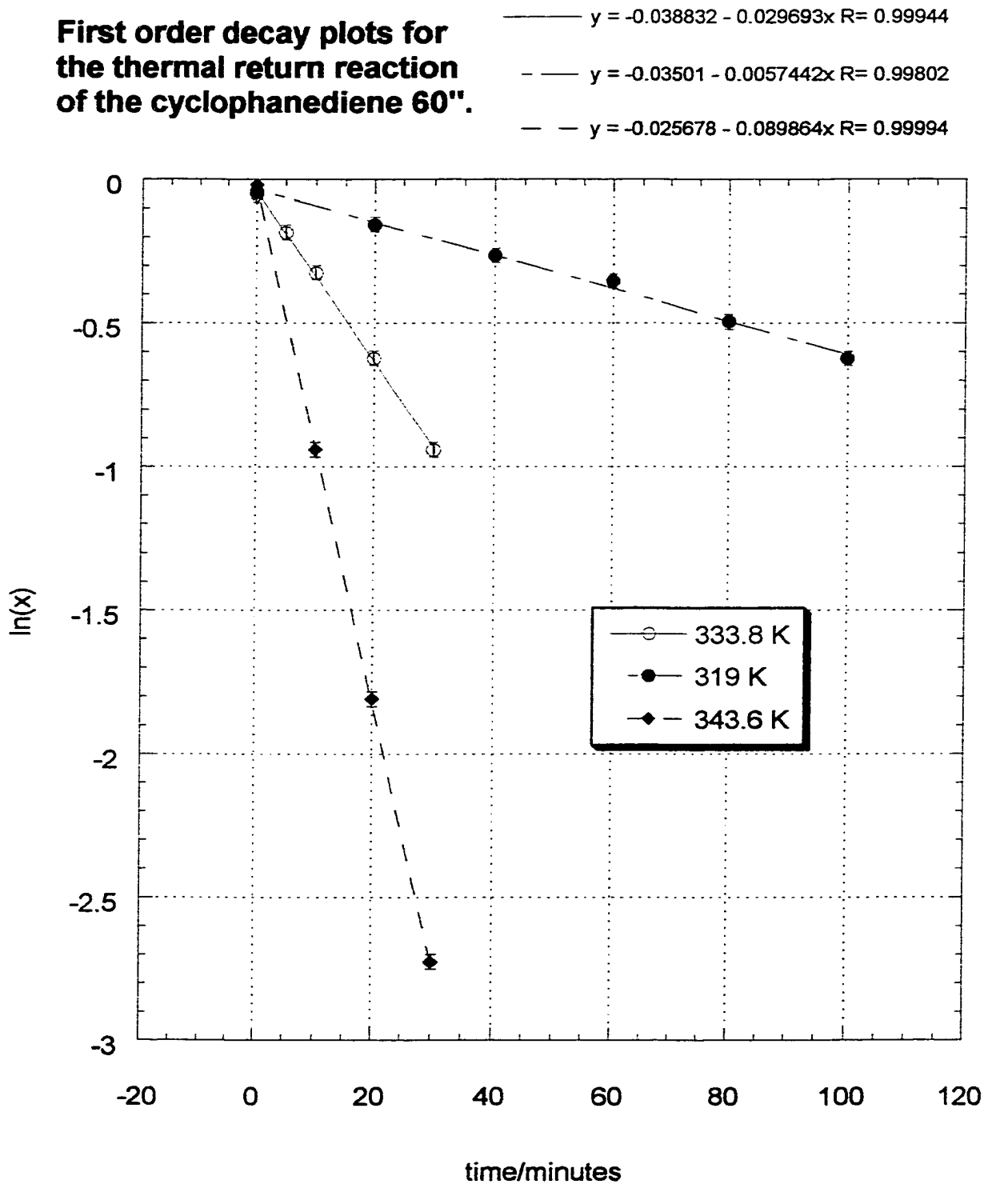

First order decay plots for the thermal return reaction of the cyclophanediene 68a'

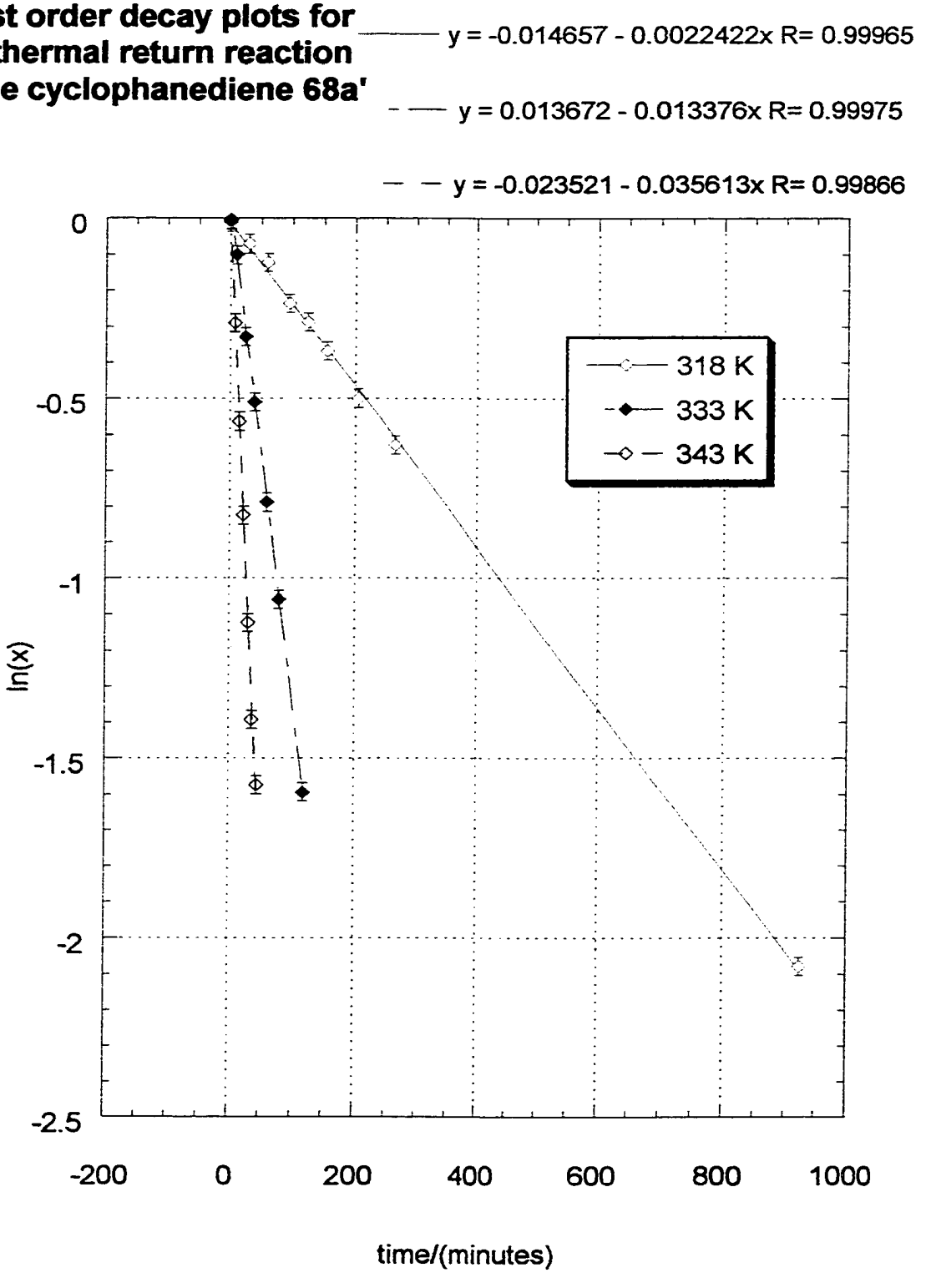

First order decay plots for the thermal return reaction of the cyclophanediene 55'.